CHARACTERISATION OF THE EFFECTS OF DIOXINS ON Ahr THROUGH ITS HOMOLOGUE IN *Drosophila*:

Spineless

Miguel Angel Cespedes

Doctor of Philosophy

School of Life Sciences

University of Sussex

Submitted January 2010

DECLARATION

I hereby declare that this thesis has not been and will not be submitted in whole or in part to another University for the award of any other degree.

Signed…….

ACKNOWLEDGEMENTS

I would like to thank my supervisor Juan Pablo Couso for daring to enable me as a scientist. In addition, I would like to thank Inyaki Pueyo, Rose Phillips, Sylvaine Fouix, Ibo Galindo and Sarah Bishop for their invaluable help and guidance. Special mention to my partners in crime John Chesebro, Emile Magny and Rob Lanfear. Thanks also to the rest of the fly community in Sussex for the lively discussions and encouragement.

I must also acknowledge: Ian Groves for the great support from my first week in Brighton; Sheridan Nye for listening and understanding me; Mamen Cordoba for encouraging me to come to UK; and Yolanda Penya, Vanessa Gomez, Maria Warnefors, Sophie Walker and Eoin O'Connor for making me laugh in the worst times, and in the best, too.

Finally, special thanks to my parents and my sisters, Victoria and Ana, without whom I would not be here. This work is dedicated to them.

This work has been funded by the Wellcome Trust and the University of Sussex.

UNIVERSITY OF SUSSEX

Miguel Angel Cespedes

A thesis submitted for the Degree of Doctor of Philosophy

CHARACTERISATION OF THE EFFECTS OF DIOXINS ON Ahr THROUGH ITS HOMOLOGUE IN *Drosophila*; Spineless

SUMMARY

Dioxins are extremely widespread, toxic and persistent pollutants, as well as a major concern for human health. The *Aryl hydrocarbon receptor* (*Ahr*) is the key component in the metabolic response to dioxins. Ahr is a cytoplasmic bHLH-PAS transcription factor that, upon binding with dioxin, translocates to the nucleus. There it forms a complex with the Ah receptor nuclear transloator (Arnt), another bHLH-PAS protein, and binds to the eight-nucleotide XRE motif to control gene expression. Previous work with *Ahr* knock-out mice revealed the existence of dioxin-independent activity for Ahr in development, but the relationship between the two activities of Ahr remains unclear. Our work uses *Drosophila* to clarify this question, which is central for therapies seeking inactivation of Ahr. The *Drosophila Ahr* homologue, *spineless*

(*ss*), does not bind dioxins, however, it physically interacts with Tango (Tgo), Arnt's fly homologue, and controls gene expression through the XRE motif during development. Here I show that, in the absence of dioxin, Ahr can still bind Tango and Arnt and rescues *ss*⁻ phenotypes, indicating equivalent dioxin-independent activities. I next demonstrate that exposure to dioxin produces an *in vivo* hyperactivation of Ahr, which can also be achieved by increasing the dosage of either Tango or Arnt. Thus Ahr shows different levels of activity, from basal to toxic, depending on the presence of specific ligands and cofactors, and the toxic effects of dioxins represent an excess of the Ahr developmental function. I have also carried out a genetic screen in the search of genes that interact with *ss*. From this screen I have found that the genes that code for the Krüppel-type zinc-finger proteins Squeeze (Sqz) and Rotund (Rn) interact functionally with *ss*. I demonstrate that Rn and Ss interact physically *in vivo*. *Ahr* is also able to interact functionally with *rn* and *sqz* indicating that the interaction with zinc-finger proteins might be an ancestral feature of the dioxin receptor.

TABLE OF CONTENTS

LIST OF FIGURES

LIST OF TABLES

LIST OF ABBREVIATIONS

aa	amino acid
ac	acute
aha-1	*C. elegans* Arnt
Ahr	Aryl hydrocarbon receptor
Ahr-1	*C. elegans* Ahr
AhrR	Ahr Repressor
al	aristal-les
an	antenna
ap	apterous
Arnt	Ahr nuclear translocator
at	antennifer
B	Bar
β-Gal	β-Galactosidase
B[α]P	Benzo-α-Pyrene
BBC	British Broadcasting Corporation
BDGP	Berkeley Drosophila Genome Project
bHLH	basic Helix-Loop-Helix
βNF	βNaptoflavone
BTE	Basic Transcription Element
CIZ	Cas Interacting Zinc-finger
CME	CNS Midline Element
CNS	Central Nervous System

Co-IP	Coimmunoprecipitation
cx	coxa
da	dendritic arborisation
dac	dachshund
dap	dacapo
DAPI	4,6'-diamidino-2-phenylindole, dihydrochloride
Df	Deficiency
DGC	Drosophila Gold Collection
Dll	Distalles
DMP	Dimethyl Pimelimidate Dihydrochloride
Dpp	Decapentaplegic
DRA	Dorsal Rim Area
DSHB	Developmental Studies Hybridoma Bank
DV	Dorso-ventral
EAF	Eosinophil-Activating Factor
EDTA	ethylenediaminetetraacetic acid
EGFR	Epidermal Growth Factor Receptor
EMSA	Electrophoretic Mobility Shift Assay
EMT	Epithelium to mesemchyma transition
Enh	Enhancer
EPA	Environmental Protection Agency
ER	Estrogen Receptor
ey	eyeless
fe	femur
fl	flagellum

FLP	FLPase
FRT	FLP Recombination Targets
GFP	Green Fluorescent Protein
GMR	Glass Multimer Reporter
HIF	Hipoxia Inducible Factor
HRE	Hipoxia Response Element
hs	heat shock
HSP90	Heat Shock Protein 90
hth	homothorax
IARC	International Agency for Research on Cancer
Kb	Kilo base
KDa	Kilo Dalton
LBD	Ligand Binding Domain
lb	labium
md	mandible
min	minute
MMP	Metalloproteinase
mx	maxilla
NES	Nuclear Export Signal
NLS	Nuclear Localisation Signal
Or-R	Oregon R
ORF	Open Reading Frame
PAS	Per Arnt Sim
PBS	Phosphate Buffered Complex
pc	pedicellus

PCR	Polymerase Chain Reaction
PFA	Paraformaldehyde
pl	pleuropodium
PNS	Periferal Nervous System
ppt	parts per trillion
pr	pretarsus
PR	PhotoReceptor
Rh	Rhodopsin
Rn	Rotund
RT	Room Temperature
S^{35}	Sulphur 34
Sav	Salvador
sc	scapus
sc	scute
SDS	Sodium DodecylSulfate
SEM	Scanning Electron Microscope
Ser	Serrate
SOC	Super Optimal Broth
Sp1	Serpentine1
Sqz	Squeeze
Ss	Spineless
Sup	Supressor
ta	tarsus
tal	tarsal-less
TBE	Tris/Borate/EDTA

TCDD	2,3,7,8-Tetrachlorodibenzo-p-dioxin
TGF-b	Tansforming Growth Factor
Tgo	Tango
Thr	trachealess
ti	tibia
Tp	Transposition
tr	trochanter
tsc1	tuberous sclerosis complex 1
tt	tibiotarsus
w	white
wg	wing-less
X-Gal	X-Galactosidase
XRE	Xenobiotic Response Element
y	yellow

Chapter 1

Introduction

"…natural selection does not work as an engineer works. It works like a tinkerer –a tinkerer who does not know exactly what he is going to produce… who uses everything at his disposal to produce some kind of workable object."

FRANÇOIS JACOB, 1977. Evolution and Tinkering.

In nature, organisms are constantly exposed to toxic chemicals such as secondary plant metabolites, mycotoxins or venoms. These compounds act as an adaptive pressure, from which some species have evolved protection. Existing physiological systems have to be adjusted to fulfill new functions (Jacob, 1977). However, in evolution, the acquisition of new traits has to compromise with the previous ones, thus coexisting in a delicate balance. Disruption of such a balance can result in adverse effects for the organism.

An example of these compounds are polycyclic aromatic hydrocarbons (PAHs, also known as dioxins), environmental toxins that induce oxidative stress in the cell. To mitigate the effects of PAHs mammals have developed a detection system mediated by the Aryl hydrocarbon receptor (Ahr). This receptor binds dioxins and starts a signaling pathway dedicated to metabolize these compounds (Schmidt and Bradfield, 1996). This receptor also has functions during the development of the organism (Fernandez-Salguero et al., 1995; Mimura et al., 1997), however, the roles that Ahr might play in development have not been widely studied. Studies with several organisms such as *C. elegans*, *D. melanogaster* and *M. arenaria* suggest that Ahr homologues in the invertebrates do not play a role in detoxification, indicating that this function has been acquired in the evolution of the vertebrate lineage, whereas the more conserved developmental functions might represent an ancestral role of Ahr (Hahn, 2002).

During the last decades, myriad medical research investigations have been underway which study the effects of byproducts of industrialization on human health. Among these substances, the 2,3,7,8-tetrachlorodibenzo-p-dioxin (TCDD, Figure 1.1.A) has raised the greatest concern, as it is the most toxic of the dioxins and has been classified as carcinogen ((IARC), 1997). In addition, TCDD is not substrate for degradation by the pathway activated by Ahr (Schmidt and Bradfield, 1996).

Wild type mice exposed to TCDD manifest developmental defects such as cleft palate (Abbott and Birnbaum, 1991). Interestingly, *Ahr-/-* mice lines are resistant to TCDD (Fernandez-Salguero et al., 1996; Mimura et al., 1997) indicating that TCDD does not represent a threat by itself, instead Ahr mediates most, if not all, of toxic effects of this dioxin. The question is: to what extent does TCDD disrupt the balance between detoxification and developmental functions of Ahr? In other words, TCDD toxicity might be better understood as an alteration in Ahr endogenous functions. With

this work I aim to shed some light on the fine balance between the different functions of the dioxin receptor.

1.1. What are dioxins?

Dioxins are produced by industrial processes like incineration, chlorine bleaching of paper, and the synthesis of some pesticides, herbicides, and fungicides (Schecter et al., 2006). Dioxins are similar in chemical structure (Figure 1.1.A) and have alike physical properties, and cause a common series of toxic effects, such as chloracne, tumour promotion, cardiac dysfunction, and immnunosuppression (Schmidt and Bradfield, 1996). These compounds are hydrophobic and accumulate in fatty tissues of animals and humans (EPA, 2005). Every dioxin is given a toxic equivalency factor (TEF) based on its relative toxicity compared to TCDD, which has a TEF of 1 (Van den Berg et al., 1998). TCDD was classified as a group 1 carcinogen by the International Agency for Research on Cancer (IARC) in 1997. This evaluation was supported by epidemiologic studies in human populations exposed to TCDD and research conducted in animals (IARC, 1997; Steenland et al., 2004).

1.2. TCDD exposure to human populations in history

The first case of TCDD exposure to the human population was reported in 1949 after an accidental release of halogenated dioxins in a chemical plant in Nitro, West Virginia. This accident resulted in the several medical cases of chloracne, liver conditions, blood diseases, tumors, and various deaths associated with the exposure (Zack and Suskind, 1980).

During the Vietnam war, the United States used a compound called Agent Orange to defoliate large forested areas. Several studies show that the concentration of

TCDD in the lipids of Vietnam veterans exposed to the Agent Orange is 600 parts per trillion (ppt), years after they left Vietnam, compared to a 1-2 ppt of general human populations (Kahn et al., 1988; Michalek et al., 1995). A high incidence of certain types of cancer, such as prostate cancer, in Vietnam veterans has been associated with exposure to TCDD (Pavuk et al., 2005).

In 1976 an industrial accident led to the dissemination of high quantities of TCDD and other TCDD-like chemicals in Seveso, Italy. During the days following the accident, 193 human cases of chloracne were reported. The linkage between TCDD exposure and other diseases was uncertain at the time (Bertazzi, 1991). However, recent studies show that the incidence of cancer is significantly higher in people that were exposed to TCDD in the Seveso disaster than in the general Italian population (Steenland et al., 2004).

In recent history, Ukraine president Viktor Yushchenko developed severe chloracne and pancreatitis as the result of TCDD food poisoning in September 2004 (Figure 1.1.B) ((BBC), 2004; Schecter et al., 2006). In December 2008, the Irish government recalled all pork products made in the Irish Republic after tests showed that some of these products had 200 times more dioxins than the recognized safety limit ((BBC), 2008).

A

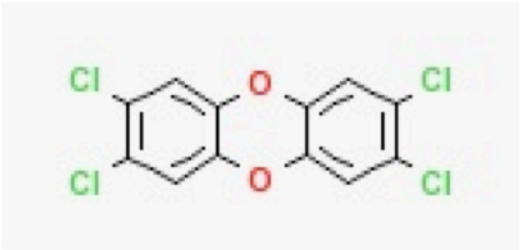

B

Figure 1.1. TCDD represents a major concern for human health. (A) TCDD is a polychlorinated dibenzodioxin. The diagram shows the quemical structure of TCDD. **(B)** Current President of Ukraine Mr. Viktor Yushchenko**.** The pictures show his face before and after September 2004, when he was poisoned with TCDD. Blisters and black heads are symptoms of Chloracne, a severe skin condition caused by exposure to TCDD. Picture was obtained from the BBC website, in: http://news.bbc.co.uk/1/hi/health/4041321.stm (BBC, 2004).

1.3. Toxic effects of TCDD

TCDD triggers a wide range of biological responses. TCDD is a non-metabolizable compound with a half life in human tissue of 7-10 years. The most common toxic effects of TCDD are chloracne, tumor promotion, immunosuppression, decreased fecundity and birth defects. Currently, it is known that most of, if not all, TCDD toxicity is mediated by Ahr (Fernandez-Salguero et al., 1996; Mimura et al., 1997). TCDD toxic effects on liver and thymus have been widely studied in *Ahr*-positive mice and compared to a mouse line in which the *Ahr* gene was disrupted by introduction of a germline-encoded null mutation (Fernandez-Salguero et al., 1995). Approximately half of the *Ahr-/-* mice died shortly after birth. Survivors reached maturity and were fertile, although these mice showed decreased accumulation of lymphocytes in the spleen and lymph nodes, and the livers were reduced by 50 percent (Fernandez-Salguero et al., 1995). TCDD effects on mice liver are characterized by hepatomegaly, cellular hypertrophy, inflammatory cell infiltration, and necrosis. Livers of *Ahr-/-* mice after TCDD exposure were un-affected with the exception of rare, scattered hepatocyte necrosis that was not present in *Ahr-/-* control groups. TCDD exposure also leads to severe regression of the thymic cortex causing thymic atrophy. Thymuses from TCDD-treated *Ahr* null mutants did not show cortical atrophy (Fernandez-Salguero et al., 1996).

A second *Ahr-/-* line was generated by Junsei Mimura's group. Individuals of this second line were viable and fertile and looked normal although displayed slower growth rate than wild-type mice. Mimura's line has been used to study the teratogenic effects of TCDD in palate and kidney. *Ahr*+/+ foetuses exposed to TCDD exhibited cleft palates and hydronephrosis, whereas *Ahr*-/- mice did not show any response to TCDD in palate and kidney compared to controls (Mimura et al., 1997; Peters et al.,

1999). Mimura's *Ahr*-deficient line was also used to study the dependence of Benzo[α]pyrene (B[α]P) toxic effects on *Ahr*. B[α]P is an environmental carcinogen and a ligand for *Ahr*. Topical application of B[α]P in adult mice leads to skin tumours in *Ahr*-positive mice, whereas *Ahr*-deficient mice do not develop tumours, indicating that Ahr mediates the effects of B[α]P (Figure 1.2) (Shimizu et al., 2000).

Most of the effects of dioxins are related directly or indirectly to disruption of the cell cycle. Many studies revealed that these effects are tissue specific. In rat liver, TCDD inhibits apoptosis in enzyme altered foci cells (EAF; carcinogenetic liver cells) while cell division is only slightly enhanced (Luebeck et al., 2000; Stinchcombe et al., 1995). In contrast, studies using rodent liver and various cell lines showed that TCDD triggers cell cycle arrest and apoptosis (Moolgavkar et al., 1996). Treatment with TCDD of carcinogenic rat liver cells leads to a decrease in the rate of apoptosis by 60% and 10% of control values after acute and chronic TCDD treatment, respectively. In normal liver tissue apoptosis rates are only slightly decreased after treatment with TCDD whereas cell division rates are unaffected (Luebeck et al., 2000; Stinchcombe et al., 1995).

In the following sections I review the mechanisms of dioxin toxicity in pathological conditions and the role of Ahr in the affected physiological systems.

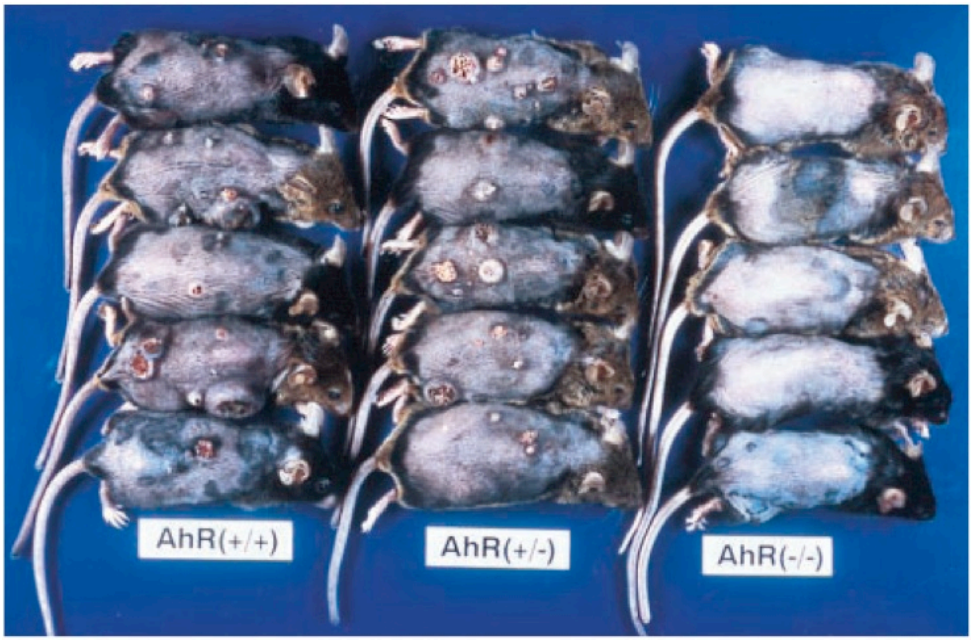

Figure 1.2. *Ahr-/-* mice are resistant to BαP. From left to right: wild type (*Ahr*+/+), *Ahr*+/- mice, *Ahr*-/- mice. Mice were treated with BαP topically. Mutants for *Ahr* do not develop skin tumours. Picture was obtained from Shimizu et al., 2000.

1.3.1. Chloracne

Chloracne is a skin condition that affects the hair follicles, sebaceous glands and interfollicular epidermis. It causes black heads, cysts, and pustules. Since the first reports of humans exposed to TCDD, chloracne has been the most common observed pathological disorder (Poland and Knutson, 1982). Sustained and inappropriate Ahr activation by TCDD is thought to cause chloracne, although the molecular mechanisms remain unknown (Bock and Kohle, 2006). *Ahr-/-* mice show other skin conditions such as alopecia and ulcers of variable severity (Fernandez-Salguero et al., 1997).

1.3.2. Carcinogenicity and tumor promotion

Cancer mortality was studied in humans that were exposed to TCDD in the Seveso disaster. Among men, 20 years after the accident, lung cancer and rectal cancer mortality were higher than normal. Among women, after 15 years, there was an elevated incidence of liver cancer (Pesatori et al., 2003; Steenland et al., 2004). Furthermore, a separate study in 1981 showed positive correlation between the incidence of breast cancer and the levels of TCDD in the serum of the analyzed patients (Warner et al., 2002).

Cell to cell contact is involved in the regulation of cell proliferation and differentiation. Disruption of the normal cell-contact state can lead to cancer and tumor development (Bock and Kohle, 2006). Studies in cell culture show that, in absence of dioxins, Ahr cellular localization depends on cell density. In a keratinocyte cell linage Ahr localizes in the cytoplasm under high cell densities. When the cell density declines, Ahr translocates to the nucleus driving changes in gene expression. The same studies show that Ahr activates expression of *Slug*, a gene that codes for a zinc-finger protein involved in epithelium to mesemchyme transition (EMT) (Ikuta et al., 1998; Ikuta and Kawajiri, 2006). Slug downregulates the transcription of E-cadherin disrupting E-

cadherin mediated cell-cell adhesion, which is considered a first step in EMT and tumor cell invasion (Nieto, 2002). In a different study conducted in liver stem cell-like culture, exposure to TCDD was associated with a reduction of contact-inhibition of cell growth (Kohle et al., 1999).

Suppression of both growth arrest and apoptosis are a key element in carcinogenesis and tumor promotion. In rat hepatocytes, TCDD leads to the inhibition of p53 by hyperphosphorilation. p53 is a tumor suppressor with functions in cell-cycle control, DNA repair and apoptosis (Bock and Kohle, 2006). Interestingly, Ahr activates c-Jun in a ligand-dependent manner leading to the inhibition of p53 and, subsequently, to the suppression of growth arrest and apoptosis resulting in tumour formation (Bock and Kohle, 2006; Henklova et al., 2008).

1.3.3. Immunosuppression

TCDD can act as an immunosuppressor via the degeneration of the thymus. This was one of the first characterised effects of TCDD in rodents (Poland and Knutson, 1982). In laboratory animals, B and T cell responses and the resistance to viral and bacterial infection are affected by the addition of TCDD (Bock and Kohle, 2006). T cells are lymphocytes responsible for the cell-mediated immune response (Boag, 2007). In T cells, activation of Ahr increased the expression of the *IL-2* gene by directly binding to a regulatory region of the gene (Jeon and Esser, 2000). *IL-2* is a pro-apoptotic gene that is involved in the induction of T-cell death (Refaeli et al., 1998).

1.3.4. Fecundity

Ahr deficient mice show functional impairment of male and female reproductive organs (Baba et al., 2005; Lin et al., 2002). In accordance with this phenotype, perinatal exposure to TCDD permanently reduces sperm production in males and the reproductive potential of females (Gray and Kelce, 1996). In nonhuman primates TCDD

increases the prevalence and severity of endometriosis, a medical condition in females that consists of uterine thickening and affects the attachment of the embryo (Rier and Foster, 2003).

Dioxins also interfere with sex hormone signalling. For instance, ligand-dependent activated Ahr acts as an E3-ubiquitin ligase that targets the estrogen receptor-α (ERα) for protein degradation (Ohtake et al., 2007). GST pull-down and *in vivo* coimmunoprecipitation studies have described direct interactions between Ahr and ERα (Klinge et al., 2000) and Arnt and ER (Brunnberg et al., 2003). Interestingly, exposure to TCDD during pregnancy in the Seveso accident was associated with a lowered male:female ratio (Mocarelli et al., 2000).

1.3.5. Cleft palate

The most common birth defect in human and rodents exposed to TCDD is a cleft palate (Abbott and Birnbaum, 1991; Abbott et al., 1992). In order to form a barrier between the nasal and oral cavities opposing palatal shelves have to grow and fuse. In normal development, once the two halves meet, cells undergo ephitelium to mesemchyma transition (EMT) to form a single fused tissue (Bock and Kohle, 2006). During individuals exposed to TCDD the two shelves meet but EMT does not occur. As a consequence, a cleft is formed as the tissue keeps growing but fails to fuse (Abbott and Birnbaum, 1991). As mention above, Ahr might play a key role in EMT by disrupting cell adhesion by indirect inhibition of E-cadherin transcription (Ikuta and Kawajiri, 2006). However, physiological functions of Ahr in the fusion of palatal shelves remain unknown.

1.4. Other functions of *Ahr* in embryonic development

It is known that *Ahr* has endogenous functions. *Ahr* is expressed in early murine embryonic development and adult tissues. *Ahr* is first expressed at gestation day 10 and the overall expression expands from the day 13 to 15 (Abbott and Probst, 1995; Mimura et al., 1997). In adult mice *Ahr* is highly expressed in the oocyte, epidermis, bladder, lung, digits, vomeronasal organ, liver, trachea, olfactory epithelium, and retina (Su et al., 2002).

Three independent *Ahr* null mouse lines have been generated. Despite of some phenotypic differences, all three share characteristics such as reduced fecundity, portal fibrosis and smaller livers, as well as resistance to TCDD (Fernandez-Salguero et al., 1995; Mimura et al., 1999; Schmidt et al., 1996).

1.4.1. Portal fibrosis

Another actively studied effect on the liver is portal tract fibrosis (development of excess fibrous connective tissue around the portal tract, the system that transports blood from the intestines to the liver) (Fernandez-Salguero et al., 1995; Schmidt et al., 1996). Lack of *Ahr* leads to increased secretion of active TGF-β, which is a potent pro-fibrotic agent (Border and Noble, 1994; Branton and Kopp, 1999). This increase is regulated post-translationally (Santiago-Josefat et al., 2004; Zaher et al., 1998) and it is thought to be a consequence of deficient retinoid metabolism (Andreola et al., 1997; Andreola et al., 2004) and direct transcriptional regulation of latent TGF-β-binding protein-1 (Corchero et al., 2004; Santiago-Josefat et al., 2004).

1.4.2. Smaller liver size

Defects in the development of the foetal vascular system leads to decreased liver size (25-50% smaller than controls) (Fernandez-Salguero et al., 1995; Mimura et al., 1997; Schmidt et al., 1996). In the foetus, blood flow bypasses the liver via a shunt

called Ductus Venosus (DV). Shortly after birth the DV closes so the blood rich in oxygen and nutrients is forced to pass through the liver (Edelstone et al., 1978; Kiserud, 2000). In *Ahr*-/- mice the DV fails to close slowing postnatal liver growth due to nutrient deprivation (Lahvis et al., 2000; Lahvis et al., 2005).

1.5. Mechanisms of regulation of Ahr protein

Ahr belongs to the family of bHLH-PAS proteins. The basic-helix-loop-helix (bHLH) is a DNA-binding and a protein dimerization domain (Figure 1.3.A) (Murre et al., 1989). A characteristic of many bHLH proteins is the presence of a secondary dimerization surface adjacent to the HLH motif, such as the Per-Arnt-Sim (PAS) domain (Figure 1.3.A) (Schmidt and Bradfield, 1996). In dissecting Ahr regulatory mechanisms we could differentiate between nuclear import/export, protein degradation, and DNA binding (Figure 1.3.B).

1.5.1. Nuclear import/export

The subcellular localization of Ahr has been shown to affect Ahr function (Pollenz et al., 1994). The inactive form of Ahr forms a cytoplasmic complex with two 90 KDa Heat Shock Proteins (Hsp90) (Pollenz, 2002), the immunophilin like protein XAP2 (Kazlauskas et al., 2000) and the co-chaperone p23 (Figure 1.3.B) (Cox and Miller, 2002). Hsp90 is known to maintain the high-affinity ligand binding conformation of Ahr (Pongratz et al., 1992). XAP2 stabilizes the Ahr/Hsp90/p23 complex, preventing transient unmasking of the N-terminal nuclear localisation sequence (Kazlauskas et al., 2001). XAP2 also protects inactive Ahr form proteosome-mediated degradation (Kazlauskas et al., 2000). The role of p23 remains unclear; however, reconstitution studies in yeast showed that p23 increases the Ahr response but it is not essential for *Ahr* signalling (Cox and Miller, 2002).

The Ligand Binding Domain (LBD) represses Ahr activity in the absence of an exogenous ligand. Upon ligand binding, Ahr undergoes a conformational change in the LBD that allows Ahr to be released from the cytoplasmic complex and shuttled to the nucleus (Figure 1.3.A and B) (Ikuta et al., 1998; Kudo et al., 2009). This change exposes a bipartite nuclear localization sequence (NLS) located in the bHLH domain (aa13-17 and 37-42) (Figure 1.3.A) (Ikuta et al., 1998) leading to Ahr nuclear translocation. Ahr dissociates from the receptor complex and once Ahr is in the nucleus it binds the Ahr nuclear translocator, Arnt (Figure 1.3.B). It remains unclear whether Ahr releases the receptor complex in the cytoplasm or in the nucleus. Ahr/Arnt complex binds Xenobiotic Response Elements (XRE, minimal consensus TNGCGTG) leading to changes in expression of downstream genes (Swanson et al., 1995; Whitlock, 1990).

Ahr has two nuclear export signals (NES). One is located in the bHLH (aa49-53) and mediates nuclear export of ligand activated receptor (Pollenz, 2002). The second is at the end of PAS-A (aa216-224) and mediates nuclear export of unliganded receptor (Figure 1.3.A) (Pollenz, 2002).

1.5.2. Protein degradation

It remains unclear whether Ahr is degraded in the nucleus or whether the NES motifs control Ahr degradation by exporting it to the cytosol. However, it is reported that ligand activation leads to ubiquitin-mediated degradation of Ahr (Pollenz, 2002). Thus, Ahr is depleted upon treatment with TCDD (Pollenz, 1996). The sequences that mediate degradation are still unknown.

1.5.3. DNA binding

The Ahr/Arnt transcription factor complex specifically binds XREs (Xenobiotic response elements) to control gene expression (Swanson et al., 1995). One of the up-regulated genes encodes the Ahr repressor protein (AhrR) (Baba et al., 2001; Mimura et

al., 1999). This protein shows high homology with Ahr in the N-terminal. AhrR is able to heterodimerize with Arnt and bind XRE motifs (Mimura et al., 1999). In cell culture experiments, overexpression of *AhrR* suppresses dioxin mediated reporter induction. Thus, AhrR might repress Ahr activity by competing for the same partner and DNA-binding site (Mimura et al., 1999).

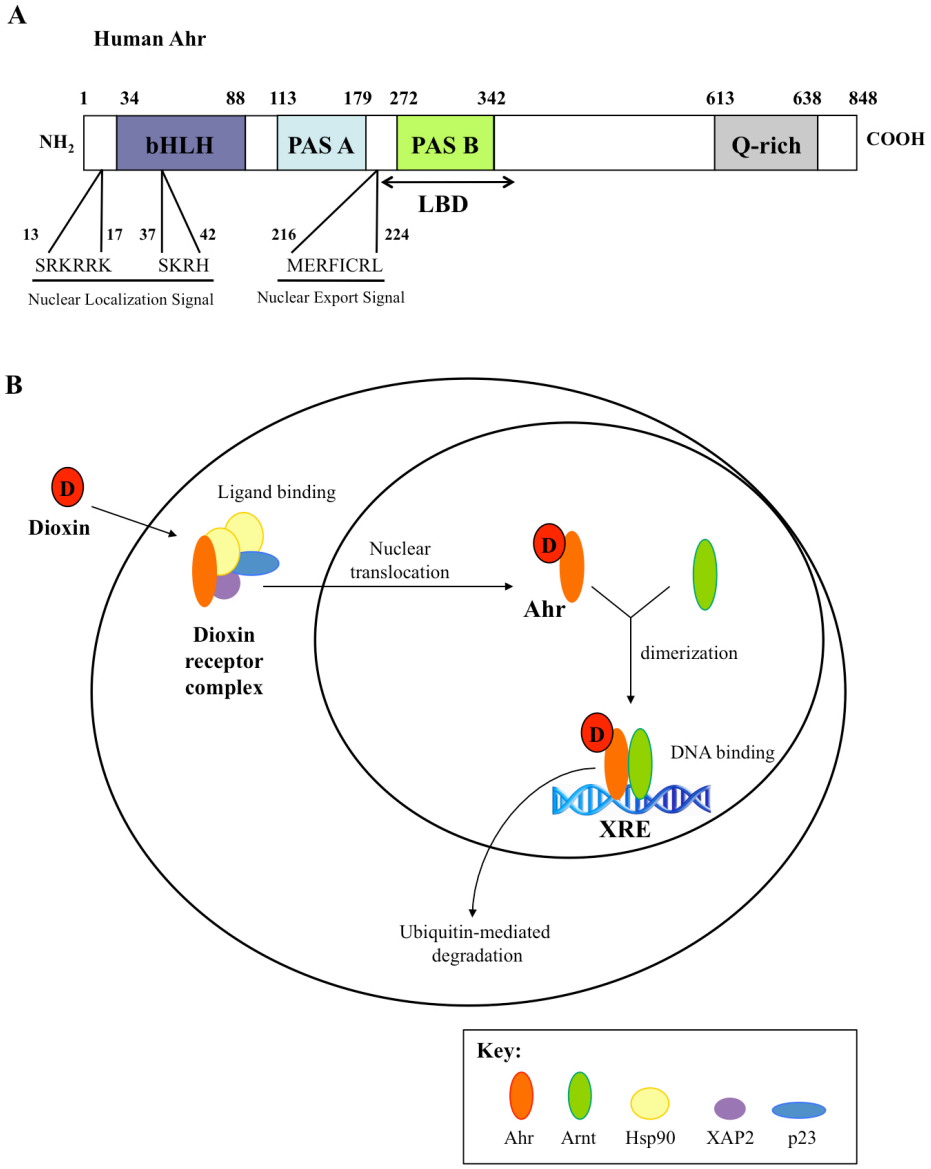

Figure 1.3. Ahr is a bHLH-PAS protein with dual function: receptor and transcription factor. (A) Ahr protein. The diagram shows the DNA binding and dimerization domain (bHLH and PAS domains respectively), the glutaimine rich (Q-Rich) domain, the location of the Nuclear Localization Signal and the Nuclear Export Signal, and the Ligand Binding Domain (LBD). **(B)** Model of dioxin signaling. Ahr binds dioxin as part of a receptor complex. Upon ligand binding, Ahr translocates to the nucleus and forms a heterodimer with Arnt. Ahr/Arnt drives changes in gene expression through the binding of XRE motifs. Ahr undergoes Ubiquitin-mediated degradation.

1.6. *Drosophila melanogaster*'s *Ahr* homologue: *spineless*

Spineless (*ss*) is the closest *Ahr* homologue in *Drosophila melanogaster*. Ss and Ahr share high conservation in the amino acid sequence in the bHLH domain (71%) and the PAS domain (45%) (Figure 1.4.A). Also, the five splicing sites within the bHLH and the PAS coding sequences are conserved (Duncan et al., 1998). Ss dimerises with Tango (Tgo), the closest homologue of Arnt in *Drosophila* (Sonnenfeld et al., 1997), to form a transcription factor complex (Emmons et al., 1999). Cell culture and *in vivo* experiments have shown the ability of Ss/Tgo to bind XRE motifs to control gene expression. In SL2 cells the Ss/Tgo complex was able to upregulate the expression of a reporter gene under the control of a promoter containing several XREs (Emmons et al., 1999). In *Drosophila melanogaster ss* represses *Bar* (*B*) expression in the distal part of the leg imaginal disc during early third larval instar (Kozu et al., 2006; Pueyo and Couso, 2008). This has been reported to be a consequence of direct binding of a XRE by *ss* in a regulatory region of *Bar* called the *ta5* enhancer (Kozu et al., 2006).

While many features are conserved between *Ahr* and *ss*, there are also several differences in their mechanisms of action. Until now Ss has always been described as a nuclear protein (Duncan et al., 1998), whereas Ahr can be cytoplasmic and nuclear (Pollenz et al., 1994). This indicates that Ss activity is not regulated by its subcellular localization and that Ss might not be able to bind Ahr's cytosolic partners. Also, Ss is unable to bind dioxins and its activity has never been reported to depend on a ligand (Butler et al., 2001; Hahn, 2002). All known *Ahr* homologues in any species of invertebrates lack the ability to bind dioxins (Butler et al., 2001). Aryl hydrocarbon signaling might be a new function acquired after the vertebrates and invertebrates lineages split, whereas Ahr developmental functions might be an evolutionary conserved feature within this protein family.

Both *Arnt* and *tgo* are ubiquitously expressed throughout development in all tissues (Pollenz et al., 1994; Ward et al., 1998) and both are partner factors for several members of the bHLH-PAS family (Sonnenfeld et al., 1997; Swanson et al., 1995). However, Arnt is always nuclear (Pollenz et al., 1994), whereas Tgo can be cytoplasmic, as well (Ward et al., 1998). This difference might represent an alternative way of regulating Tgo activity by controlling the subcellular localization of its functional partner.

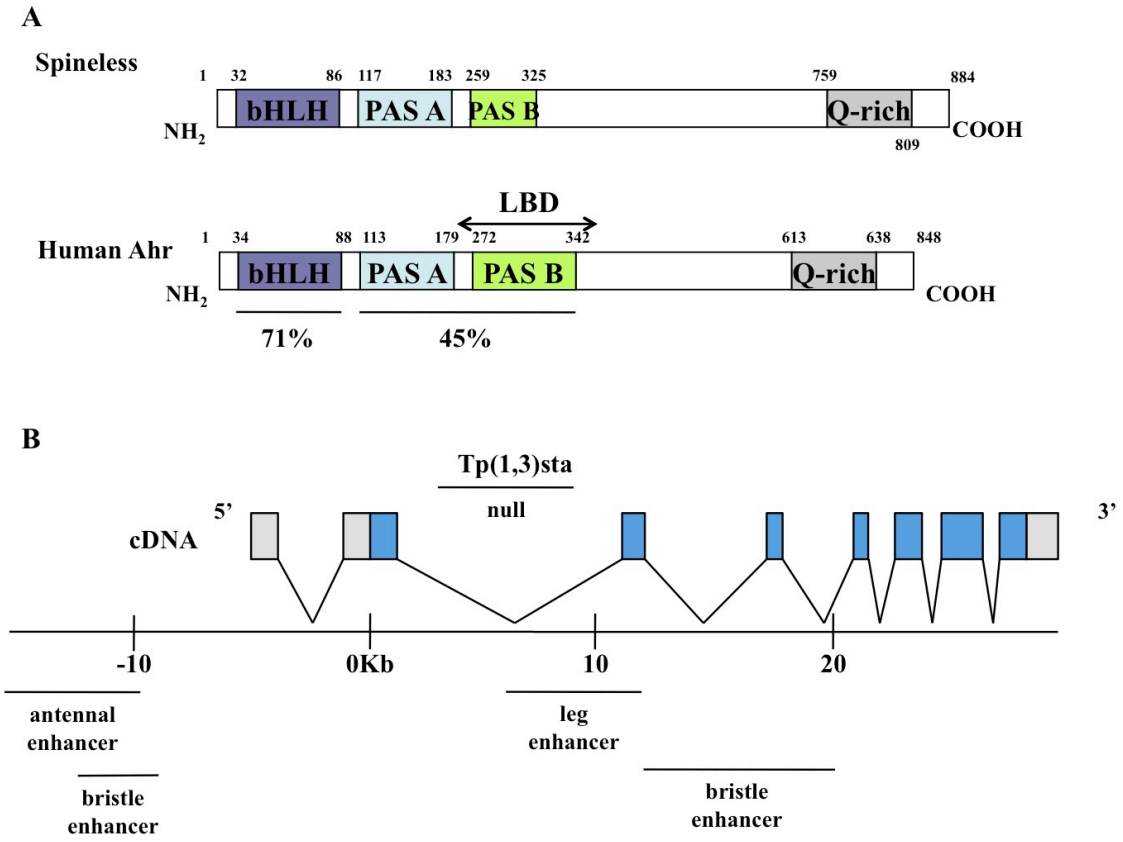

Figure 1.4. The *spineless* locus and the protein that it encodes. (A) Ss and Ahr proteins. The percentage of homology between the different bHLH and PAS domains are shown below. **(B)** The structure of the *spineless* locus showing the exons (blue boxes), non-coding sequences (grey box), the antennal and leg enhancers, and the insertion that generates the ss^{sta} allele (*Tp(1,3)*ss^{sta}).

1.7. The role of *ss* in *Drosophila*'s development

The gene *ss* plays a key role in the development of the leg, antenna, bristles (Lindsley, 1992; Struhl, 1981), mouthparts (Joulia et al., 2006), embryonic PNS (Kim et al., 2006), and ommatidial eye mosaic (Wernet et al., 2006). Null alleles of the gene *ss* cause transformation from antenna to distal leg and deletion of the three intermediate tarsal segments (Lindsley, 1992; Struhl, 1981). In all *ss* mutants bristle size is affected to some degree (Struhl, 1981). Recently it is been reported that there is also a loss of dendrite diversity among the da neurons in the embryonic PNS (Kim et al., 2006). In ommatidia, all R7 cells and most of R8 acquire a pale photoreceptor fate in *ss* mutants (Wernet et al., 2006). Expression of *ss* can be detected by *in situ* hybridation in embryonic development from the stage 8 till the late stages (Figure 1.5.A-F). *ss* transcript can be also found in eye-antennal, leg and wing imaginal disc in larvae and pupae (Figure 1.5.G-M) (Duncan et al., 1998).

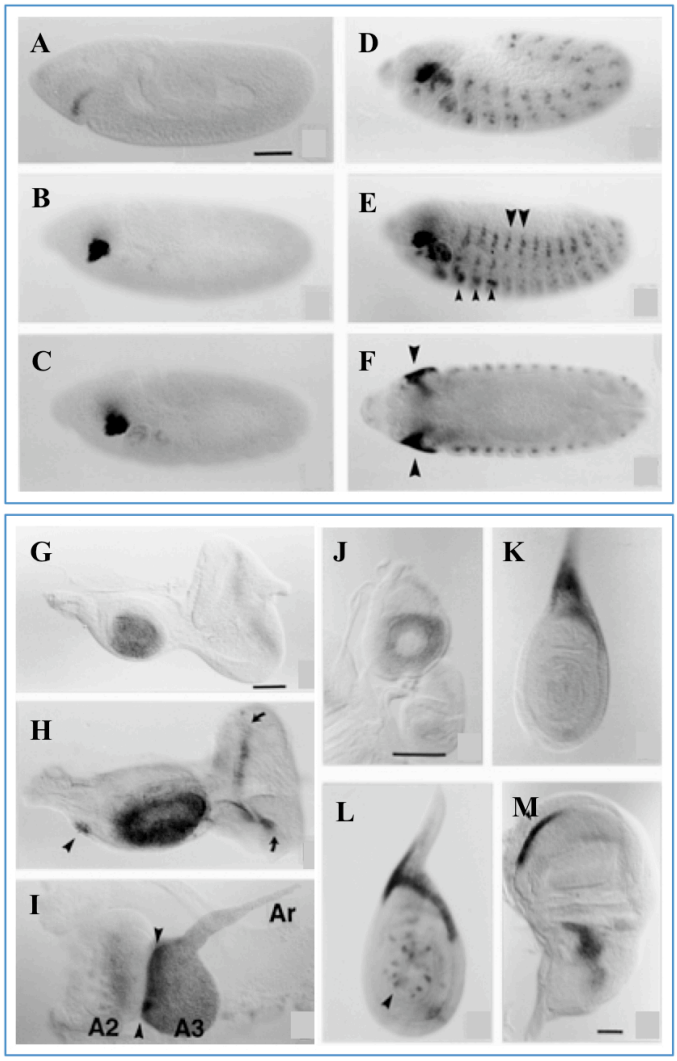

Figure 1.5. *ss* expression during embryonic and larval development. Figure extracted from Duncan et al., 1998. *ss* expression was detected by *in situ* hybridation **(A-F)** Distribution of the *ss* transcript in embryos from stage 8 **(A)** till late stages of embryonic development. The leg anlages and the Peripheral Nervous System are indicated in **E** by the small and large arrowheads, respectively. In **F**, the arrowheads point at the eye-antennal discs. **(G-M)** *ss* expression in larval imaginal discs. **(G-H)** Eye–antennal discs from early and late wild-type third instar larvae. **(I)** *ss* expression in an everted antennal disc. **(J–L)** *ss* expression pattern in early **J** and late **K** third instar leg discs, and in a leg disc just prior to eversion **(L).** The arrowhead in **L** indicates labelling of bristle precursor cells. **(M)** *ss* expression in a third instar wing disc. Scale bars, 50 μm.

1.7.1 *ss* in leg development

In the leg imaginal disc the conjugation of three main signals lead to the formation of proximo-distal genetic domains. Those signals are: *Dpp* expressed dorsally, *Wg* expressed ventrally, and EGFR signalling coming from the centre of the disc (Galindo et al., 2002; Lecuit and Cohen, 1997). *Dpp* and *Wg* cooperate to activate *Distal-less* (*Dll*) and *dachshund* (*dac*) in the distal and medial presumptive regions, respectively (Diaz-Benjumea et al., 1994; Lecuit and Cohen, 1997). EGFR signalling activates *B* expression in the most distal domain (Galindo et al., 2002). *B* represses *dac* expression, creating two major expression domains in the distal part of the disc. Around 80-96 hours AEL the gene *tarsal-less* (*tal*) is expressed in the boundary of *dac* and *B* expression domains (Galindo et al., 2007; Pueyo and Couso, 2008). *tal* activates *ss* and *rn* in a ring in the distal half of the leg imaginal disc during mid-third instar. *ss* and *rn* repress *dac* proximally and *B* distally to create an expression domain that contains the presumptive intermediate tarsal segments (Figure 1.6) (Pueyo and Couso, 2008). *ss* expression in the leg imaginal disc is controlled by an intronic region approximately 10 kb downstream of the start of *ss* ORF (Figure 1.4.B) (Emmons et al., 2007). *ss* mutants lack most of the tarsal segments: distal part of the first tarsus, and second to fourth tarsi (Lindsley, 1992; Struhl, 1981). *ss* is also expressed in the most proximal region of the disc by the end of the third larval instar. However, proximal structures remain unaffected in *ss* mutants (Duncan et al., 1998).

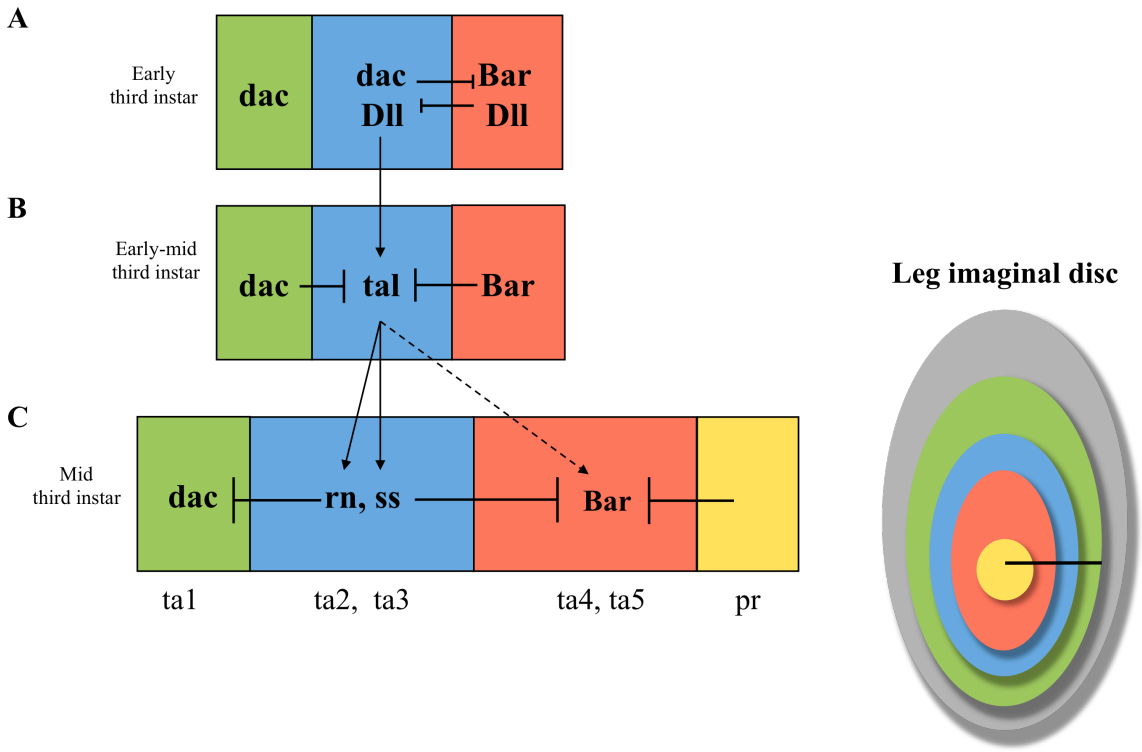

Figure 1.6. A combinatorial code of transcription factors determine tarsal fate. (A) During early 3rd larval instar the genes *dac* and *Bar* are expressed in abutting rings in the distal part of the leg imaginal disc. **(B)** The gene *tal* is expressed between both domains during early-mid 3rd larval instar. **(C)** During mid 3rd larval instar *tal* activates the expression of *rn* and *ss*, which in turn repress expression of *Bar* distally and *dac* proximally so creating an intermediate expression domain that will form the second and third tarsal segments. Other factors repress expression of *Bar* in the centre of the disc, thus creating the presumptive pretarsus. The first, second, third, fourth and fifth tarsal segment, and the pretarsus are represented by ta1, ta2, ta3, ta4, ta5, and pr, respectively.

1.7.2. *ss* in antennal development

ss and the homeobox genes *homothorax* (*hth*) and *Distal-less* (*Dll*) play key roles in antennal development. *ss* expression in antenna imaginal disc starts as a solid domain in the centre of the disc at late second instar (Duncan et al., 1998). The expression resolves in to a ring by mid-third instar. *ss* antennal expression is controlled by an enhancer region approximately 15 Kb upstream of the *ss* ORF (Figure 1.4.B) (Duncan et al., 1998; Emmons et al., 2007). *Dll* and *hth* activate *ss* expression, whereas *cut* represses it determining the proximal limit of expression (Emmons et al., 2007). *ss* mutants show a homeotic transformation of the distal antenna into distal second-thoracic leg, indicating that *ss* has a function in the determination of antennal identity (Lindsley, 1992; Struhl, 1981).

1.7.3 *ss* in bristle development

Expression of *achaete* (*ac*) and *scute* (*sc*) lead to the formation of mechanosensory bristles (Alonso and Cabrera, 1988; Ghysen and Richelle, 1979). The large bristles, macrochaetes, are arranged into specific patterns (Simpson, 2007). In *ss* mutants, *ac* is not expressed (Tsubota et al., 2008) and macrochaetes are shorter or absent (Melnick et al., 1993). According to this phenotype, *ss* drives the expression of *ac* in a group of cells in the distal/dorsal region of the mesothoracic leg imaginal disc. This set of cells will develop in to sternopleural bristles –a group of three bristles in the mesothoracic segment. Recently, three bristle enhancers have been found in a region upstream of *ss* and in two *ss* intronic regions (Figure 1.4.B) (Emmons et al., 2007).

1.7.4. *ss* in mouthparts development

During late third instar *ss* is expressed in the antennal imaginal disc in the region that corresponds to the adult mouthparts (Duncan et al., 1998). *ss* mutants have not detectable effect on the mouthparts. *proboscipedia* (*pb*) mutants show transformation

from labium to prothoracic leg (pretarsus and two partially formed tarsae). Loss of function of *ss* enhances pb^{-} phenotype giving rise to a tripartite leg (pretarsus and three tarsae) (Joulia et al., 2006).

1.7.5. *ss* in the determination of the retinal mosaic

The compound eye of *Drosophila* consists of approximately 800 optical units called ommatidia (Wolff, 1993). Each ommatidium has eight photoreceptor cells (PRs). PRs are subdivided in two categories: six "outer" PRs (R1-R6 cells), and two "inner" PRs (R7 and R8 cells). The "outer" PRs express the broad-spectrum rhodopsin, Rh1, which is required for motion detection in dim light (Heisenberg, 1977; Miller, 1981; Zuker et al., 1985). The "inner" PRs express a range of different rhodopsins that are responsible for colour vision (Chou et al., 1999). There are three major ommatidial subtypes depending on the rhodopsins that are expressed in the "inner" PRs: "Pale" ommatidia, "yellow" ommatidia, and the dorsal rim area (DRA) (Chou et al., 1999; Feiler et al., 1992). In "pale" ommatidia, R7 cells express the ultraviolet–sensitive Rh3, and R8 cells express blue-sensitive Rh5. In "yellow" ommatidia, R7 cells express the ultraviolet opsin Rh4, and R8 cells express the green-sensitive Rh6. In the DRA both R7 and R8 cells express ultraviolet-sensitive Rh3 (Fortini and Rubin, 1990; Wernet et al., 2003).

In wild type flies, different ommatidial subtypes are randomly distributed, whereas in *ss* mutants all ommatidia (apart from the DRA) acquire "pale" ommatidial fate. Ectopic expression of *ss* during mid-pupation is sufficient to induce the "yellow" fate (Wernet et al., 2006). *ss* is expressed at 50% pupation in R7 cells. The ommatidial levels of expression of *ss* vary across the eye. In a model suggested by Wernet et al. in 2006, retinal mosaic is established in two steps. First, stochastic levels of expression of *ss* determine the "pale" or "yellow" fate in R7 cells. Second, the R7 cell instructs the

fate of the R8 cell in the same ommatidial cluster, thus *ss* is necessary and sufficient for the determination of the retinal mosaic. (Wernet et al., 2006).

1.7.6. *ss* in dendrite morphogenesis in the embryonic PNS

In the PNS, dendritic arborisation (da) neurons are responsible for thermosensory, nociceptive, and rhythmic locomotory functions (Ainsley et al., 2003; Liu et al., 2003; Tracey et al., 2003). da neurons have branched and complex dendrites. da neurons can be subdivided in four categories, in order of increasing dendritic complexity: class I, II, III, and IV. da dendritic complexity is predictable and characteristic. Class I and II are relatively simple in branching. Class III contain F-actin-rich dendritic filopodia distributed about the dendritic tree. Class IV da neurons have extensive branching, and dendritic branches are longer than the other subtypes (Grueber et al., 2002).

ss is expressed in the four da subtypes. Interestingly, in *ss* mutants da dendritic diversity is reduced. In absence of *ss*, class I and II da neurons show increased branching, whereas in class III and IV branching and complexity are reduced. In class III da neurons the actin-rich dendritic spikes are also absent (Kim et al., 2006).

1.8. *Ahr* in the worm *C. elegans*

C. elegans Ahr (Ahr-1) shares a 38 % amino acid identity with the human homologue. Ahr-1 contains the bHLH, PAS-A and PAS-B domains. It also interacts physically with the homologue of Arnt (Aha-1) to bind XRE motifs. Like Tgo, Aha-1 is not constituvely nuclear, instead it requires dimerization with a partner to remain nuclear (Powell-Coffman et al., 1998). Velocity sedimentation analysis show that Ahr-1 is not able to bind to ligands such as TCDD and BNF, indicating that Ahr-1 activity might be ligand-independent (Butler et al., 2001). Ahr-1 binds to human chaperon

hsp90 in *in vitro* coimmunoprecipitation assays, however, *C. elegans* homologue of hsp90 is not involved in Ahr-1 functions. Mutations in Ahr-1 indicate a role in neuronal development and feeding behaviour relative to ambient oxygen concentration (Huang et al., 2004; Qin and Powell-Coffman, 2004). *ahr-1* is expressed in early stages of embryonic development. By the first larval stage many cell express *ahr-1*, including different subtypes of neurons (Qin and Powell-Coffman, 2004).

1.9. *Ahr* in the soft shell clam *M. arenaria*

The soft shell clam homologue of *Ahr* (referred here as *clam-ahr*) has been cloned. The clam-ahr protein has bHLH, PAS-A and PAS-B domains, and as Ahr-1 and Ss it fails to bind TCDD or BNF in *in vitro* assays. Expression analysis by RT-PCR showed that the *clam-ahr* gene is expressed in the seven tissues examined (adductor muscle, digestive gland, foot, gill, gonad, mantle and siphon). The role of *clam-ahr* in the development of molluscs is to be determined (Butler et al., 2001).

1.10. The use of invertebrates as models for human research

The worm *Caenorhabditis elegans* and the fruit fly *Drosophila melanogaster* are two of the most widespread experimental systems in biology research. Work in *C. elegans* and *D. melanogaster* has made great contributions in genetics and developmental biology. Nevertheless, the fruit fly stands out as a better experimental system for human research given its phylogenetic position and its mode of development. Also, in *C. elegans*, organ growth does not depend on cell proliferation, and the nervous system has a very singular structure (Dahmann, 2008).

Drosophila was first used as a model animal in the beginning of the 20th century for the study of evolutionary biology. Soon it became an invaluable tool in different

aspects of biology research due to its simplicity of culturing and low maintenance cost (Dahmann, 2008). About 75% of genes related to a human disease are present in the fruit fly (Reiter et al., 2001) and about a third of these genes still show homology in *Drosophila* when the scoring stringency indicates functional conservation (Fortini et al., 2000).

Given the high degree of gene conservation, *Drosophila* has been successfully used to approach different questions in human genetics. In vertebrates, genetic redundancy is greater than in flies, making it difficult to obtain an overt phenotype for a specific mutation, and therefore the contribution of that mutation in a medical condition. On the other, in flies, phenotypes are very sensitive to gene dosage (Muller and Kaplan, 1966). making it easier to identify the role of a gene in a disease with a complex genetic background.

In the following sections, I will describe briefly some of the most common genetic tools used in the work in Drosophila, and how they can be employed in human disease research.

1.10.1 Balancer Chromosomes

"Balancer chromosomes are what set fly genetics apart from genetics in all other organisms" (quoting Ralph J. Greenspan (Greenspan, 2004)).

Balancer chromosomes are multiply inverted chromosomes that are very unlikely to undergo recombination with a homologue (Greenspan, 2004; Muller, 1918). They also contain several dominant and recessive markers that make them easy to genotype, and are often lethal in homozygosis (Greenspan, 2004). Thanks to balancer chromosomes specific homozygous lethal mutations can be kept in perpetuated heterozygous stocks where all the siblings have the same genotype, i.e. mutant allele/balancer.

For instance homozygous lethal alleles of the tumor suppressor *salvador* (*sav*), such as *sav1*, can be kept in stocks balanced with *TM3 Ser* (a third chromosome balancer with the dominant marker *Serrate*, which shows indentations in the wing margin). In this way, a stock *sav1/TM3 Ser* will never give homozygous offspring because both *sav1/sav1* and *TM3/TM3* individuals will die (Figure 1.7).

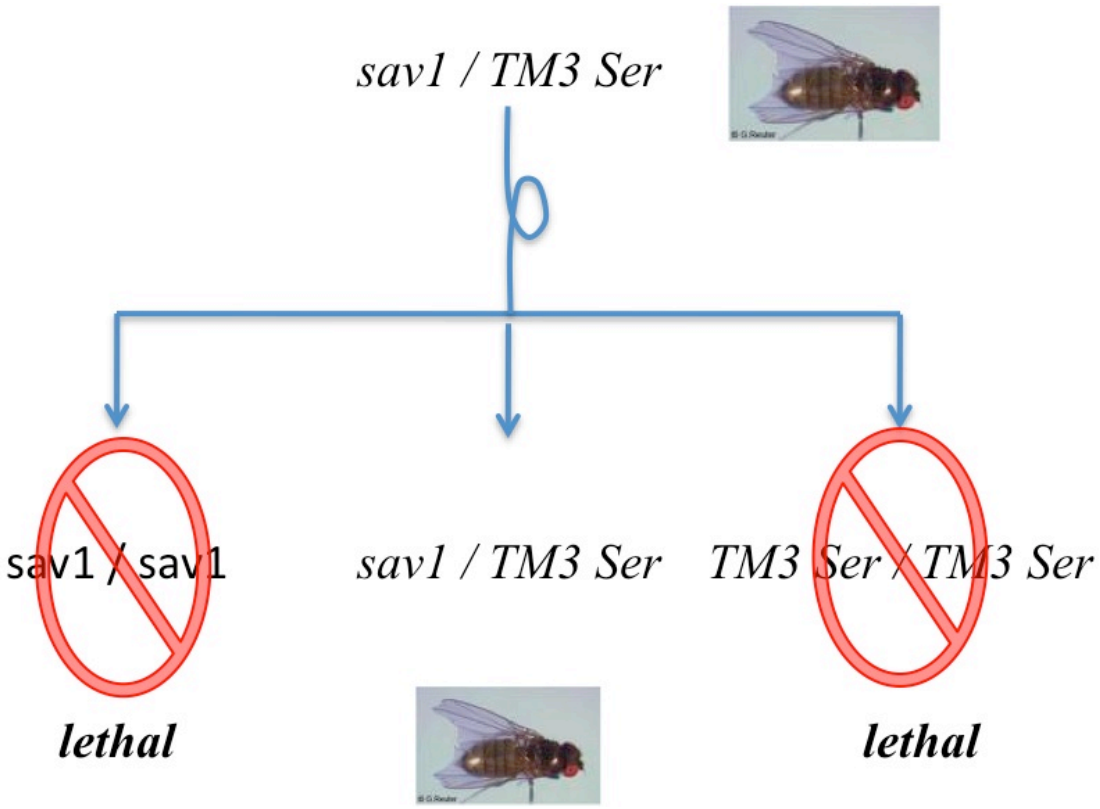

Figure 1.7. Balancing a lethal mutation. A lethal allele of *sav1* can be kept in a perpetuated fly strain. Either *sav1*$^{-}$ or the balancer *TM3Ser* are homozygous lethal. The only viable genotype is the trans-heterozygote *sav1*$^{-}$*/TM3Ser*. Segregation of the balancer chromosome can be tracked by the presence of the phenotypic marker *Serrate* (*Ser*). *Ser* flies have characteristic indentations in the wing margin.

1.10.2. Gain of function assays

In *Drosophila* it is possible to over-express a specific gene in its own pattern or in a new pattern (ectopic expression) by using the *UAS/Gal4* system, also called gain of function assay (Greenspan, 2004). It uses the yeast transcription factor *Gal4* downstream of a known promoter. Gal4 protein targets *UAS* sites that have been inserted upstream of a given transgene (Figure 1.8.A) (Brand and Perrimon, 1993; Fischer et al., 1988).

The *UAS/Gal4* system has been used in genetic screens on the search for negative regulators of the cell cycle. For instance, ectopic expression of the cdk inhibitor (CKI) *dacapo* (*dap* (de Nooij et al., 1996)) or its human homologue *CKIp21* (de Nooij and Hariharan, 1995) driven by *eyeless-Gal4* (*ey-Gal4* (Hauck et al., 1999)) gave rise to smaller adult eyes when compared with wild-type flies (Figure 1.8.A and B). The size of the eye imaginal discs was also reduced (Tseng and Hariharan, 2002). *ey-Gal4* is expressed in eye imaginal disc during early larval development, when cells are proliferating (Hauck et al., 1999). This shows that both *Drosophila* and human negative regulators of the cell-cycle are able to inhibit cell proliferation in eye development, indicating high degree of conservation in the mechanisms of control of cell growth (Tseng and Hariharan, 2002).

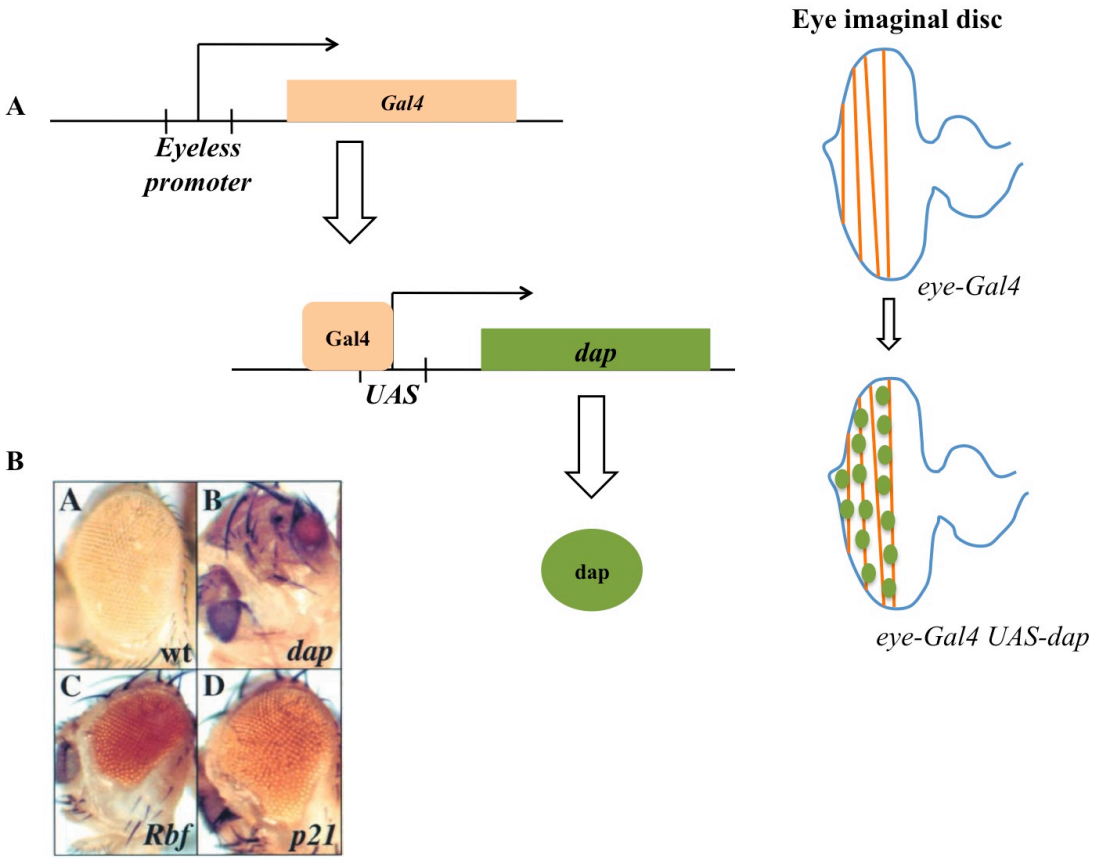

Figure 1.8. Gain of function assays. A. The Gal4 protein is expressed under the control of the promoter of *eyeless* (expressed in the eye imaginal disc, orange bars). Gal4 targets *UAS* sites to activate the expression of the transgene *dap* (green circles). **B.** Ectopic expression of *dap* or its human homologue *p21* led to a reduction in eye size. Image was obtained from Tseng and Hariharan, 2002.

1.10.3. Mosaics

One of the main advantages in *Drosophila* is that mitotic clones of cells homozygous for a given mutation can be generated during development, so the adults are a mosaic composed of mutant clones coexisting with wild-type cells (Figure 1.9.A) (Dahmann, 2008). The analysis of clonal mosaics allows the study of mutations that are embryonic or larval lethal (Blair, 2003) allowing the study of genes that give mutant cells a growth advantage compared to normal cells; one of the main characteristics of cancer (Brumby and Richardson, 2005).

Nowadays, one of the most common ways to induce mosaics is FRT-mediated recombination between the arms of homologous chromosomes (Figure 1.9.A). This consists of a system derived from yeast: targeted DNA recombination at *FLP recombinase* (*FLPase*) *recombination targets* (*FRTs*) (Blair, 2003). The *FLPase* gene is driven by a temperature sensitive promoter (heat shock), which activates *FLPase* expression at 37^{o}C. FLPase drives recombination between two *FRT* sites located in the same position on homologous chromosomes. If a mutation of interest is in the same arm, one of the daughter cells of a cell undergoing recombination will be homozygous for the mutation (Figure 1.9.A) (Blair, 2003; Golic and Lindquist, 1989). This system has the advantage that the researcher can control the period in development in which the mitotic clones are generated, so the rate of recombination is sufficient but low enough as to support lethal mutations. In other words, the researcher can control the extent of the mutant clones in the animal's body.

Clonal analysis has been widely used to study the cellular response to mutations in tumor suppressor genes, when mutant cells coexist with wild-type cells; a context that resemble cancer development (Brumby and Richardson, 2005). For instance, mitotic clones homozygous mutant for the gene *tuberous sclerosis complex 1* (*tsc1*) exhibit increased cell size when compared to the neighboring cells (Figure 1.9.B)

(Tapon et al., 2001). Interestingly, *tsc1* is homologue of the human tumor suppressor gene *TSC1* (Tapon et al., 2001; Young et al., 1998). Mutations in *TSC1* also cause a rise in cell size, what is associated with the development of tuberous sclerosis (Young et al., 1998); consisting of tumorous growths in many tissues such as brain, skin and kidneys (Gomez, 1988).

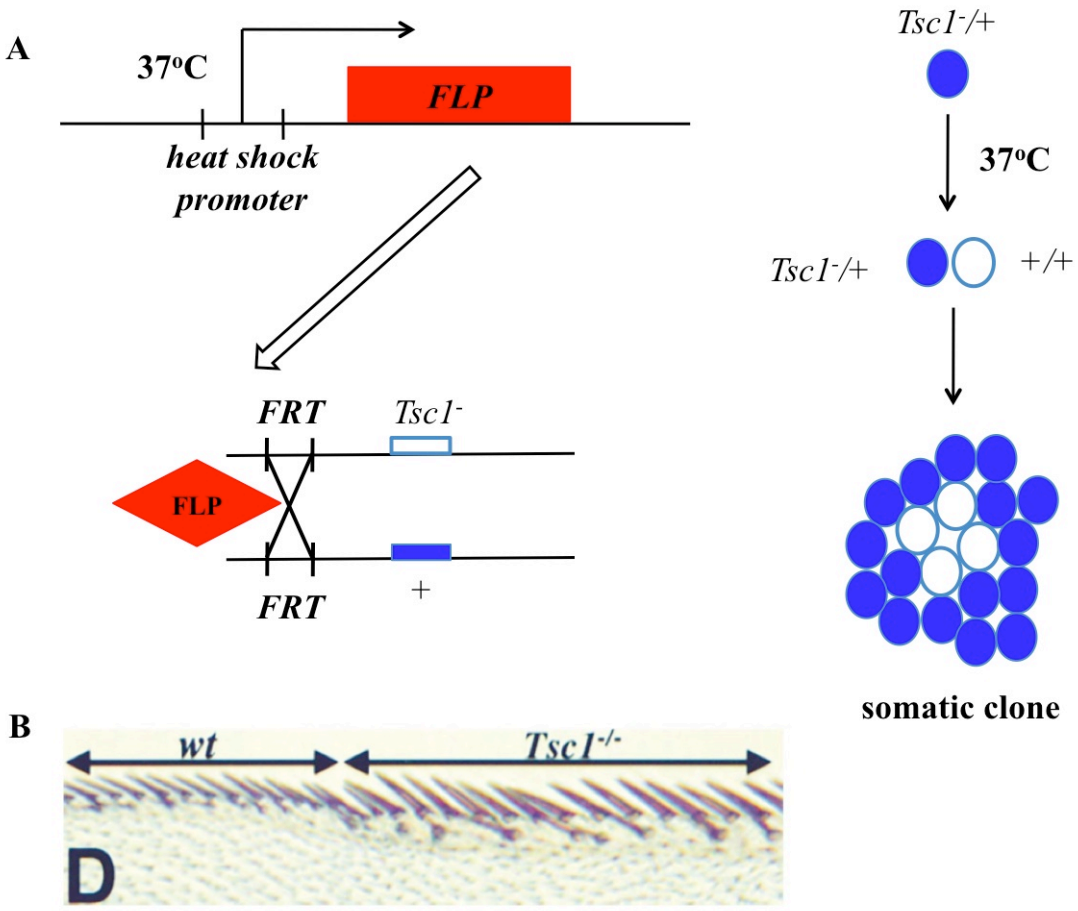

Figure 1.9. Mosaic analysis. A. FLPase is expressed when the individuals are incubated at 37°C. FLPase targets FRT sites, which in turn undergo recombination. As a result, a clone *TSC1*$^{-/-}$ is formed. **B.** Mosaic analysis of *TSC1* mutant clones show that *TSC1* defective cells overgrow when compared to wild type cells. Picture was extracted from Tapon et al., 2001.

1.11. Objectives of this thesis

There is a vast amount of research on the physiological conditions caused by TCDD toxicity in mammals and the implication of Ahr on these. However, it remains unknown to what extent dioxins interfere with the developmental functions of Ahr, in other words, whether dioxin toxicity might be understood as a gain or loss of function of endogenous Ahr activity. From this perspective, three scenarios can be considered. First, TCDD might enhance Ahr's activity acting as a hypermorphic version of the ligand free Ahr. Second, TCDD might inhibit endogenous Ahr activity leading to a lack of function. Binding affinity for the XRE motif and molecular partners such as Arnt might decrease, leaving them free for other competitors to bind. Third, Ahr might act by different means in the presence of TCDD; this would be better understood as a neomorphic transformation of Ahr activity.

Most of work in the field has been conducted in perpetuated cell lines. These systems have been highly useful in understanding the physiological response to TCDD. However, the development of a disease depends on the interaction between different cell types. For instance, in tumorigenesis, the interactions between the tumour and a specific microenvironment are important for the development of the disease (Bissell and Radisky, 2001). For this reason, in cancer research it is crucial to develop systems in which self-sufficiency and growth signals, cell-death and anti-proliferative signals, and tissue invasion can be studied (Brumby and Richardson, 2005).

The use of vertebrate systems is ideal given the physiological similarities with humans. However, the number of genetic assays that can be performed in these systems is limited given the life cycle, the high cost of maintenance and the low number of offspring. On the other hand, several comparative studies have shown a high degree of conservation of human disease genes in the fruit fly genome (Fortini et al., 2000; Reiter et al., 2001). *Drosophila* offers a multicellular system in which it is easy to conduct

genetic assays and that has been used in the past to approach the molecular basis of certain medical conditions (Bier, 2005; Brumby and Richardson, 2005).

The issues addressed in this work can be summarized in the following points:

- The degree of functional homology between Ahr and Ss. I aim to shed some light on the degree of conservation on the mechanisms of action of Ahr signaling. To do this I will test the ability of Ahr to fulfill Ss functions in the fruit fly and whether they undergo the same cellular and molecular interactions. The data regarding this point will be shown in the third chapter.
- Dioxins as disruptors of Ahr endogenous functions. I will express *Ahr* in a purely developmental context and I will analyze the effects of TCDD exposure over Ahr's endogenous activity. This will be addressed in chapter 4.
- New elements in Ss and Ahr signaling. In chapter 5 I will describe the results of a systematic screen performed on the search for genes that interact with *ss*. I will test the ability of the obtained candidates to interact with Ahr, in doing so I will also bring some knowledge in the mechanisms of action of Ss.
- What can we learn from the fruit fly? In the sixth chapter (discussion) I will build up a new model of dioxin toxicity. This will be based on the effect of TCDD on the delicate balance between detoxification and endogenous functions of Ahr. I will also show other mechanisms of regulation of Ahr activity and constitutive molecular features that remain conserved in Ss.

Chapter 2

Material and Methods

In this chapter I describe all the material and experimental protocols used to obtain the results shown in the following chapters.

2.1. Preparation and maintenance of Fly stocks

Fly stocks were kept in plastic tubes at 18^{o}C on a modified Lewis medium containing yeast, agar, cornmeal and glucose with Nipagen (Lewis, 1960) . Stocks were transferred to new tubes every three weeks. In order to facilitate the collection of virgins, tubes were incubated at 25^{o}C during the day and at 18 ^{o}C during the night. Virgins were collected twice a day, first time in the morning and in the evening. Experiments with flies were carried out at 18^{o}C, 25^{o}C, or 29^{o}C, unless specified, depending on the experimental requirements.

For dioxin exposure experiments flies had to be fed TCDD. In this case, food tubes were melted in a microwave and left to cool down for 10 min. TCDD was diluted

in water to make a stock solution of 0.01 mg/ml. 0.25 ml of the stock solution were added per tube for a final concentration of 200 ng TCDD/g food and 0.5ml for a final concentration of 400 ng TCDD/g. Food was allowed to solidify over night. Next morning, fly crosses were transferred to the dioxin-food. All the dioxin handling procedures were done in an extraction fume-hood, where the temperature was kept between 21-27^{o}C.

2.1.1. Fly stock genotypes

The following table shows a list of stocks used in this thesis detailing genotype and source.

Table 2.1

Stock name	**Genotype**	**Source**
AB1-Gal4	*y^{1}w*; AB1-Gal4*	1
ta5-lacZ	*w; BB2.4-lacZ*	T. Kojima
dac^{-}	*w; dac^{3} FRT40A/CyO*	J.P. Couso
Df(3L)BSC14	*Df(3L)BSC14, rho p e/ TM3, Ser*	1
Df(3L)Delta1AK	*Df(3L)Delta1AK ru h ry sr e ca/ TM3, ry^{RK} Sb Ser*	1
Df(3L)ED4470	*w;; Df(3L)ED4470, w^{+}/ TM6C, cu Sb*	1
Df(3L)Exel6115	*w;; Df(3L)Exel6115,w^{+}/ TM6B, hu Tb*	1
Df(3L)HD1	*w;; Df(3L)HD1/ TM3, Sb Ser*	1
Df(3L)Ten-m-AL29	*Df(3L)Ten-m-AL29/ TM3, ry^{RK} Sb Ser*	1
Df(3L)vin2	*Df(3L)vin2 ru h gl e ca/ TM3, Sb*	1
Df(3L)vin5	*Df(3L)vin5, ru h gl e ca/ TM3, Sb Ser*	1
Df(3L)vin7	*Df(3L)vin7, h gl e ca/ TM3, Sb Ser*	1

Df(3R)07280	*Df(3R)07280/MKRS*	1
Df(3R)BSC24	*Df(3R)BSC24, st ca/ TM3, Ser*	1
Df(3R)BSC38	*Df(3R)BSC38, st ca/ TM2, p^p*	1
Df(3R)BSC42	*Df(3R)BSC42, st ca/ TM3, Sb*	1
Df(3R)Cha7	*Df(3R)Cha7, red/ TM6B, hu Tb*	1
Df(3R)DG2	*Df(3R)DG2/ TM2, red*	1
Df(3R)Dl-Bx12	*Df(3R)Dl-Bx12, ss^1 e ro/ TM6B, hu Tb*	1
Df(3R)ED5331	*w;;Df(3R)ED5331, w^+/ TM6C, cu Sb*	1
Df(3R)ED5339	*w;;Df(3R)ED5339, w^+/ TM6C, cu Sb*	1
Df(3R)ED5495	*w;;Df(3R)ED5495, w^+/ TM6C, cu Sb*	1
Df(3R)ED5911	*w;;Df(3R)ED5911, w^+/ TM6C, cu Sb*	1
Df(3R)ED5942	*w;;Df(3R)ED5942, w^+/ TM6C, cu Sb*	1
Df(3R)Ed6025	*w;;Df(3R)ED6025, w^+/ TM6C, cu Sb*	1
Df(3R)Exel6155	*w;;Df(3R)Exel6155, w^+/ TM6B, hu Tb*	1
Df(3R)Exel6183	*w;;Df(3R)Exel6183, w^+/ TM6B, hu Tb*	1
Df(3R)Exel6184	*w;;Df(3R)Exel6184, w^+/ TM6B, hu Tb*	1
Df(3R)Exel6185	*w;;Df(3R)Exel 6185, w^+/ TM6B, hu Tb*	1
Df(3R)Exel6265	*w;;Df(3R)Exel6265, w^+/ TM6B, hu Tb*	1
Df(3R)H-B79	*Df(3R)H-B79, e*/ TM2*	1
dpp-Gal4 (strong)	*w; wg^{Sp-1}/CyO; $dppGal4^{blk1}$/ TM6B, hu Tb*	T.Klein
dpp-Gal4 (weak)	*w;; Ser^{94C} dppGal4/ TM6B, hu Tb*	1
FRT82B $sqz^{1.e}$	*w; FRT82B cu $sqz^{i.e}$/ TM6B, hu Tb*	2
GMR-Gal4	*w;; GMR-Gal4*	1
GMR-Gal4 UAS-ssC2	*w; UAS-ssC2, w^+/SM6a-TM6B/ GMR-Gal4, w^+*	S. Bishop

hs-Gal4	*w; HSP70-Gal4 PB*	1
l(3)02102^{021012}	*ry^{506} P[PZ]l(3)021012^{021012}/ TM3 ry^{RK} Sb Ser*	1
l(3)03675^{03675}	*ry^{506} P[PZ]l(3)03675^{03675}/ TM3 ry^{RK} Sb Ser*	1
ms(3)98B^{6302}	*ry^{506} P[PZ]m(3)98B^{06302}/ CxD ry^{BW}*	1
ptc-Gal4 UAS-EGFP	*w; ptc-Gal4/SM6a-TM6B/UAS-eGFP*	I. Pueyo
rn-Gal4(13)	*w; rn-Gal4(13)/ TM3 Sb fz-lacZ*	S. Thor
rn-Gal4(13) ss^{sta}	*w; ru rn-Gal4(13) cu ss^{sta}/ TM6B hu Tb*	2
rn-Gal4(5)	*w; rn-Gal4(5)/ TM3 Sb fz-lacZ*	S. Thor
rn-Gal4(5) ss^{aBr}	*w;; rn-Gal4(5) ss^{aBr}/ TM3, Ser GFP*	S. Bishop
sqz-lacZ	*ry^{506} P[PZ]l(3)021012^{021012}/ TM3, ry^{RK} Sb Ser*	1
sqz^{Df}	*Df(3R)Dl-kx23, e*/TM3, Ser*	1
sqz$^{i.e}$	*w; sqz$^{i.e}$/ TM6B, hu Tb*	S. Thor
ss^{aBr}	*red^{1} ss $^{aBR30-71}$ e^{1}/ TM3, Sb*	I. Duncan
ss^{sta}	*Dp(1;3)ss^{sta}/ TM6B, hu Tb*	I. Duncan
tgo^{-}	*tgo^{5} FRT82B/ TM6B, hu Tb*	S. Crews
UAS-Ahr-eGFP G2	*w; UAS-Ahr-eGFPG2/ (CyO)*	I. Galindo
UAS-AhrH1	*w; UAS-AhrH1*	I. Galindo
UAS-AhrH1; ss^{sta}	*w; UAS-AhrH1/(CyO); Dp(1;3)sta/ TM6B, hu Tb*	I. Galindo
UAS-Arnt5.2	*w; UAS-Arnt5.2/CyO*	2
UAS-GFP (II)	*w; UAS-GFP.S65T T2*	1
UAS-GFP (III)	*w;; UAS-GFP.S65T T10*	1
UAS-rn1a	*w; UAS-rn1a/ CyO*	S. Thor

UAS-sqz7.2	*w; UAS-sqz7.2/ (CyO)*	S. Thor
UAS-ss-eGFP 32.1	*w; UAS-ss-eGFP 32.1/ TM6B, hu Tb*	I. Galindo
UAS-ssC2	*w;; UAS-ssC2*	I. Duncan
UAS-ssC3	*w;; UAS-ssC3*	I. Dunacn
UAS-tgo	*w; UAS-tgo/CyO*	S. Crews
WT	*Or-R*	1

*Stocks requested from Bloomington or generated by myself are denoted as 1 and 2, respectively.

2.1.2. Injection of transgenics

Transgenic lines were generated by injection of freshly purified plasmid DNA at a concentration of 500 ng/µl into embryos w^{118} (which give rise to flies with white eyes) by Vanedis (www.vanedis.no). The plasmid contained a copy of the gene *white* (*w*), which gives color to the adult eye. Single G_0 flies were separately crossed with the balancer stock *w; CyO/If; TM6B/MKRS*, and transgenic flies were selected in F_1 according to their eye colour. Insertions were mapped and balanced again using the same balancer stock by following standard chromosomal markers.

2.2. Adult cuticle preparations

Pharates and eclosed adults were kept in SH medium (ethanol 100%:glycerol, 3:1; v/v) prior to mounting. They were rinsed with ethanol several times to remove traces of glycerol. Head and abdomen were pulled from the thorax using forceps. Samples were washed twice with water, incubated for 5 minutes at 60^{o}C in NaOH 1M, washed again with water and cooked in Hoyer's medium (Hoyers: lactic acid, 1:1; v/v) for 20 min at 60^{o}C. Finally the different body parts were mounted in Hoyer's medium. In this last step, legs were separated from the rest of the thorax.

Adult cuticle preparations were observed under the Leica DMRB optical microscope, and the pictures were taken with one of the following softwares: Q-win or Simple PCI 6.6.

2.3. Collection and fixation of imaginal discs

Mid to late third instar larvae were collected from the food surface and tube walls. They were placed into a glass well with cold PBS1x (PBS10x: 0.01M KH2PO4, 0.1M Na2HPO4, 1.37M NaCl, 0.0227M KCl; pH7.4). Larval stages were sorted according to their sizes, posterior spiracles, and mouthparts. Larvae were dissected under the dissecting microscope using a pair of forceps. To dissect them, the posterior third of the larvae was removed, and cuticle was turned inside out by pressing in the mouthparts. In this way imaginal discs are left exposed. The dissected larvae were placed in 0.5 ml eppendorf tubes (about 7-10 larvae per tube) and fixed at room temperature (RT) for 10 min in 4% paraformaldehyde (PFA). Larvae were then rinse with PBS1x and incubated twice for 10 min in PBS1x at RT. At this point larvae were used straight away for immunocytochemistry or detection of β-galactosidase activity, or kept at -20^{o}C in methanol. Ethanol 70% was used instead of methanol if the sample was used to visualize expression of GFP.

2.4. Detection of β–Galactosidase activity in imaginal disc

Dissected larvae were washed twice with PBTx (0.03% Triton x-100 in PBS1x) after fixation or incubation at -20^{o}C in ethanol. Then, they were washed once for 15 min in PBS prior to incubation in X-Gal at 37^{o}C. Discs were checked periodically for the presence of β–Galactosidase activity (blue staining). Larvae were washed twice in PBS for 15 min to remove X-Gal. CNS and imaginal discs were pulled from the cuticle and

mounted in Aqua Polymount (Polysciences cat£18606). Discs were observed under the Leica DMRB optical microscope, and the pictures were taken with one of the following softwares: Q-win or Simple PCI 6.6.

2.5. Antibody staining of imaginal discs

Larvae were collected and fixed as described in section 2.3. Samples stored at -20^{o}C were rinsed in PBTx, washed in PBTx for 20 min, and then blocked in PBTA (0.4% Bovine Albumine in PBTx) for 20 min. Primary antibodies were diluted in PBTA to a dilution given in table 2.2. Samples were incubated overnight at 4^{o}C in the primary antibody. If a second primary antibody was needed, the first one was washed twice in PBTA for 20 min, and then the samples were incubated with the second primary for three hours at RT. Samples were washed twice in PBTA for 20 min, incubated in the secondary antibody for two hours, washed again twice in PBTA for 20 min and incubated in the tertiary antibody, if needed. Otherwise, the samples were washed for 20 min in PBTx, 20 min in PBTx with DAPI (1:80000), and twice in PBS. Samples were kept in the dark after addition of fluorescent conjugated secondary antibodies. Finally, the samples were mounted in Vectashield mounting media by pulling the imaginal discs from the brain and cuticle. Fluorescence pictures were taken in a Zeiss Axiovert confocal microscope equipped with a LSM520 Meta.

Table 2.2. Antibodies used in this work.

antibody	organism	staining	western-blot	provider
Primary				
Bar	rabbit	1:20	-	Kojima
Dac	mouse	1:200	-	DSHB
Tgo	mouse	1:10	-	DSHB
GFP	mouse	-	1:1000	Roche
Rn	rabbit	-	1:400	D. del Alamo
Secondary				
mouse-biotin	donkey	1:200	-	Jackson
rabbit-rho	donkey	1:100	-	Jackson
mouse-HRP	goat	-	1:5000	St. Cruz
rabbit-HRP	swine	-	1:2000	DAKO
Tertiary				
streptavidin-FITC	-	1:200	-	Vector

2.6. Preparation of adult eyes

To take the pictures of the eye of the adults, flies were put to sleep with CO2 and placed under a dissecting microscope (Leica MZ75). Pictures were captured with the software Leica FireCam. Some flies were prepared for the Scanning Electron Microscope (SEM). These flies were dehydrated by washing for 10 min in 70%, 80%, 90%, and 100% ethanol, and finally washed twice for 10 min in hexamethyldisilazane. Then samples were left to dry for an hour before they were mounted and coated with a thin layer of gold. Eyes were scan in a Leo420 Steroscan SEM.

2.6.1. Estimation of bristle size

SEM pictures taken at 1000x were analyzed by the imaging program Image J. Sections of the 500 x 200 pixels from the dorsal part of the eye were cropped. The resulting image was binarized using an appropriate threshold of brightness to isolate the bristles from the rest of the ommatidia. The background was removed by eroding once. The effect of the erosion on bristle size was corrected by dilating once. The size of each bristle was estimated by the number of covered pixels (Figure 2.1). The output data below 80 pixels or above 300 pixels were discarded to remove any artefacts caused by the background. These limits were determined empirically. Between five and ten eyes were observed per sample. The data of each sample was analyzed using the program SPSS. The data did not show a normal distribution, therefore I compared the samples in pairs using the non parametric test of Mann-Whitney U (Mann and Whitney, 1947).

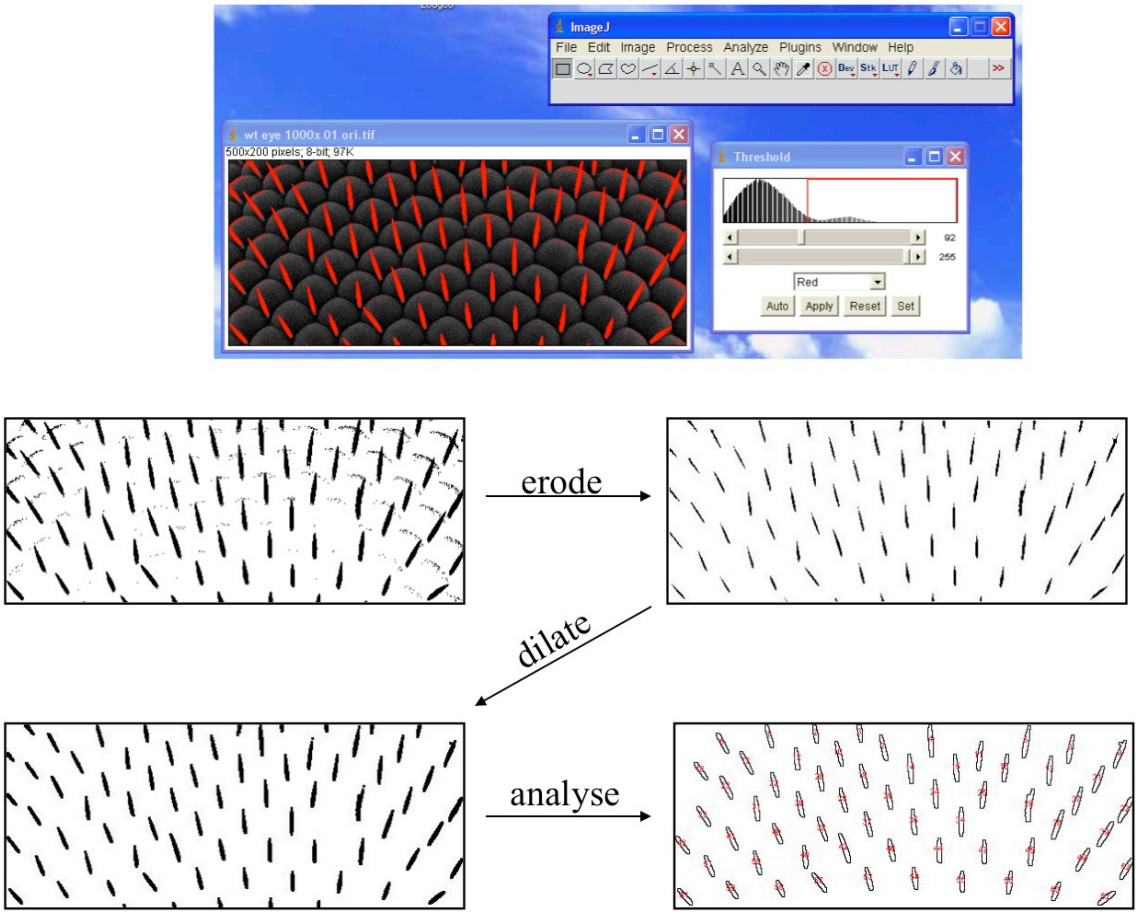

Figure 2.1. Estimation of eye bristle size using Image J. Areas of 500x200 pixels from 1000x SEM images of adult eyes were cropped, and binarised. The resulting pictures were eroded to remove background, dilated to correct the effect of the erosion, and analyzed. The number of pixels covered by bristle was used to estimate the bristle size.

2.7. Clonal analysis

sqz mutant somatic clones were generated by mitotic recombination induced by the FRT/FLPase system (Golic and Lindquist, 1989). Females of a line *y FLP9P; FRT82B CD2* y^+ *min/TM6B, hu Tb* were crossed with males *w; FRT82B* $sqz^{i.e}$*/TM6B, hu Tb*. Heat shock was induced at 37°C for 40 min at about 50 hours A.E.L. (after egg lying). From the offspring, males with the genotype *y FLP9P; FRT82B CD2* y^+ *min/ FRT82B* $sqz^{i.e}$ were selected following the absence of the phenotypic markers of the balancer chromosome *TM6B*. Clones were detected by *yellow* (*y*) phenotype, which consists of lack of pigmentation. Notice that clones could not be visible in females as they are heterozygous for the recessive phenotypic marker *y*.

2.8. Balancer Chromosomes

Balancer chromosomes are used to keep populations of flies in which all the individuals are heterozygous for a lethal mutation. Balancers prevent recombination between homologous chromosomes and have dominant phenotypic markers that are easily tractable. Such a markers affect negatively the reproductive fitness when carried homozygously (see section 1.10.1 and Figure 1.7) (Greenspan, 2004).

In the following table I have listed the balancer chromosomes more frequently used in this work.

Table 2.3 . Balancer chromosomes used in this work.

Balancer	Chromosome	Markers	Phenotype
CyO	Second	CyO (Curly O)	Posterior part of the wing is bent upwards.
TM6B	Third	Tb (Tubby) and Hu (humeral)	Tb: pupae and larvae are shorter Hu: extra humeral bristles in the adult

TM3 Ser	Third	Ser (Serrate)	Idented wing margins
TM3 Sb	Third	Sb (Stubble)	Shorther and thicker macrochaetea

2.9. Cloning tools.

2.9.1. Polymerase Chain Reaction (PCR)

PCR reactions were performed on an Eppendorf Mastercycler Gradient thermocycler, using the Expand Long Template PCR System (Roche cat# 1681834) or the Taq PCR Core Kit (QIAGEN cat# 201223) following the manufacturer's instructions. Each PCR reaction was optimized according to the characteristics of the primers being used (length and C-G composition), and the length of the expected DNA fragment.

2.9.2. Purification of PCR products

PCR products were purified before cloning in order to remove all the PCR reagents. Purification was carried out using the QIAquick PCR Purification Kit (QIAGEN cat# 28106) following the manufacturer's instructions. This protocol first binds DNA to a silica filter, then several washes remove small oligonucleotides and PCR reagents. Finally DNA is eluted in DEPC-treated H_2O.

2.9.3. Agarose gel electrophoresis

Quantification and separation of DNA fragments was performed by agarose gel electrophoresis. Gels were made of 0.8% agarose in TBE1x (TBE10x: 89 mM boric acid, 2 mM EDTA). 0.5 μg/ml of ethidium bromide was added for visualisation of the DNA under UV light. A mass ruler DNA ladder (Fermentas cat#SM0403) was used to determine the molecular weight of DNA bands.

2.9.4. Extraction of DNA from agarose gels

In order to extract DNA fragments of a particular length from a pool of other fragments, the specific DNA bands were cut with a razor from the agarose gel on an UV transilluminator at 365nm. Gel slices were placed in 1.5 ml centrifuge tubes and weighed for purification. Purification was carried out by QIAquick Gel extraction kit (QIAGEN Cat# 28706) following the manufacturer's instructions. The samples were analyzed by agarose gel electrophoresis.

2.9.5. Cloning, screening of bacterial colonies and DNA preparations

PCR or restriction digest products were inserted into the specific vectors using the T4 DNA Ligase (Promega cat# M1804) following the manufacture's instructions. 10 μl of the ligation reaction were incubated on ice for 30 min with 50 μl of Transforming One Shot TOP10 Competent *E. coli* cells (Invitrogen cat# k4580-40). Transformation was induced by heat-shock at 42^{o}C for 30 sec. Cells were then incubated with SOC medium (Invitrogen cat# 15544-034) in a shaker at 225 rpm for one hour at 37^{o}C. Finally, transformed cells were plated in agar and allowed to grow overnight. Plates were supplemented with antibiotics to select positive transformants. The antibiotic used depends on the vector (table 2.4).

In order to isolate and amplify plasmid DNA from bacterial colonies that had grown successfully, minipreparation was performed using the QIAprep Miniprep Kit (QIAGEN cat# 27106) according to the manufacturer's instructions. When a greater yield of DNA was required, midipreparation was carried out using the QIAfilter Plasmid Purification Kit (QIAGEN cat# 12243).

Cloning in the pCR4-TOPO vector was carried out using the TOPO TA Cloning Kit (Invitrogen cat# k4575-02) following the manufacturer's instructions.

Table 2.4. Vectors and antibiotic selection used in this work.

Vector	Antibiotic resistance	Provider
pCR4-TOPO	kanamycin, ampicillin	Invitrogen
pEGX-2T	ampicillin	GE Healthcare
pUASt	ampicillin	Fisher, 1988
pOT2	chloranfenicol	BDGP
pcMV-Sport6	ampicillin	Gene Service

2.9.6. Sequencing

Sequencing was done by MWG Biotech (www.mwg-biotech.com). Sequencing reactions were sent as 2μg of plasmid DNA in 5mM Tris HCl, pH 8.5. Primers used are listed in appendix I. Sequences were checked using the SeqMan program (DNA star package).

2.10. DNA Constructs

In the following section I describe the cloning of the transgenic constructs that I have employed in this work. *pOT2-tgo* was obtained from the *Drosophila* Gold Collection from the BDGP (Berkeley *Drosophila* Genome Project (Stapleton et al., 2002)), identified as clone LD32037. Dr. Ibo Galindo generated the constructs *pUASt-Ahr, pUASt-Ahr-eGFP* and *pUASt-ss-eGFP*. I made the rest of the constructs. Maps of the following constructs are shown in the appendix II.

2.10.1. *pUASt-Ahr* and *pUASt-AhrGFP*

pEGFP-Ahr (kindly provided by Dr. P. Fernandez-Salguero) was digested with NheI and BglI to extract the whole *eGFP-Ahr* coding sequence, and digested with NheI

and XbaI restriction sites to extract *Ahr* coding sequence. Both *eGFP-Ahr* and *Ahr* were then cloned in an XbaI restriction site in *pUASt*. This was possible as NheI and BglI restriction sites generate overhangs that are complementary to XbaI restriction sites.

2.10.2. *pUASt-eGFP-ss*

ss was extracted from *pGEX-2T-ssA1* (kindly provided by Dr. I. Duncan) by PCR. An XbaI restriction site was inserted upstream of *ss* in a tail in the forward primer (appendix I). The *ss* coding sequence was then sub-cloned in an XbaI restriction site in *pBK-eGFP*, leaving *eGFP* ORF in the *ss* N-terminal side. *eGFP-ss* was then cloned in the *pUASt* vector using the NotI and SpeI restriction sites.

2.10.3. *pCR4-TOPO-SDK-Ahr* and *pCR4-TOPO-SDK-ss*

In order to drive the expression of the mouse *Ahr* and *ss* under the control of the T7 promoter in a cell-free translation system (see section 2.13) both genes were cloned in the *pCR4-TOPO* vector, leaving the T7 promoter upstream of the their coding sequence. Mouse Ahr was extracted from *pUASt-Ahr* and *ss* was extracted from *pGEX-2T-ssA1* (kindly provided by Dr. I. Duncan) using the Expand Long Template PCR System. The Kozak sequence was added in a tail in the forward primers (appendix I). The size of the products were verified by DNA electrophoresis (2449 bp for *Ahr* and 2673 bp for *ss*) and purified to remove the PCR reagents. The products were then cloned into the *pCR4-TOPO* vector using the TOPO TA Cloining kit (Invitrogen cat#k4575-02). The orientation of the insert in the positive transformants was checked by PCR using the QIAGEN Taq DNA Polymerase Kit with the T7 primer, and the Ahr and ss reverse primers (appendix I). Minipreparations were done on positive clones, of which several were sequenced. Sequences were verified using the SeqMan program (DNASTAR package). Finally, I did midipreparations for each of the constructs.

2.10.4. *pUASt-Arnt*

Arnt cDNA was extracted from *pCMV-sport6-Arnt* (obtained from Gene Service), identified as clone AV-21A3. Arnt was minipreped and digested with EcoRI and XhoI restriction sites. The digested product was run on an 0.8% agarose gel. A band of the expected size of *Arnt* (2733 bp) was extracted from the agarose and cloned into the *pUASt* vector in the EcoRI and XhoI restriction sites (see appendix II). Several positive transformants were minipreped and then checked by digesting with BamH1. Finally, one of the clones that gave the right band pattern was chosen to do a midipreparation.

2.10.5. *pOT2-Arnt*

In order to express *Arnt* under the contol of the T7 promoter in a cell-free translation system, the cDNA of *Arnt* was cloned into the *pOT2* vector, leaving the T7 promoter upstream of the insert. *Arnt* was extracted from *pUASt-Arnt* and *pOT2* was extracted from *pOT2-tgo*. *pUASt-Arnt* was digested with EcoRI and XhoI restriction enzymes and *pOT2* was digested with EcoRI, XhoI and NdeI. NdeI cuts in the coding sequence of *tgo*, stopping *tgo* from being reinserted in *pOT2* after the digestion (see appendix II). *Arnt* was then cloned into *pOT2* in the EcoRI and XhoI restriction sites. Several positive transformants were minipreped and then checked by digesting with EcoRI and XhoI restriction enzymes. One of the clones that gave the right band pattern was chosen to do a midipreparation.

2.11. Tools for protein interaction assays

2.11.1. Gel casting

SDS-PAGE denaturing gels were casted in pairs with a BioRad Protean II minigel casting system. Gels were made of a stacking phase (0.125M Tris-HCl pH6.8,

0.1% w/v SDS, 4% acrylamide/bisacrylamide, 0.05% w/v Ammonium Persulfate, 0.1% TEMED) and a resolving phase (0.375M Tris-HCl pH8.8, 0.1% w/v SDS, 10% acrylamide/bisacrylamide, 0.05% w/v Ammonium Persulfate, 0.05% TEMED). The volume used for each phase varied depending on the thickness of the gel (0.75mm or 1.5mm). Gels could be kept for several days at 4^{o}C if wrapped in wet filter paper and cling film.

2.11.2. Protein electrophoresis

Electrophoresis was carried out in a BioRad electrophoresis cell (cat#165-2975). The tank was filled with running buffer (0.3% w/v Tris, 1.45% w/v Glycine, 0.1% w/v SDS). Samples were diluted 50% with 2x loading buffer (100mM Tris-HCl pH 6.8, 4% w/v SDS, 0.1% bromophenol blue, 20% glycerol). 5μl of β-mercaptoethanol were added per 40μl of sample before boiling. Electrophoresis was performed at about 30 mA. A protein ladder (BioRad, cat#161-0374) was used to determine the molecular weight of the protein bands.

2.11.3. Protein Blotting

Protein blotting was performed in a BioRad semidry electrophoretic transfer cell (cat#170-3940) following the instructions of the manufacturer. Proteins were transferred to a PVDF membrane in transfer buffer (0.35% w/v Tris-base, 1.5% w/v glycine, 25% methanol, 0.012% w/v SDS). Prior to the blotting, the membrane was washed for one minute in methanol and then in water for an additional minute. Transference was conducted for 1hr at 20V).

Membranes were rinsed several times in PBT (01% Tween-20 in PBS) and incubated overnight at 4^{o}C in 5% milk (5% dry skimmed milk in PBT). Membranes were then incubated with the primary antibody (diluted in milk solution, table 2.2) for an hour at R.T. Membranes were then washed in PBT for 1hr 30 min changing the PBT

every 5-10 min. The secondary antibody (also diluted in milk solution, see table 2.2) was then added for 1hr. The blottings were washed for 1hr 30min in PBT and developed with the chemiluminiscence ECL-Plus detection system (Amersham cat#RPN2132) following the manufacturer's instructions in high performance chemiluminescence films (Amersham cat#90292) using a Konica SRX-101A developer.

2.11.4. Autoradiography

Gels of proteins labeled with S^{35} (see section 2.13) were incubated after electrophoresis in fixing buffer (50% methanol, 10% Acetic acid) for 30 min, and washed in 10% glycerol to avoid cracking during the drying process. Gels were flattened in a piece of filter paper and covered with cling film. Finally, the gels were dried in a vacuum gel dryer for 1hr for 0.75 mm gels and 2hr for 1.5mm gels. Gels were then exposed to a phosphoplate (Molecular Dynamics) overnight, after which, the plate was scanned in a Typhoon Trio scanner (GE healthcare).

2.12. GFP Co-immunoprecipitation assays.

In order to express the GFP quimeric proteins, late-3rd instar larvae *hs-Gal4 UAS-ssGFP*, *hs-Gal4 UAS-AhrGFP* and *hs-Gal4 UAS-GFP* heterozygotes were heat-shocked for 1hr 30 min at 37^{o}C. Immediately after, the larvae were placed in dry ice inside 1.5 ml eppendorf tubes for 30 min. Samples were stored at -80^{o}C until the moment of the extraction. About 100 larvae were collected per sample. For the extraction, 1ml of lysis buffer (50mM Tris-HCl pH8.0, 150mM NaCl, 0.5% Triton x-100, 1 tablet of Roche protein inhibitors per 10ml of buffer cat#04693159001) was added to each sample. Larvae were then mashed with a sterile pestle and kept on ice for 15 min. Samples were then centrifuged for 5 min at maximum speed (13,000 rpm). Supernatant was transferred to a new 1.5 ml tube (50µl of each sample were kept apart

for the “before assay” sample). In order to remove any unspecific binding, the supernatant was incubated with 50µl protein G sepharose beads (GE Healthcare cat#17-0618-01, 50% slurry in lysis buffer) for an hour at 4^{o}C in constant rotation and then centrifuged at maximum speed for 3 min. The supernatant was again transferred to a new 1.5ml tube. The supernatant was incubated with 40µl of mouse monoclonal anti-GFP (Roche, cat#11814460001) for 2 hr at 4^{o}C. In order to precipitate the anti-GFP antibody, the samples were then incubated with 100µl of protein G sepharose (50% slurry in lysis buffer) for 2hr at 4^{o}C and centrifuged at 500g for 5min. The white precipitate was then washed three times in lysis buffer and centrifuged at 500g for 5 min. The final precipitates were then resuspended in 2x sample buffer according to the protocol in section 2.11.2. 15µl of each sample were run in a SDS-PAGE 0.75 mm gel.

2.13. Co-Immunoprecipitation from a cell-free translation system

In order to increase the efficiency of the Co-Ip assays, the protein G sepharose beads were covalently bound to mouse monoclonal antibodies anti-Tgo (Developmental Studies Hybridoma Bank) and anti-Arnt (Thermo Scientific MA1-515). 500µl of beads were washed three times in 500µl PBS and pelleted at 500g for 5 min. The final pellet was resuspended in one volume of PBS with Roche proteinase inhibitors. 30µl of either anti-Tgo or anti-Arnt were incubated with the beads for 1hr at RT in constant rotation. To induce the covalent binding, beads were washed once with 1ml of Borate buffer (0.2M Boric acid pH 9.0), prior to incubation for one hour at RT in Borate buffer with 20µM of DMP (Dimethyl Pimelimidate Dihydrochloride; Sigma cat#D8388). In order to stop the covalent reaction, beads were then washed twice and incubated for 2hr at RT in ethanolamine buffer (0.2M ethanolamine pH8.0, Sigma cat#398136). Beads were

finally washed three times and resuspended in one volume of PBS with proteinase inhibitors.

Midipreparations of the DNA constructs *pCR4-TOPO-SDK-Ahr*, *pCR4-TOPO-SDK-ss, pOT2-Arnt* and *pOT2-tgo* were used to express Ahr, Ss, Arnt and Tgo proteins, respectively, using the rabbit TnT Coupled Transcription/Translation system (Promega cat# L1170) following the manufacture's instructions. Proteins were tagged with methionine labeled with S^{35}.

Protein extracts were mixed according to the interaction assay. Every mix was then filled up to 300µl with RIPA buffer (20mM HEPES pH 7.9, 50mM NaCl, 1%Np40, 0.1%, 1 tablet of Roche protein inhibitors per 10ml of buffer). TCDD was added to a final concentration of 10nM when required. Samples were incubated with 80µl of 50% slurry of protein G sepharose beads conjugated with mouse monoclonal anti-Tgo or anti-Arnt for 4hr at RT. Samples were centrifuged at 500g for 5min, supernatant was discarded and the pellet was resuspended in RIPA buffer. The later step was repeated five times. The final pellet was resuspended in 2x sample buffer as shown in section 2.11.2. 25µl of each sample was run in a 1.5mm SDS-PAGE gel for autoradiography.

Chapter 3

Functional conservation between Ahr and Ss

3.1. INTRODUCTION

Some of the protein domains of Ss and Ahr are highly conserved, sharing 71% of aminoacid identity in the bHLH domain and a 45% in the PAS domain (Duncan et al., 1998). The bHLH and PAS domains are involved in DNA binding and protein dimerization properties. These similarities indicate that the ability to undergo interactions with specific DNA motifs and proteins might also remain preserved. In agreement with this observation Ss forms a protein complex with Tgo (Emmons et al., 1999), the orthologue of Arnt (Ahr's partner) (Ward et al., 1998), and drives changes in gene expression through the binding of the XRE motif (Emmons et al., 1999). Nevertheless, differences exist between Ahr and Ss. Ss is not able to bind dioxins and the ligand binding domain is poorly conserved (Butler et al., 2001; Kudo et al., 2009). In the following sections I will review the similarities and differences between Ahr and Ss.

3.1.1 Binding to Tgo and Arnt

In 1991 it was reported that Ahr activity required a second locus, which encoded for another bHLH-PAS protein. This protein was given the name of the Aryl hydrocarbon receptor nuclear translocator (Arnt), since Ahr was found nuclear in cells expressing Arnt (Hoffman et al., 1991). However, subsequent work demonstrated that Arnt is not required for the nuclear translocation of Ahr (Pollenz et al., 1994). Instead, Ahr shuttles to the nucleus upon ligand binding (Ikuta et al., 1998) and there it binds Arnt to form a transcription factor complex (Dolwick et al., 1993).

tgo, the fruit fly orthologue of *Arnt* (Ward et al., 1998), has a close relationship with *ss* in leg and antennal development (Emmons et al., 1999). Like *Arnt*, *tgo* encodes for a bHLH-PAS transcription factor that act as a partner for many other bHLH-PAS proteins (Ohshiro and Saigo, 1997; Sonnenfeld et al., 1997). *tgo* mutant alleles enhance ss^{-} phenotypes and tgo^{-} somatic clones show antennal, leg, and bristle defects that are very similar to ss^{-} mutants. The physical interaction between Tgo and Ss was proven by yeast two hybrid assays (Emmons et al., 1999). In contrast to mammals, Tgo is located all over the cell in absence of any other bHLH-PAS protein (Ward et al., 1998). In cells that express *ss*, Tgo translocates to the nucleus (Emmons et al., 1999).

3.1.2. The Xenobiotic Response Element

Ahr and Arnt control gene expression through the binding to the XRE (Swanson et al., 1993). This feature is also conserved in Ss and Tgo. In cell culture experiments, transfection with transgenic constructs containing *ss* and *tgo* led to the activation of a reporter downstream of XREs (Emmons et al., 1999). Recently, it has been shown that Ss downregulates the expression of the gene *Bar* in leg imaginal disc through the binding to a genomic region called *ta5-enhancer*. The sequence of the *ta5-enhancer* has a XRE motif that is highly conserved in other species of *Drosophila*. Ss represses the

expression of the reporter gene *lacZ* under the control of the *ta5-enhancer*. When the XRE is removed, Ss is not longer able to control the expression of the reporter gene (Kozu et al., 2006).

3.1.3. Ss does not bind dioxins

Ahr's ligand binding domain (LBD) is located in the N-terminal region, overlapping with the PAS-B repeat (Ikuta et al., 1998). This part of the PAS domain is poorly conserved in Ss (Kudo et al., 2009). This agrees with *in vitro* assays in which Ss failed to bind TCDD or β-naphthoflavone (BNF) (Butler et al., 2001). Recently it was shown that a quimeric murine-fly Ahr, in which the LBD was replaced with *Drosophila*'s LBD, does not require an exogenous ligand to be active (Kudo et al., 2009). This supports the theory that, in absence of dioxins, the murine LBD keeps Ahr in an inactive form (Ikuta et al., 1998). However, we must not forget that Ahr has dioxin-independent functions in development (Fernandez-Salguero et al., 1995; Mimura et al., 1999; Schmidt et al., 1996). For this reason it is important to address the mechanisms of regulation of Ahr in a developmental context.

In summary, many similarities exist between Ahr and Ss such as protein and DNA binding properties. However, there are still several differences that might undermine the use of *Drosophila* as a model for dioxin toxicity. For this reason, in this chapter I aim to ascertain whether Ahr and Ss mechanisms of action remain conserved, thus determining whether the fruit fly can be employed as a tool to study the effects of TCDD on Ahr. The use of transgenics and the *UAS/Gal4* system has allowed me to work with the dioxin receptor in a purely developmental context and to determine to what extent Ahr is able to undergo the same cellular and molecular interaction than Ss. First, I will show the ability of *Ahr* to rescue the *ss* mutant phenotype. Second, I will

describe the effects of expression of *Ahr* in *Drosophila* and compare them with those caused by misexpression of *ss*. Third, I will demonstrate that Ahr protein interacts both functionally and physically with Tgo. These results indicate that functional equivalence exits between the dioxin receptor and Ss and that this conservation extends to cellular and molecular interactions. This brings an interesting opportunity to use *Drosophila* as a new vehicle that will help us to understand in which way dioxins disrupt the role of the Dioxin Receptor in development.

3.2. RESULTS

3.2.1. *Ahr* is able to fulfill *ss* functions in the leg imaginal disc

In the first place, I aim to test whether *Ahr* is able to fulfill *ss* functions. For this purpose I used the adult leg as experimental system. The leg is a tubular organ composed of ten segments with a stereotyped bristle pattern, from proximal to distal: coxa, trochanter, femur, tibia, five tarsi and claw. This well-known pattern makes the leg a good system to study and detect the effects of changes on gene expression. *ss* is expressed in a ring in the presumptive tarsal region of the leg imaginal disc at the mid-third larval instar. *ss* mutants lack tarsus from distal part of the first tarsal segment (ta1) to the fourth tarsal segment (ta4) in adult leg (Figure 3.1.B) (Duncan et al., 1998). In order to test a functional conservation between *ss* and *Ahr*, I aim to rescue the *ss* mutant phenotype in adult leg by expressing *Ahr*. To do this I have expressed *UAS-ss* and *UAS-Ahr* transgenic lines in a ss^{abr}/ss^{sta} background (referred as ss^{-} in this section). ss^{abr} is an hypomorph allele (McMillan and McGuire, 1992), whereas ss^{sta} is an amorph allele (Melnick et al., 1993). I have selected this allelic combination because the use of a null does not give viable offspring. Expression of either *UAS-ss* or *UAS-Ahr* was driven by *rn-Gal4*. *rn* and *rn-Gal4* are expressed in a ring in the distal portion of the leg imaginal disc during mid larval instar in a pattern that is very close to the *ss* expression domain (Pueyo and Couso, 2008; St Pierre et al., 2002). Despite being co-expressed, *rn* and *ss* do not regulate each other (Pueyo and Couso, 2008), so *rn-Gal4* is expressed in a *ss* mutant background.

Females *w;; rn-Gal4* ss^{abr}*/TM3 Ser* were crossed with males *w; UAS-Ahr/CyO;* ss^{sta}*/TM6B*. The offspring were sorted following the dominant markers from the balancer chromosomes (i.e. Serrate wings from TM3 Ser; see section 1.10.1). Flies

expressing Ahr in the ss^- background (*w; UAS-Ahr; rn-Gal4* ss^{abr}/ss^{sta}) were classified as the experimental class (Figure 3.1.C). ss^- flies that did not express Ahr were used as negative control (*w; CyO/+; rn-Gal4* ss^{abr}/ss^{sta}) (Figure 3.1.B). Experiments were performed at 25°C. Among the experimental class, about an 80% of the flies recovered two out of the three missing tarsi (Figure 3.1.C and Figure 3.2). In the negative controls about 50% of the flies had three tarsi, and the rest had two or less (Figure 3.1.B and Figure 3.2). These data indicate that *Ahr* partially rescues the *ss* mutant phenotype.

Misexpression of *ss* driven by *rn-Gal4* in ss^- flies also rescues the *ss* mutant phenotype, although it does not recover the wild-type phenotype, about 20 % had three tarsi or less, and none had five tarsi (Figure 3.1.D and Figure 3.2). This incomplete rescue might be due to the dominant effects caused by over-expression of *ss*, which leads to a partial transformation to antenna; notice that tarsi of *w; UAS-ss; rn-Gal4* ss^{abr}/ss^{sta} are thinner than wild-type and lack bristles and sex-combs, although the presence of joints (arrows) indicates the formation of actual tarsi (Figure 3.1.D). This resembles the phenotypes of legs of *rn-Gal4 UAS-ss* heterozygotes in which extra *ss* causes a partial transformation from distal leg to an antennal aristae (Figure 3.1.E). This transformation is also supported by previous reports on the role of *ss* in determining antennal fate in which ectopic expression of *ss* across the leg imaginal disc driven by *ptc–Gal4* caused the transformation of a claw to an aristae (Duncan et al., 1998).

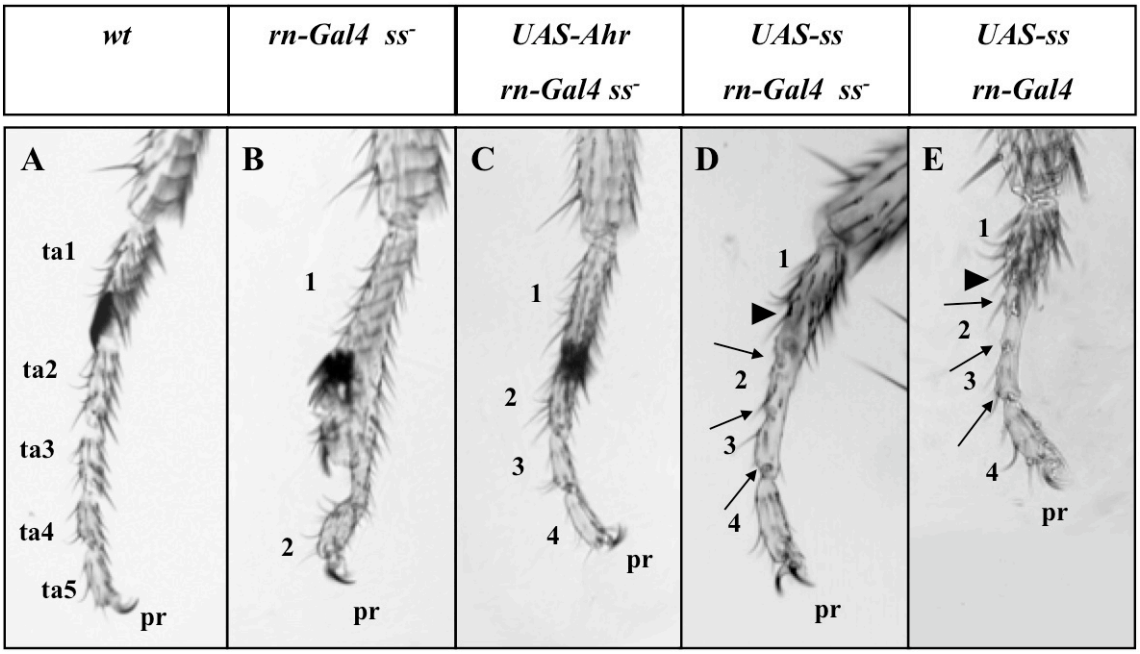

Figure 3.1. Ahr rescues *ss*⁻ phenotype in adult leg. All images represent the tarsal region of a leg from the first thoracic segment of a male. Dorsal to the left and proximal to the top. **(A)** Tarsal region of a wild-type leg. First, second, third, fourth and fifth tarsal segment, and pretarsus referred as ta1, ta2, ta3, ta4, ta5, and pr, respectively. **(B)** Leg of a *w; rn-Gal4 ss^{abr}/ss^{sta}*. 1 and 2 represent the only two present tarsi. **(C)** Leg of a *w; UAS-Ahr; rn-Gal4 ss^{abr}/ss^{sta}*. Notice the presence of four well formed tarsi. **(D)** Leg of a *w; UAS-ss; rn-Gal4 ss^{abr}/ss^{sta}*. **(E)** leg of a *w; UAS-ss; rn-Gal4 ss^{abr}* heterozygote. Tarsi morphology is severely affected due to a partial transformation to distal antenna. The arrows indicate the presence of joints that separate four tarsi. The arrowheads point to the missing sex-combs. Numbers indicate the number of present tarsi.

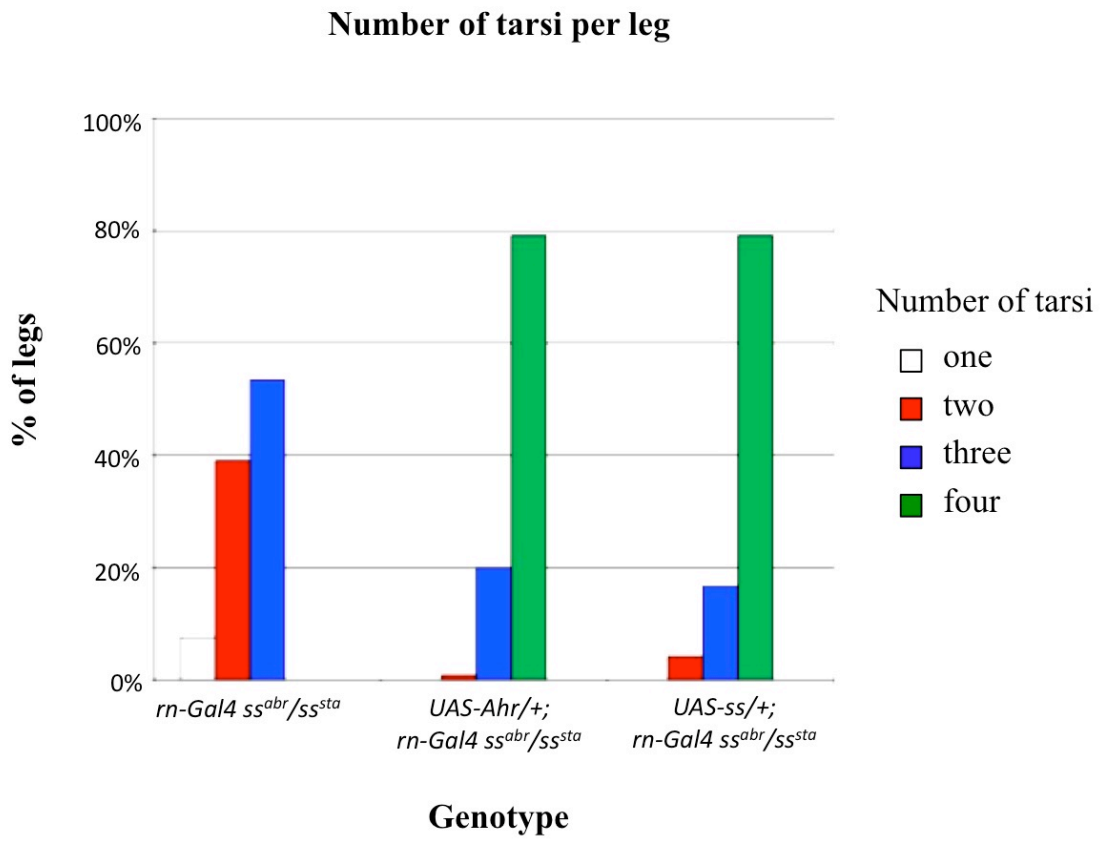

Figure 3.2. Frequency of phenotypes in the rescue experiments sorted by number of tarsi per leg and genotype. White, red, blue, and green bars represent the percentage of legs with one, two, three, or four tarsi respectively.

3.2.2. *Ahr* is able to regulate the expression of the *ss* targets *Bar* and *dachshund*

ss is a key element in the formation of intermediate tarsal segments (from ta2 to ta4) as shown by the ss^{-} phenotype (Figure 3.1.B). As a transcription factor the role of Ss is to regulate changes in gene expression. Whether Ahr is able to drive the same changes in gene expression as Ss is a crucial point to test the functional conservation between both proteins. During second instar, the leg imaginal disc is subdivided into different PD domains by two signaling proteins: Decapentaplegic (Dpp) expressed dorsally and Wingless (Wg) expressed ventrally. Dpp and Wg cooperate to activate *Distal-less* (*Dll*) and *dachshund* (*dac*) in the distal and medial presumptive regions respectively (Estella and Mann, 2008; Lecuit and Cohen, 1997). In the most distal region, EGFR signalling coming from the centre of the disc activates *B* expression (Galindo et al., 2005). *B* represses *dac* expression, creating two major expression domains in the distal part of the disc. Around 80-96 hr AEL the gene *tarsal-less* (*tal*) is expressed in the boundary of the *dac* and *B* expression domains. *tal* activates *ss* and *rn* expression. *ss* and *rn* repress *dac* proximally and *B* distally, thus creating a third expression domain abutting with *dac* and *B* (Figure 1.6). Ectopic expression of *ss* driven across a proximal to distal stripe in the dorsal half of the disc with *dpp-Gal4* led to the suppression of *dac* and *B* (Figure 3.3.B) (Pueyo and Couso, 2008). Also, adult flies *dpp-Gal4*; *UAS-ss* heterozygotes showed shorter legs with thickened and fused segments with the absence of a pretarsus (Figure 3.3.G). Notice that the presence of sex-combs in the first pair of legs indicates the presence of tarsal identity (arrows in the Figure 3.3.G).

In order to find whether Ahr and Ss are functional homologues I aimed to test if ectopic expression of *Ahr* mimics the effects of *ss* in gene expression, in other words if *Ahr* is able to repress *dac* and *B*. Ectopic expression of one or two copies of *Ahr* driven

by *dpp-Gal4* did not down-regulate *dac* and *B* expression and adult flies showed wild-type legs (Figure 3.3.E and J). However, combined ectopic expression of *Ahr* and its partner *Arnt* driven by *dpp-Gal4* suppressed *dac* and *B* in the *dpp* pattern (Figure 3.3.C). The flies *dpp-Gal4; UAS-Arnt UAS-Ahr* heterozygotes showed a phenotype in leg that resembles the ectopic *ss* phenotype: shortened and thickened segments, fusion of the tarsal segments, absence of joints, and absence of the claw (Figure 3.3.H). The presence of an indentation between tarsi and sex-combs in the pair of legs from the first thoracic segment suggests that there are no changes in segment identity (arrows in Figure 4.H). Notice that ectopic Arnt had not effect on the expression of *dac* and *B* (data not shown). This indicates that Ahr and Arnt are able to interact functionally in this system, and that addition of Arnt enhances Ahr activity.

Interestingly, a similar effect was observed with Tgo. Overexpression of Tgo on its own does not trigger any ectopic phenotype (data not shown), whereas overexpression of Ahr and Tgo (*w; UAS-Ahr UAS-tgo/+; dpp-Gal4/+*) suppressed *dac* and *B* expression (Figure 3.3.D). In adult leg tarsal segments were slightly shorter than wild type and claw was missing (Figure 3.3.I). Notice that the latest phenotype is milder than the phenotype caused by coexpression of Ahr and Arnt (Figure 3.3.H).

Ectopic Ss or Ahr downregulates the expression of a *lacZ* reporter, which is under the control of the *ta5-enhancer* (*ta5-lacZ*) (Figure 3.4.C and D). The *ta5-lacZ* contains a XRE site (Kozu et al., 2006) (Figure 3.4.A), suggesting that Ahr is able to drive changes in gene expression in *Drosophila* through the binding of its specific DNA binding site.

These results demonstrate that: 1) Tgo is able to interact with Ahr and enhances its activity; 2) there is a high degree of functional conservation between Tgo and Arnt;

and 3) Ss and Ahr undergo similar molecular interactions in terms of protein partners and DNA binding sites.

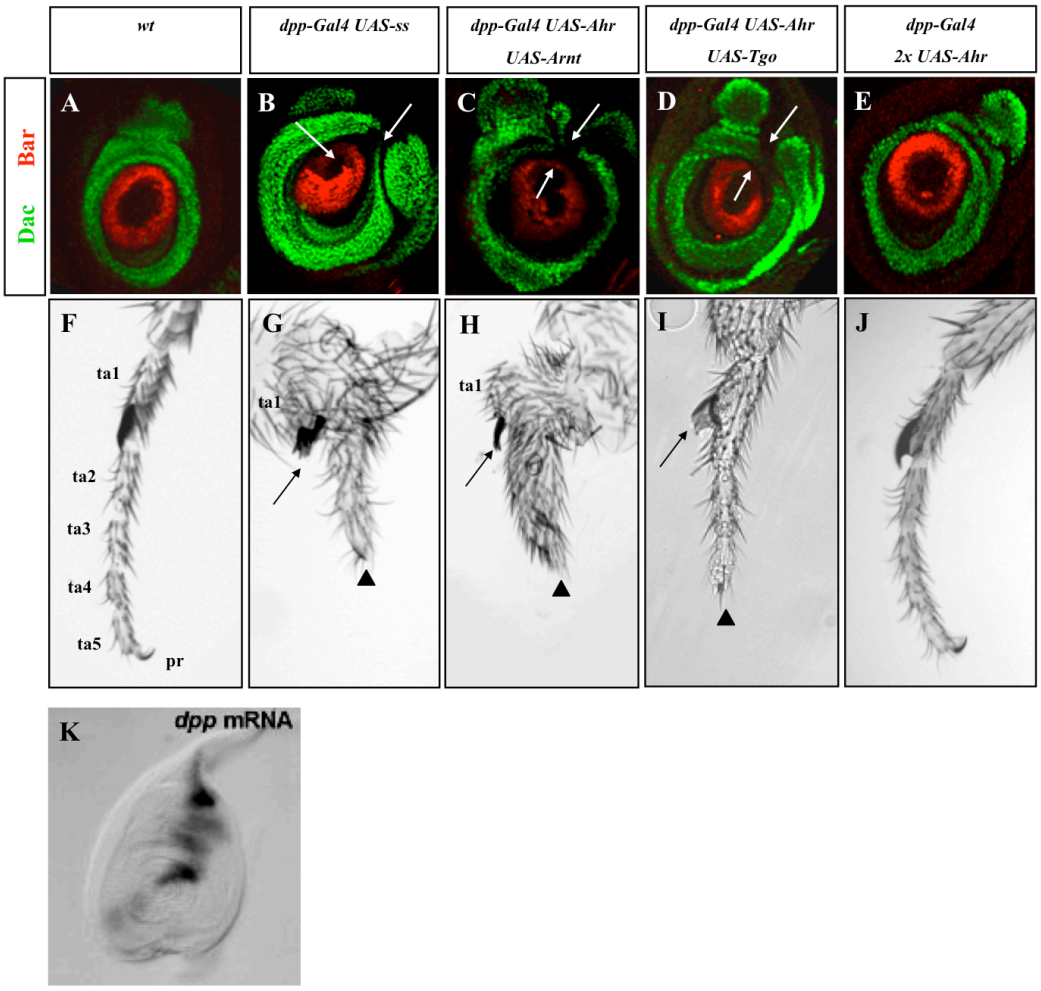

Figure 3.3. Effects of ectopic expression of Ahr and Arnt on leg development. (A-E) Expression of *dac* (green) and *Bar* (red) in leg imaginal disc during third larval instar. Dorsal to the top. **(F-J)** Tarsal regions of legs from the first thoracic segment of adult males. Dorsal to the top, anterior to the left. **(A and F)** Wild type. **(B and G)** Ectopic expression of Ss, *w; UAS-ss; dpp-Gal4* heterozygote. **(C and H)** Ectopic expression of Ahr and Arnt, *w; UAS-Ahr UAS-Arnt; dpp-Gal4* heterozygote. **(D and I)** Ectopic expression of Ahr and Tgo, *w; UAS-Ahr UAS-Tgo; dpp-Gal4* heterozygote. **(E and J)** Ectopic expression of two copies of Ahr, *w; UAS-Ahr/UAS-Ahr; dpp-Gal4/+*. (K) dpp expression pattern in leg imaginal disc as shown by in situ hybridation. The latest panel was extrated from Theisen et al., 2010. The white arrows indicate the repression of *dac* and *Bar* in the dorsal region of the disc. ta1, ta2, ta3, ta4, ta5, and pr represent the first, second, third, fourth and fifth tarsal segment, and pretarsus, respectively. The black arrow points to the sex-combs, which seem to be reduced in number.

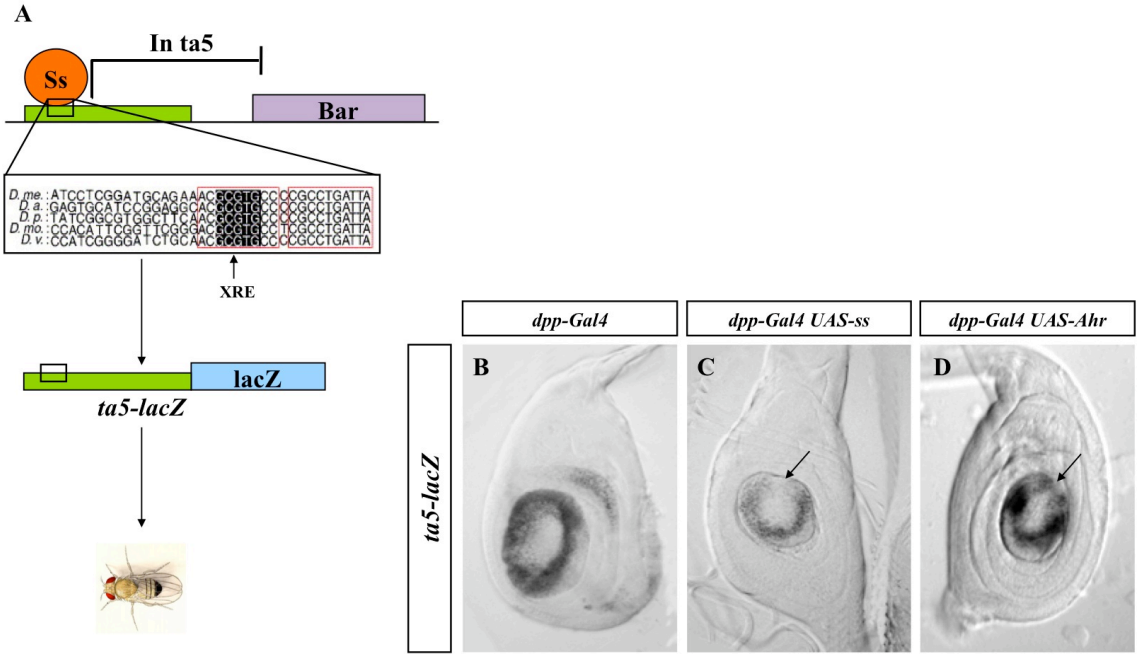

Figure 3.4. Ectopic expression of Ss and Ahr repress the *ta5-lacZ* reporter. (A) Ss downregulates *Bar* in the presumptive fifth tarsal segment of the leg imaginal disc through the direct binding to the *ta5-enhancer*. The *ta5-ehnacer* was cloned upstream of a *lacZ* reporter (*ta5-lacZ*). The *ta5-lacZ* was injected in flies to set a transgenic line. **(B)** Expression of the *ta5-lacZ* reporter gene in leg imaginal discs from mid-late 3rd instar larvae (*lacZ* expression was detected by X-Gal staining). **(C)** *ta5-lacZ* expression in *ta5-lacZ/+; dpp-Gal4/UAS-ss* larvae. **(D)** X-Gal staining in *ta5-lacZ/UAS-Ahr; dpp-Gal4/+* larvae. Notice that the *ta5-lacZ* reporter is repressed by the ectopic expression of Ss and Ahr (arrows in C and D respectively).

3.2.3. Effects of misexpression of *Ahr* depend on the dose of *Tgo*

The results shown above suggest the need for further analysis on the functional interaction between Ahr and Tgo proteins. To test such an interaction I aimed to study the dependency of Ahr activity on Tgo. I used the GMR-*Gal4* to drive expression of Tgo and Ahr on the eye imaginal disc, and observed the effects on the eye of the adult flies. Ectopic expression of *Ahr* during the 3rd larval instar in the eye imaginal disc driven by *GMR-Gal4* at 25^{o}C had no obvious effects on the adult eye morphology (Figure 3.5.B). Overexpression of Tgo driven by *GMR-Gal4* gave rise to wild type eyes, as well (Figure 3.5.C). However, flies *w; GMR-Gal4; UAS-Ahr UAS-tgo* heterozygotes (referred as *Ahr+tgo* hereafter) showed a strong phenotype: the surface of the eye looks rough, the bristles seem thicker and longer and more abundant in the anterior-posterior part of the eye, and lack of color in the centre of the eye (Figure 3.5.D). This resembles the phenotype of flies with ectopic expression of Ss in the eye (*w; UAS-ss/+; GMR-Gal4/+*) (Figure 3.5.E), which is also enhanced by overexpression of Tgo (Figure 3.5.F).

In order to corroborate with further detail the nature of this interaction, the surface of eyes of flies of the genotypes mentioned above were observed under the scanning electron microscope and the size of the bristles was measured to test whether the effect of Ahr+Tgo is similar to the effect of ectopic expression of Ss. The analysis shows, that there is a significant increase in bristle size in *w; GMR-Gal4; UAS-ss* heterozygotes (Figure 3.6.B) and *w; GMR-Gal4; UAS-Ahr UAS-tgo* heterozygotes (Figure 3.5.C) when compared to the wild type (Figure 3.6.A and Figure 3.7). On the other hand, there is not significant difference between *w; GMR-Gal4; UAS-ss* (Figure 3.6.B) and *w; GMR-Gal4; UAS-Ahr UAS-tgo* (Figure 3.6.C and Figure 3.7). The analysis also shows that there is no significant difference in the size of bristles between *OR-R* flies and *w; GMR-Gal4; UAS-tgo* (Figure 3.6.D and Figure 3.7) or between *OR-R*

flies and *w; GMR-Gal4; UAS-Ahr* heterozygote flies (Figure 3.6.E and Figure 3.7), demonstrating that ectopic expression of *Ahr* or *tgo* in the eye imaginal disc does not cause any obvious phenotypes in the adult eye (see averages and standard errors in Figure 3.7). Notice that the bristles are also bent on the tip. Greater magnification reveals that ectopic Ss or Ahr+Tgo triggers the formation of little ectopic structures that resemble bracts or trichomes (Figure 3.8.B and C, red arrows). Bracts are cuticular projections secreted by a single cell that is located in the base of the bristles that grow in the leg or in the costa –proximal region of the adult wing (Hannah-Alava, 1958). These bristles use EGFR signaling to recruit a nearby cell to form a bract (Held, 2002). Trichomes are sensory structures. In the wing blade, each cell forms a trichome (Mitchell et al., 1990). The identity of these structures is unknown, but will be addressed in the future as they might indicate changes in cell identity. Nevertheless, this analysis corroborates that extra Tgo enhances Ahr activity giving rise to a specific phenotype that closely resembles the phenotype caused by ectopic Ss.

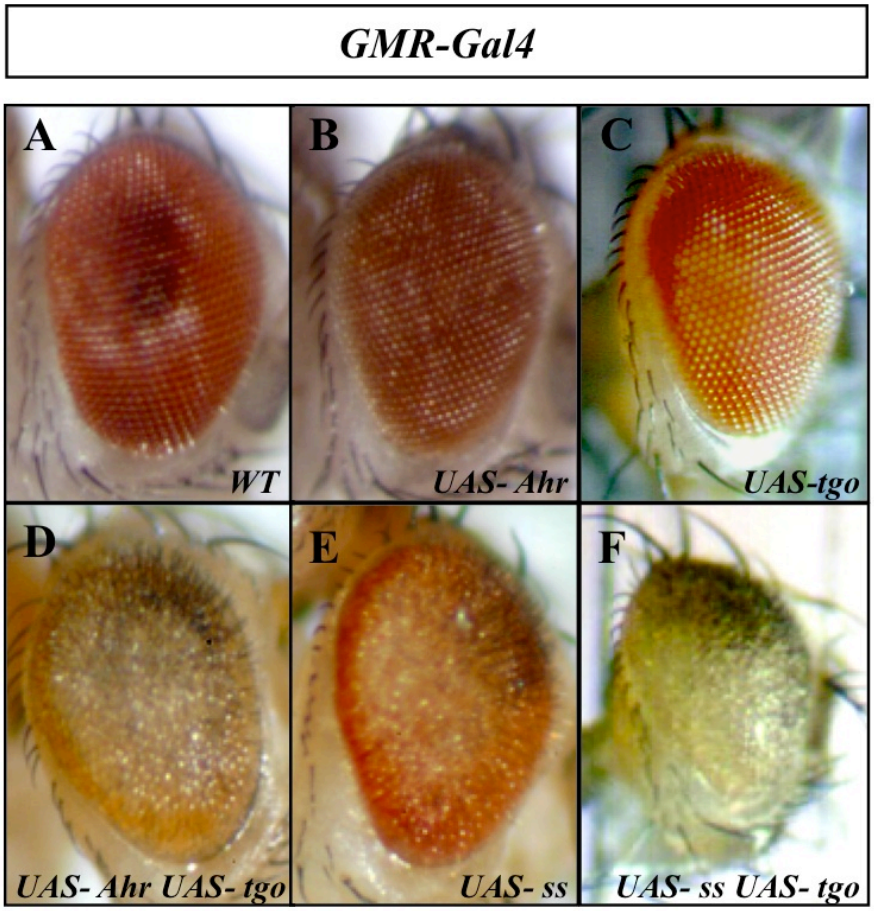

Figure 3.5. Ahr ectopic phenotypes depend on the dose of Tgo. (A) The eye of a wild-type fly. Top is dorsal, right is anterior. **(B)** Eye of a *w; GMR-Gal4; UAS-Ahr* heterozygote. **(C)** Eye of a *w; GMR-Gal4; UAS-tgo* heterozygote. **(D)** Eye of a *w; GMR-Gal4; UAS-Ahr UAS-tgo* heterozygote. **(E)** Eye of a *w; GMR-Gal4; UAS-ss* heterozygote. **(F)** Eye of a *w; GMR-Gal4; UAS-ss UAS-tgo* heterozygote. Notice that in the three bottom panels the ommatidial arrangement is disrupted, eye pigmentation is partially or completely lost, and bristles are very apparent.

Figure 3.6. Effects on eye morphology caused by ectopic expression of Ss, Ahr, and Tgo. (A) The eye of a wild-type fly. Top is dorsal, right is anterior. **(B)** Eye of a *w; GMR-Gal4; UAS-ss* heterozygote. **(C)** Eye of a *w; GMR-Gal4; UAS-Ahr UAS-tgo* heterozygote. **(D)** Eye of a *w; GMR-Gal4; UAS-tgo* heterozygote **(E)** Eye of a *w; GMR-Gal4; UAS-Ahr* heterozygote. The red section represents the area of 500x200 pixels that was cropped for the bristle size analysis. The bottom panels are an amplification at 1000x of the red areas.

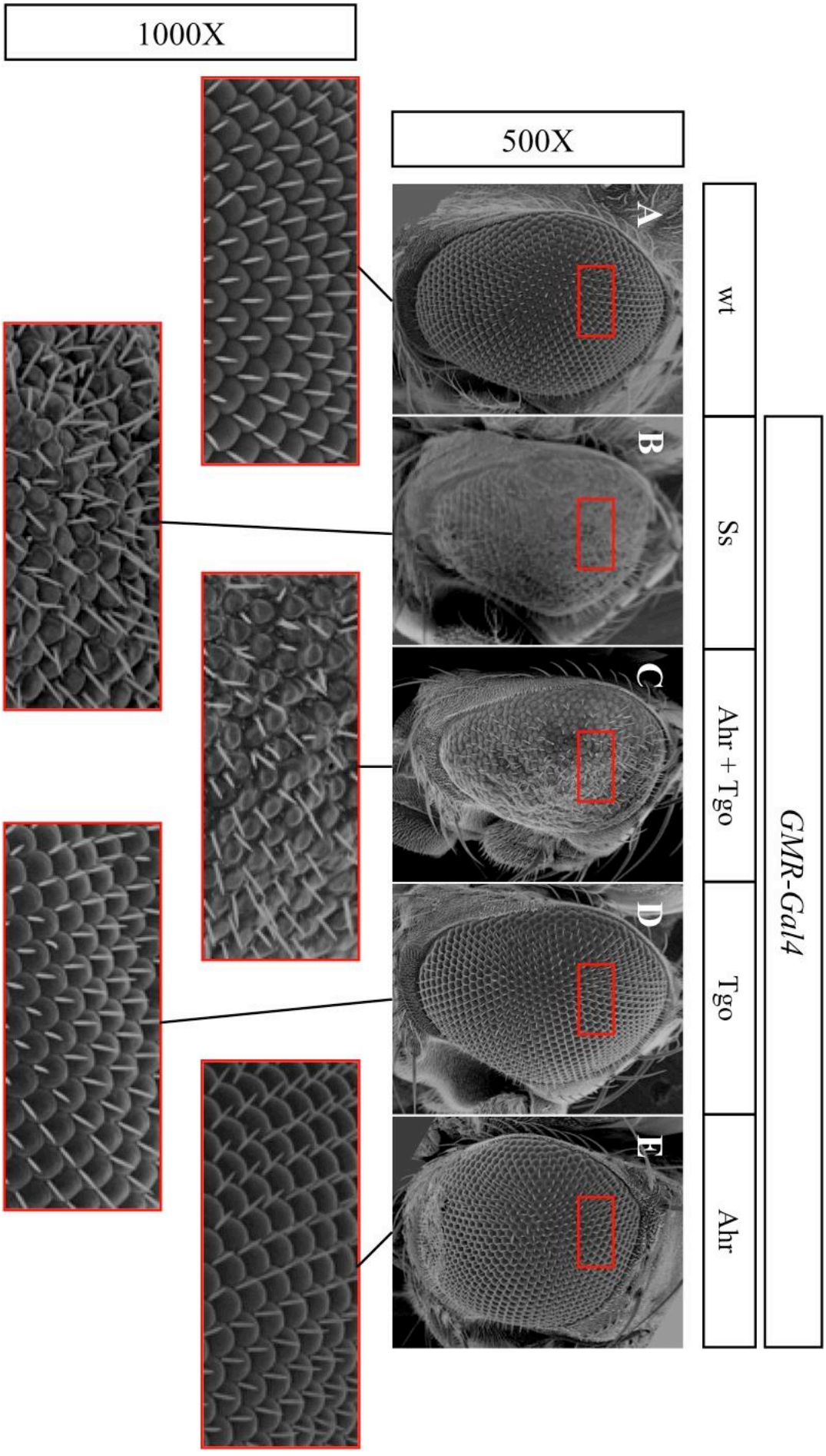
1000X
500X
A
B
C
D
E
wt
Ss
Ahr + Tgo
Tgo
Ahr
GMR-Gal4

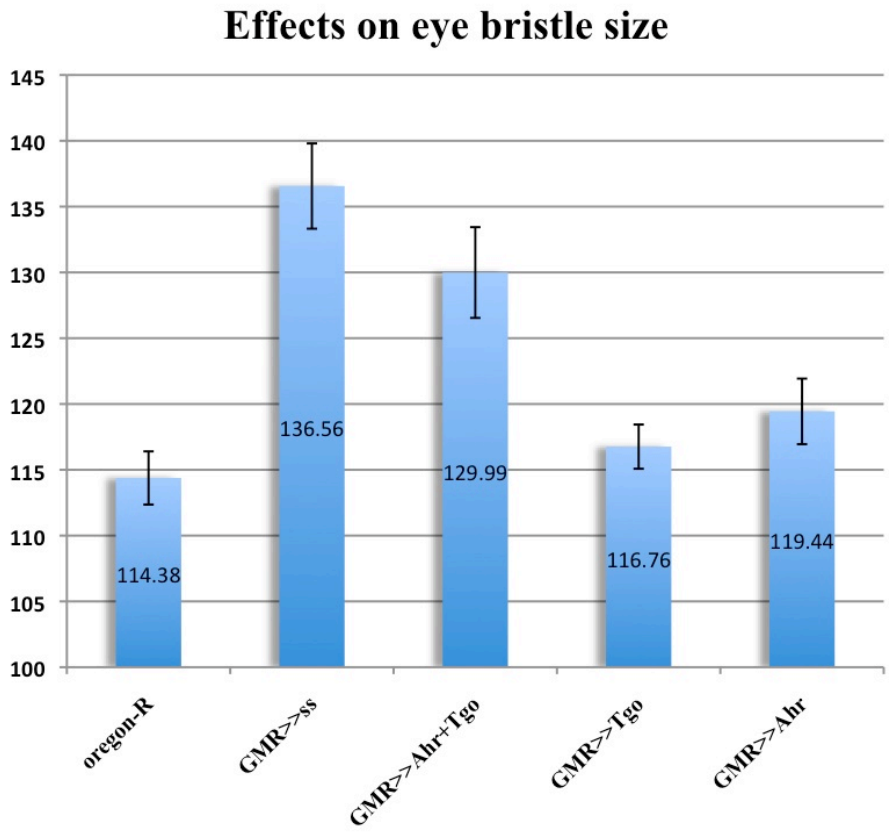

Figure 3.7. Average bristle size and standard error bars in each sample. The size of the eye bristles of 5 eyes per genotype were analyzed. Notice that the average size in flies *w ;GMR-Gal4 UAS-ss* and *w; GMR-Gal4 UAS-Ahr UAS-tgo* is significantly higher than the rest of genotypes. The numbers inside the graph indicate the average size for each genotype, and the bar indicates the standard errors.

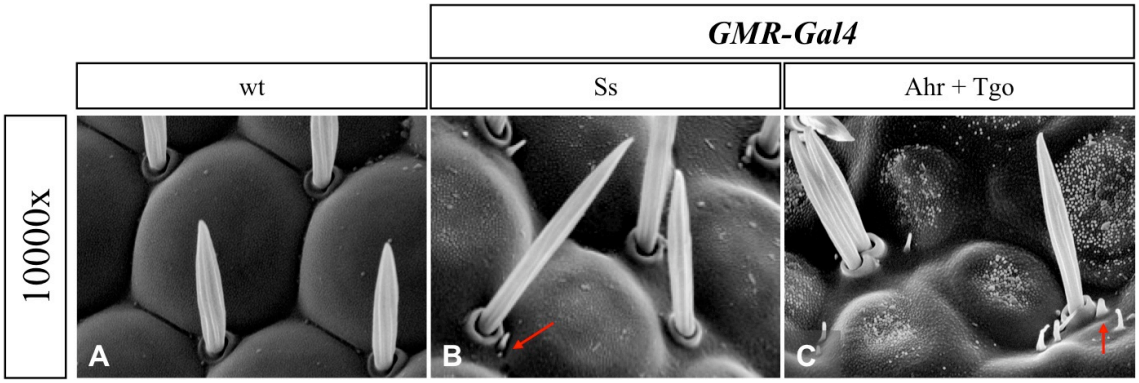

Figure 3.8. Detailed view of the surface of eyes expressing ectopic Ss and ectopic Ahr+Tgo. Pictures of the eye surface taken with the scanning electron microscope at 10000x. **(A)** Wild type. **(B)** Ectopic Ss, *w; GMR-Gal4; UAS-ss* heterozygote. **(C)** Ectopic Ahr+Tgo, *w; GMR-Gal4; UAS-Ahr UAS-tgo* heterozygote. The red arrows point to ectopic structures that resemble bracts or trichomes. Notice that bristles are longer and bent on the tip in B and C.

3.2.4. Ahr protein is nuclear in *Drosophila* and drives the translocation of Tgo into the nucleus

Ss is a nuclear protein and requires its partner Tgo to carry out its developmental role. In mitotic recombination experiments it was shown that *tgo*$^{-}$ somatic clones in the antenna cause a transformation from arista to distal leg (tarsal segments and a claw) and loss-of-function alleles of *tgo* act as dominant enhancers of *ss* mutants (Emmons et al., 1999). Also, Ss and Tgo interact physically in yeast two-hybrid assays (Emmons et al., 1999; Kim et al., 2006). In the absence of Ss or any other partner, Tgo is distributed homogeneously in the cell, whereas the presence of Ss drives translocation of Tgo to the nucleus (Emmons et al., 1999; Ward et al., 1998). The fact that expression of Ahr rescues *ss*$^{-}$ phenotypes and interacts with Tgo in leg development suggests that the Ahr protein might be able to drive Tgo to the nucleus. In order to test this hypothesis, I set a model system in which I could easily detect the changes in Tgo cellular location in regard to the presence or absence of Ss or Ahr. For this purpose I used larval salivary glands from 3rd instar larvae. Salivary glands are organs composed of big cells that are ideal to distinguish cytoplasmic and nuclear localization. I studied the location of Tgo in salivary glands in which ectopic expression of the contructs *UAS-ss-GFP* or *UAS-Ahr-GFP* was driven by *AB1-Gal4* (Figure 3.9). Expression of either *ss-GFP* or *Ahr-GFP* is able to rescue the *ss* mutant phenotypes in adult leg (data not shown). In this experiments the presence of Tgo was reported with the monoclonal mouse anti-Tgo anti-body (Ward et al., 1998).

In the salivary glands of wild-type larvae, Tgo was located throughout the cell (Figure 3.9.A). In cells where the fusion protein Ss-eGFP was expressed, both Ss-eGFP and Tgo were nuclear, indicating that the presence of Ss leads to Tgo accumulation in the nucleus (Figure 3.9.B). In the same way, in salivary glands expressing ectopic Ahr-

eGFP fusion protein, Tgo was retained in the nucleus, as well (Figure 3.9.C). Notice that, Ahr-eGFP was nuclear (Figure 3.9.C). The conservation of the chaperone complex that keeps Ahr in the cytosol has not been addressed in this work. Therefore, it remains unclear whether Ahr is nuclear as it is not retained in the cytosol, or whether Ahr is responding to a ligand-independent pathway triggered by the insect machinery. This issue might be approached in the future.

Ahr and Arnt form a nuclear complex to drive changes in gene expression in mammals. *tgo* is the closest homologue of *Arnt* in *Drosophila* (Sonnenfeld et al., 1997). This indicates that both the presence of Ss or Ahr is sufficient to drive Tgo translocation to the nucleus, suggesting that Ahr protein might functionally and physically interact with Tgo and that Ss and Ahr share a high degree of conservation in terms of the co-factors that they interact to and their mode of interaction.

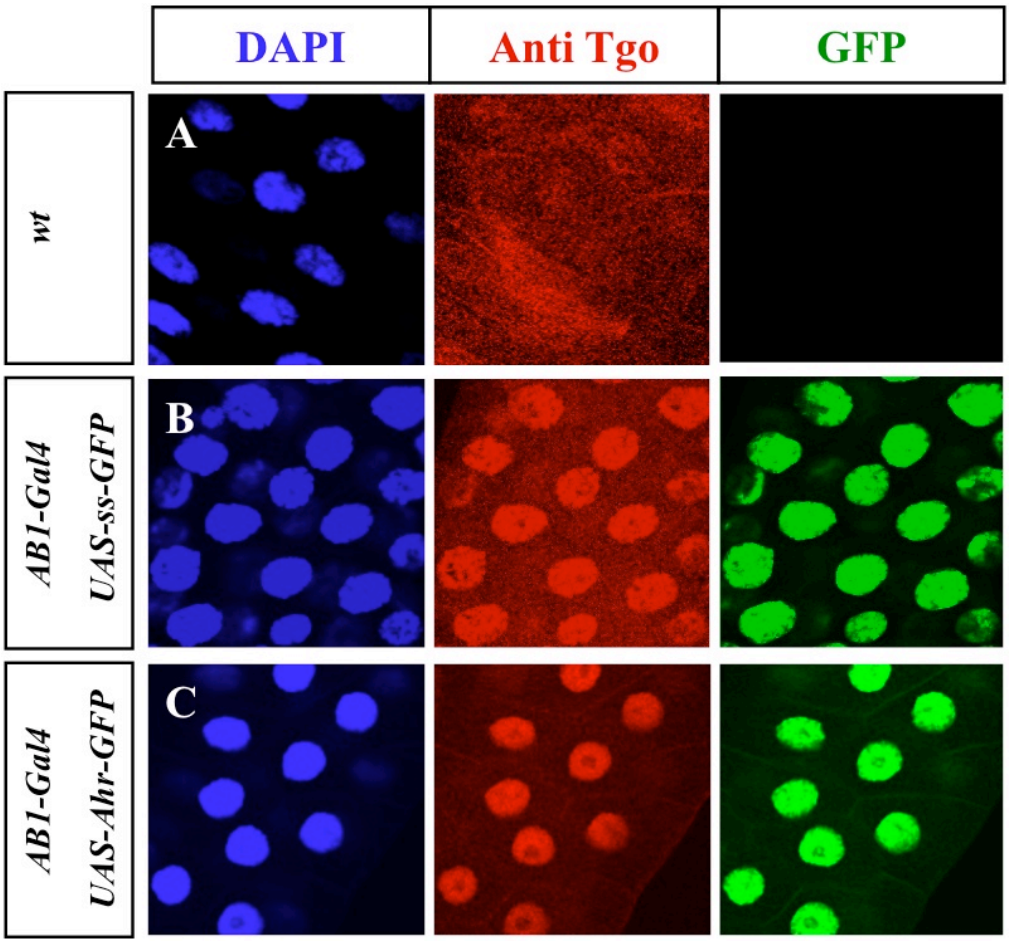

Figure 3.9. Tgo is nuclear in the presence of Ahr or Ss in salivary glands. (A) Wild type salivary gland showing endogenous Tgo (red). **(B)**. *w; AB1-Gal4; UAS-ss-GFP* heterozygote; Ss-GFP (green) and endogenous Tgo (red) are nuclear. Notice that there is still some Tgo in the cytoplasm. **(C)** *w; AB1-Gal4; UAS-Ahr-GFP* heterozygote; Ahr-eGFP (green) is nuclear and endogenous Tgo (red) is nuclear. Nuclei are stained by the DNA marker DAPI (blue).

3.2.5. Ahr interacts physically with Tgo

It is likely that Ahr and Tgo proteins are interacting physically. In order to test this hypothesis I carried out co-immunoprecipitation assays. Ahr-GFP and Ss-GFP proteins were expressed in third instar larvae using the *hs-Gal4* driver (heat shock driver). Anti-GFP mouse monoclonal anti-body (Crameri et al., 1996) was used to precipitate Ahr-GFP and Ss-GFP from the protein extracts. After precipitation Tgo remains in the samples (Figure 3.10.A, lanes 2 and 4), indicating that it interacts physically with Ahr and Ss. Notice that Ahr-GFP seems to be more abundant than Ss-GFP (Figure 3.10.B). However, the interaction Tgo-Ahr looks weaker than Tgo-Ss, suggesting that Tgo has greater affinity for Ss-GFP (Figure 3.10.A, lanes 2 and 4).

In order to test whether these proteins require other factors to interact physically, the assays were carried out with proteins that were synthesized using the TNT quick transcription/translation system. Ahr and Ss were labeled with methionine tagged with S^{35} (Figure 3.10.C, lanes 1 and 6 respectively). Protein lysates were mixed and incubated according to the interactions being tested. Tgo and Arnt proteins were precipitated with anti-Tgo (Ward et al., 1998) and anti-Arnt (Wenger et al., 1998) monoclonal antibodies, respectively. The assay showed that under these conditions Ahr is still able to interact with Tgo and Arnt (Figure 3.10.B, lanes 2 and 3, respectively). As expected, Ss is also able to interact with Tgo (Figure 3.10.B, lane 7). These results indicate that Tgo and Ahr do not require other factors to interact physically, indicating that the interaction seen *in vivo* is due to direct binding.

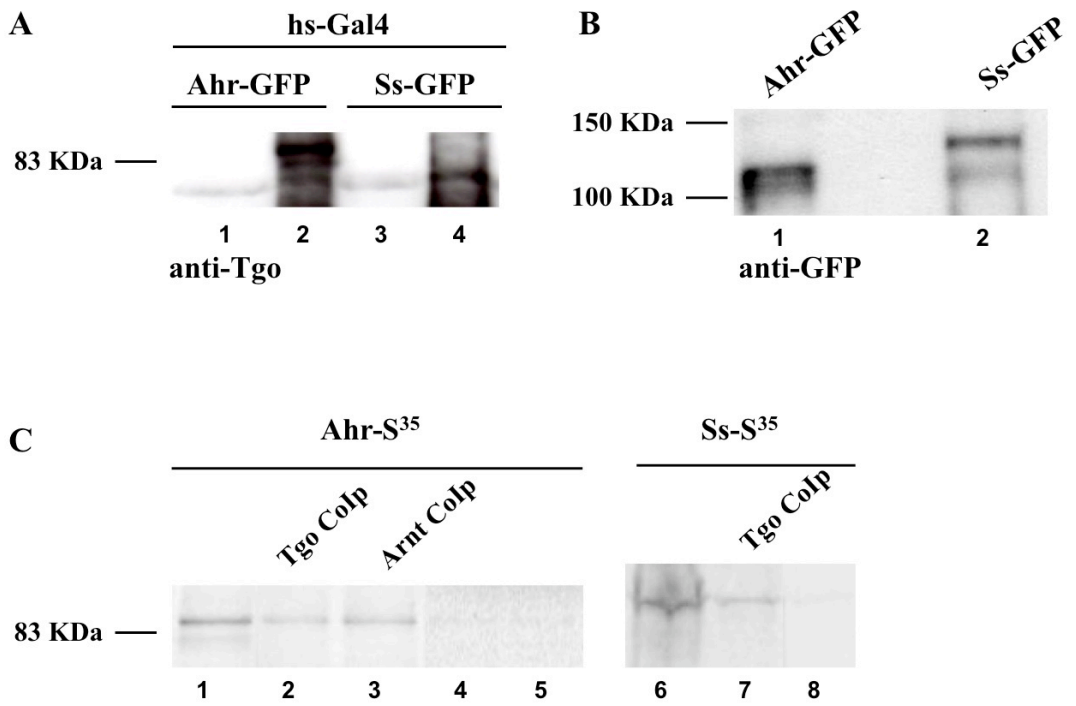

Figure 3.10. Ahr and Tgo interact physically. (A) Ahr-GFP and Tgo, and Ss-GFP and Tgo interact in *in vivo* co-immunoprecipitation assays. Ahr-GFP and Ss-GFP from *in vivo* extracts were precipitated using anti-GFP, the presence of Tgo was detected before (lanes 1 and 3) and after (lanes 2 and 4) the interaction assay by western-blot with anti-Tgo monoclonal antibody. **(B)** Western-blot with anti-GFP monoclonal antibody revealing the presence of Ahr-GFP (lane 1) and Ss-GFP (lane 2) in the co-immunoprecipitation assays. Notice that Ahr-GFP seems to be more abundant. **(C)** *in vitro* coimmunoprecipitation assays. Ahr interacts with Tgo (lane 2), and Arnt (lane 3). Ss interacts with Tgo (lane 7). Assays were also carried out in the absence of Tgo (lane 4 and 8), and Arnt (lane 5), as negative controls. Proteins were synthesized with the TNT coupled transcription/translation system. Ahr and Ss were labeled with methionine tagged with S^{35} (lanes 1 and 6 respectively). Tgo and Arnt were precipitated with anti-Tgo and anti-Arnt monoclonal antibodies.

3.3. DISCUSSION

3.3.1. Ahr and Ss are functionally conserved

Ss and Ahr share high conservation in aminoacid sequence in the bHLH and PAS domains. The bHLH domain is essential for DNA-binding and interaction with other proteins (Murre et al., 1989). The PAS domain is a secondary dimerization domain that gives partner specificity and increases the strength of dimerization (Schmidt and Bradfield, 1996). DNA-binding and protein interactions represent the major features of transcription factors. The degree of similarity between the bHLH and the PAS domains of Ss and Ahr indicate that their conservation might extend to the level of protein function. Here, I have shown that Ahr can carry out Ss functions in *Drosophila* leg development, allowing the formation of mid-tarsal segments in *ss* mutants. However, ss^{-} phenotypes are not completely rescued to the wildtype. This might be due to two different factors. On one hand, the degree of functional conservation is enough as to partially rescue ss^{-} phenotype but not as to fully fulfill Ss functions. On the other hand, the amount of Ahr protein might not be enough to equal endogenous levels of Ss. This is a likely scenario since Ss functions are dosage-dependent. In flies heterozygous for deletions that cover the Ss region, the antenna undergoes an homeotic transformation; the arista is transformed to a distal leg (tarsi and claw), whereas the legs are unaffected (Duncan et al., 1998). Also, the addition of extra Ss leads to a phenotype that resembles a transformation to a distal antenna (thinner tarsi without bristles). However, the two rescued structures are actual tarsi in terms of morphology and size, which leads me to the conclusion that *Ahr* is able to, at least partially, fulfill *ss* functions in leg development.

This is also demonstrated at the level of gene regulation. Ectopic expression of *Ahr* on its own did not have any effect, whereas co-expression of *Ahr* together with *Arnt* causes the repression of *dac* and *B* expression in leg imaginal disc. This clearly indicates that Arnt is able to interact with Ahr and to enhance its activity in the fruit fly.

I have also demonstrated that Ahr responds to doses of Tgo. Ectopic expression experiments in the *Drosophila* eye and leg show that Ahr activity is enhanced upon overexpression of Tgo. Notice that *tgo* is endogenously expressed in eye and leg imaginal disc, therefore the enhancement of Ahr activity is due to an increase in inner Tgo protein, not to the synthesis of Tgo in an ectopic pattern. In the leg, the phenotypes caused by coexpression of Ahr and Arnt are stronger than those produced by coexpression of Ahr and Tgo. It remains unclear whether this might be due to differences in the level of expression of the *UAS-Arnt* and *UAS-Tgo* constructs or to a lower transcriptional activity of the Ahr+Tgo heterodimer. This issue will be addressed in the future. In the eye, this enhancement gives rise to a specific phenotype that equals the effects of ectopic expression of Ss: ectopic bracts or trichomes in the eye surface and bigger bristles that are slightly bent on the top. The functional interaction between the dioxin receptor and Tgo explains the fact that Ahr is able to rescue ss^{-} phenotypes in absence of Arnt.

Co-immunoprecipitation assays have shown that Ahr and Tgo interact physically in *in vivo* extracts. These proteins are also able to interact in *in vitro* assays, demonstrating that Tgo and Ahr do not need other elements to undergo dimerization and form an active transcription factor complex. This indicates a high degree of functional conservation not only between Ahr and Ss, but also on the context in which these proteins operate, and it makes it more likely that other specific molecular interactions remain conserved.

Ss represses the expression of *B* in the fifth tarsal segment through a XRE motif located in a regulatory region upstream of *B* coding sequence (Kozu et al., 2006). Since both Ahr+Arnt and Ahr+Tgo are able to repress B expression in the tarsal region, the most plausible scenario is that Ahr is forming heterodimers with Tgo or Arnt, and possibly keeping DNA-binding specificity. Interestingly, Ahr downregulates the *ta5-lacZ* reporter, which contains a XRE, suggesting that Ahr is able to drive changes in gene expression through the its specific DNA binding site in Drosophila.

In this chapter, I have shown that there is a high degree of functional conservation between Ahr and Ss, and between Arnt and Tgo. This suggests that the mechanisms of action and regulation of Ahr in development have been preserved. Thus Ahr and Ss undergo similar protein and DNA interactions. We could learn more about the biology of Ahr by understanding the functions of its homologues on invertebrates. This reveals an interesting opportunity: the use of genetic assays in *Drosophila*. This will help to ascertain the mechanisms of regulation of endogenous Ahr activity and to what extend dioxins interfere with *Ahr*'s developmental signalling pathways.

Chapter 4

Dioxins increase endogenous activity of the aryl hydrocarbon receptor

4.1. INTRODUCTION

Extensive evidence demonstrates that Ahr mediates most of the adverse effects of dioxins (Fernandez-Salguero et al., 1995; Mimura et al., 1997; Schmidt et al., 1996). Abundant research has been conducted on the medical conditions caused by TCDD and the implication of Ahr on these. However, it remains unknown to what extent dioxins interfere with Ahr developmental functions, in other words, whether dioxin toxicity might be understood as a gain or loss of function of Ahr endogenous activity. From this perspective, three scenarios can be considered. First, TCDD might enhance Ahr's activity acting as a hypermorph version of the ligand free Ahr. In this case, DNA binding specificity for the XRE motif and other molecular interactions would remain the same or maybe enhanced. Second, TCDD inhibits endogenous Ahr activity leading to a

lack of function. Binding affinity for the XRE motif and molecular partners such as Arnt might decrease, leaving them free for other competitors to bind. Third, Ahr acts in different means in presence of TCDD, this would be better understood as a neomorphic transformation of Ahr activity, perhaps leading to interaction with other DNA motifs or proteins. The latest possibility does not exclude the other two. For this reason, the effects of dioxins on transgenic flies expressing Ahr must be compared with the phenotypes caused by the ectopic expression of Ss in order to determine to what extent these effects are due to an enhancement or inhibition of its developmental functions or to the acquisition of new ones.

The genetic pathways that drive the development of an organism have remained greatly preserved throughout evolution at both the genetic and biochemical level (Bier, 2005). Thus, in the previous chapter, I have demonstrated the high degree of functional conservation between Ahr and Ss. *Drosophila* can be used as an experimental system to understand Ahr's biology and its role in development. I have also set the tools to study the activity of Ahr in a developmental context.

In this chapter I aim to describe the way in which dioxins disrupt Ahr's endogenous functions. For this purpose, I compare the changes on Ahr activity in the presence and absence of TCDD. I have fed flies and larvae with dioxin, examined Ahr's ability to rescue mutant phenotypes and changes in gene expression in ss^{-} background. On doing so, I have observed that, in the presence of dioxin, Ahr is able to fully rescue *ss* mutant legs to wild type, and to induce ectopic phenotypes and changes in gene expression that resemble those caused by ectopic Ss. These data demonstrate that Ahr has two levels of activity: basal or endogenous, and activated or "toxic". Addition of TCDD results in an increase of the endogenous activity of Ahr and a shift to the "toxic" state.

4.2. RESULTS

4.2.1. TCDD increases Ahr activity

As shown in section 3.2.1 Ahr is able to partially rescue the *ss*$^{-}$ mutant phenotype in fly legs. The absence of structures, or the addition of new ectopic ones is easy to assess in the leg of adult flies. In *ss*$^{-}$ mutants three of these segments are missing (ta2-ta4). In presence of Ahr two are recovered, indicating that Ahr carries out Ss developmental functions in the absence of dioxins. This partial rescue offers a model to study the effect of the TCDD toxicity on Ahr endogenous functions.

Would dioxins interfere with the ability of Ahr to rescue *ss*$^{-}$ phenotypes? If dioxin toxicity is due to an enhancement of Ahr endogenous functions, addition of TCDD might lead to a full rescue of the leg phenotype, and Ahr might also be able to trigger ectopic phenotypes. On the other hand, if dioxin suppresses Ahr activity, TCDD could impair the ability of Ahr to rescue *ss*$^{-}$ mutants legs. Any other responses to TCDD might fit with a neomorphic transformation.

In order to discriminate between these possibilities, the rescue experiments were repeated in presence of TCDD and the offspring were studied. I carried out the crosses in corn food supplemented with TCDD to a final concentration of 200 ng TCDD/g food. This method of dioxin administration implies constant exposure to the chemical. As the fruit flies spend most of early development in the food (embryonic and larval stages) and dioxins do not require active mechanisms to enter tissues and cells, I assumed that the concentration of dioxin in the larvae/fly would be similar to the concentration in the food. This particular concentration was chosen given that it leads to a severe toxic response in mice (Fernandez-Salguero et al., 1996). However, in the assays in mice dioxin was given in a single hip injection (acute exposure). This difference must be

taken into account since acute and maintained exposure to dioxins might develop different responses. Therefore, the effects that I will show in the following sections should be considered as a consequence of constant exposure to TCDD.

In the presence of TCDD Ahr is able to fully rescue the *ss*$^{-}$ phenotype recovering all the tarsi (Figure 4.1.D). However, the penetrance of the rescue was highly variable. Legs could be classified in three categories:

- 28% of the legs had recovered two tarsi (Figure 4.1.D). I consider this phenotype as a partial rescue. In absence of TCDD, Ahr is able to partially rescue *ss* mutant legs (see section 3.2.1). This indicates that, in these legs, TCDD had no discernable effect on Ahr activity.
- 17% of the legs were fully rescued and were similar to wild-type (Figure 4.1.E). In this case, TCDD enables Ahr to recover full *ss* functions in leg development. Notice that TCDD has no discernable effects on wild type or *ss* mutant flies (Figure 4.1.A and B). Therefore, the phenotypes described above are mediated by Ahr.
- 45% showed one or two recovered tarsi, although these are thinner and lacked bristles (Figure 4.1.F). This extends to the distal region of the first tarsus, indicating that this is a dominant phenotype caused by ectopic Ahr. In flies w;*UAS-ss/+; rn-Gal4/+*, the intermediate tarsal segments are similarly thinner than the wild type, the number of bristles is also reduced, and have no sex-combs (Figure 4.1.F). This phenotype might represent a homeotic transformation to antennae. Ectopic expression of Ss in leg imaginal discs triggers the formation of ectopic aristae, indicating that excessive Ss leads to a change from leg to antennal

identity (Duncan et al., 1998). In this case, addition of TCDD seems to increase Ahr activity to levels comparable with overexpression of Ss.

The degree of variability might be due to the lack of control over the temperature in which flies that were exposed to dioxin grew. For safety reasons, crosses had to be kept in a fumehood. Unfortunately, the temperature was not under the control of a thermostat. Despite the efforts to regulate the temperature, this varied from the 21 to 27 ^{o}C, with an average of 24 ^{o}C. Despite the variability, overall these data show a tendency of TCDD to enhance Ahr activity, leading to full rescues or phenotypes that resemble excess of function of Ss. Thus, the strongest phenotypes might be understood as an excess of activity of Ahr in its developmental functions.

In wild type *ss* is expressed in a ring in the presumptive tarsal region. *ss* represses *dac* proximally and *B* distally, creating and intermediate expression domain. In *ss* mutants, *dac* and *B* expression domains are abutting (data not shown), whereas in flies *w; UAS-Ahr/+; rn-Gal4* ss^{abr}/ss^{sta} the intermediate domain is rescued. This ability remains unaffected in presence of dioxin (Figure 4.2.B), suggesting that addition of dioxin does not affect the specific changes in gene expression driven by Ahr. Hence, TCDD does not decrease activity of Ahr. Notice that dioxin has no effect on expression of *dac* or *B* in wild-type leg imaginal discs (Figure 4.2.A).

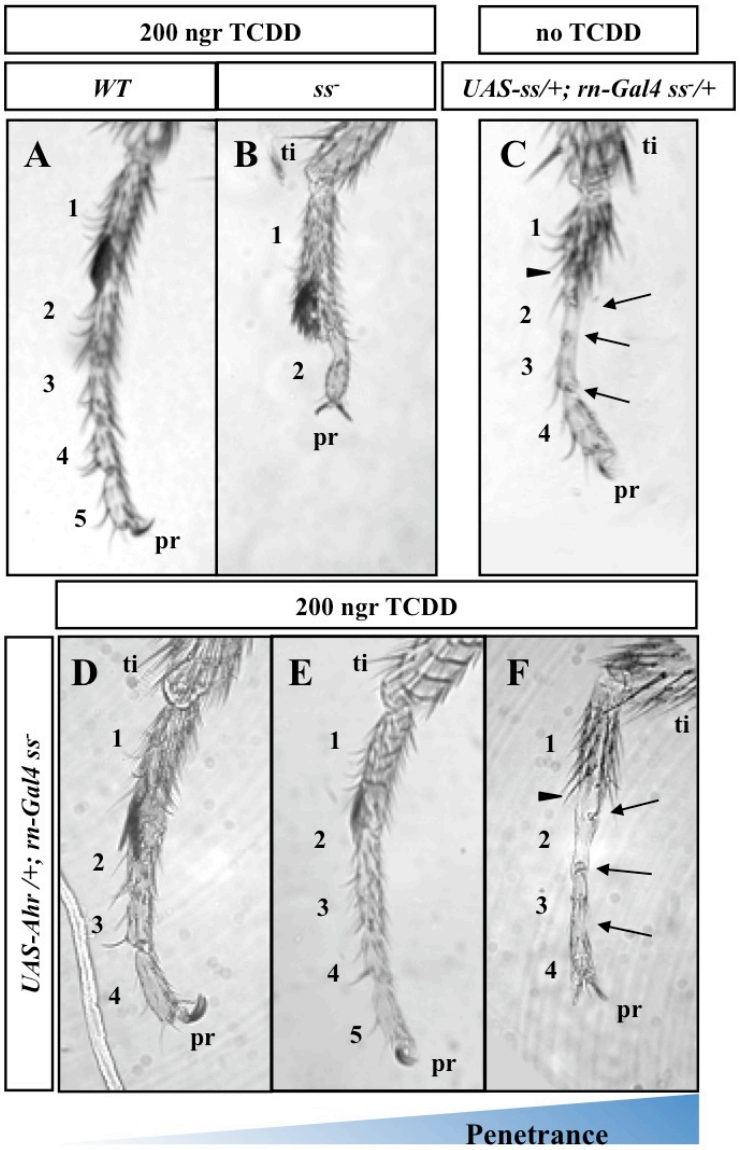

Figure 4.1. Ahr is able to fully rescue *ss*⁻ phenotype in adult leg. All the images represent the tarsal region of a leg from the first thoracic segment of male flies grown in presence of TCDD (A-B and D-F) and in absence of TCDD (C). **(A)** Leg from an Or-R fly. **(B)** Leg from a *w; rn-Gal4 ss^{abr}/ss^{sta}* fly. **(C)** Leg of a *w; UAS-ss/+; rn-Gal4 ss^{abr}/+* heterozygote. **(D-F)** Legs from *w; UAS-Ahr/+; rn-Gal4 ss^{abr}/ss^{sta}* flies. **(D)** A 28% of flies show partial rescue of the tarsal region. **(E)** In 17% the five tarsi are fully recovered. **(F)** 45% of flies show ectopic phenotpe. Notice that in this class tarsi morphology is severely affected as they are reduced in size and lack bristles. Notice that phenotypes in C and F are similar. Arrows indicate the formation of joints and identations between tarsi. Arrowheads point at the missing sex-combs. Numbers indicate the number of present tarsi. Ti and pr refer to the tibia and pretarsus, respectively.

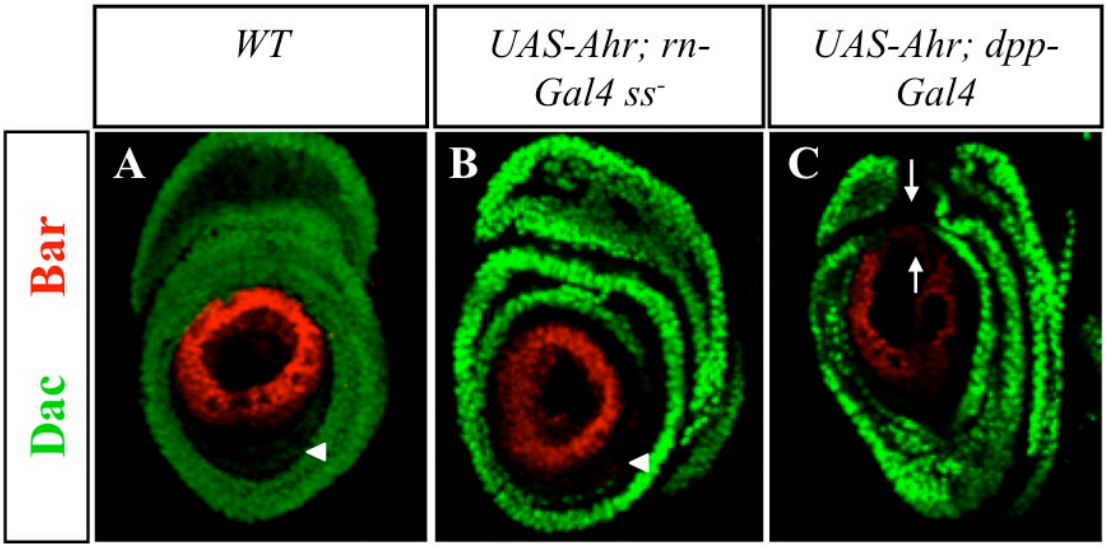

Figure 4.2. Effects of ectopic expression of Ahr in the expression of the genes *dac* and *B* in presence of TCDD. *dac* (green) and *Bar* (red) expression in leg imaginal disc during third larval instar. **(A)** Leg imaginal disc of a wild type. **(B)** leg imaginal disc of a larvae *w; UAS-Ahr/+; rn-Gal4 ss^{abr}/ss^{sta}*. **(C)** Disc of a larvae w; *UAS-Ahr/+; dpp-Gal4/+*. The white arrows indicate the repression of dac and Bar in the dorsal region of the disc. The arrowheads point to the gap between the *Bar* and *dac* expression domains.

4.2.2 Expression of Ahr triggers ectopic phenotypes only in the presence of dioxin

rn-Gal4 is expressed in the central region and the notum of the wing imaginal disc. Therefore, in the rescue experiments shown above, Ahr is expressed ectopically in the wing imaginal disc (St Pierre et al., 2002). However, despite Ahr's ability to rescue *ss* mutant legs, in absence of TCDD, wings of the flies *w; UAS-Ahr/+; rn-Gal4* ss^{abr}/ss^{sta} looked wild type. This indicates that under those experimental conditions Ahr is able to fulfil endogenous functions of *ss,* but it cannot trigger ectopic phenotypes. Interestingly, in the presence of TCDD, expression of Ahr in wing imaginal discs led to a clear reduction in the adult wing size (Figure 4.3.A-C). Individuals could be sorted into three groups depending on the penetrance of the phenotype. In the least affected flies, wings were slightly smaller (Figure 4.3.A) when compared with the negative controls (*rn-Gal4* ss^{abr}/ss^{sta}, Figure 4.3.D). In an intermediate group, wings were severely reduced in size and veins did not form (Figure 4.3.B). In the most affected flies, wing blades were almost entirely reduced (Figure 4.3.C). The severity of the phenotype correlated with the effects observed in adult legs. Notice that *ss* mutants did not show a reduction in wing size (Figure 4.3.D), whereas ectopic expression of Ss led to a great reduction of the adult wing (Figure 4.3.E).

Ectopic expression of Ahr in leg imaginal discs driven by *dpp-Gal4* did not lead to any ectopic phenotype (Figure 4.4.C). In agreement with the phenotypes observed in adult wing, in presence of dioxin, flies *w; UAS-Ahr/ UAS-Ahr; dpp-Gal4/+* showed a phenotype that resembled ectopic expression of Ss: all segments were shorter and wider, and joints and the claw were absent (Figure 4.4.B and D). Notice that the sex-combs were present, indicating that there was not change in segment identity (arrows). This phenotype is fully penetrant.

In order to test whether these phenotypic changes were a consequence of specific changes in gene expression, I checked the expression of the genes *dac* and *B* in leg imaginal disc during third instar. Ectopic expression of either Ss or Ahr repressed *dac* and *B* in the dorsal part of their expression domain (Figure 4.2.C), suggesting that the phenotypes caused by addition of TCDD are due to activation of Ahr. Notice that similar changes in phenotype and gene expression can be observed in the absence of dioxin when Ahr is over-expressed together with either Tgo or Arnt (see Figure 3.3).

Ectopic expression of Ahr in eye imaginal disc driven by *GMR-Gal4* in absence of dioxin had no effect on the adult eye, whereas the addition of TCDD gave rise to a specific ectopic phenotype (Figure 4.5.B, D and F): disruption of the ommatidial arrangement, longer bristles, and the formation of ectopic structures resembling trichomes or bracts (red arrow). The identity of these structures is of great importance, since they might indicate a change in cell identity (see section 3.2.3.). This will be addressed in future experiments. Bristle size is significantly bigger than wild type and close to the pheotype observed in ectopic expression of Ss or Ahr+Tgo (Figure 4.5.G). However, these results have to be treated with caution since, in presence of TCDD, only two *w; GMR-Gal4; UAS-Ahr* flies out of fifty siblings were recovered. This indicates a high degree of lethality of this genotype when flies are treated with TCDD.

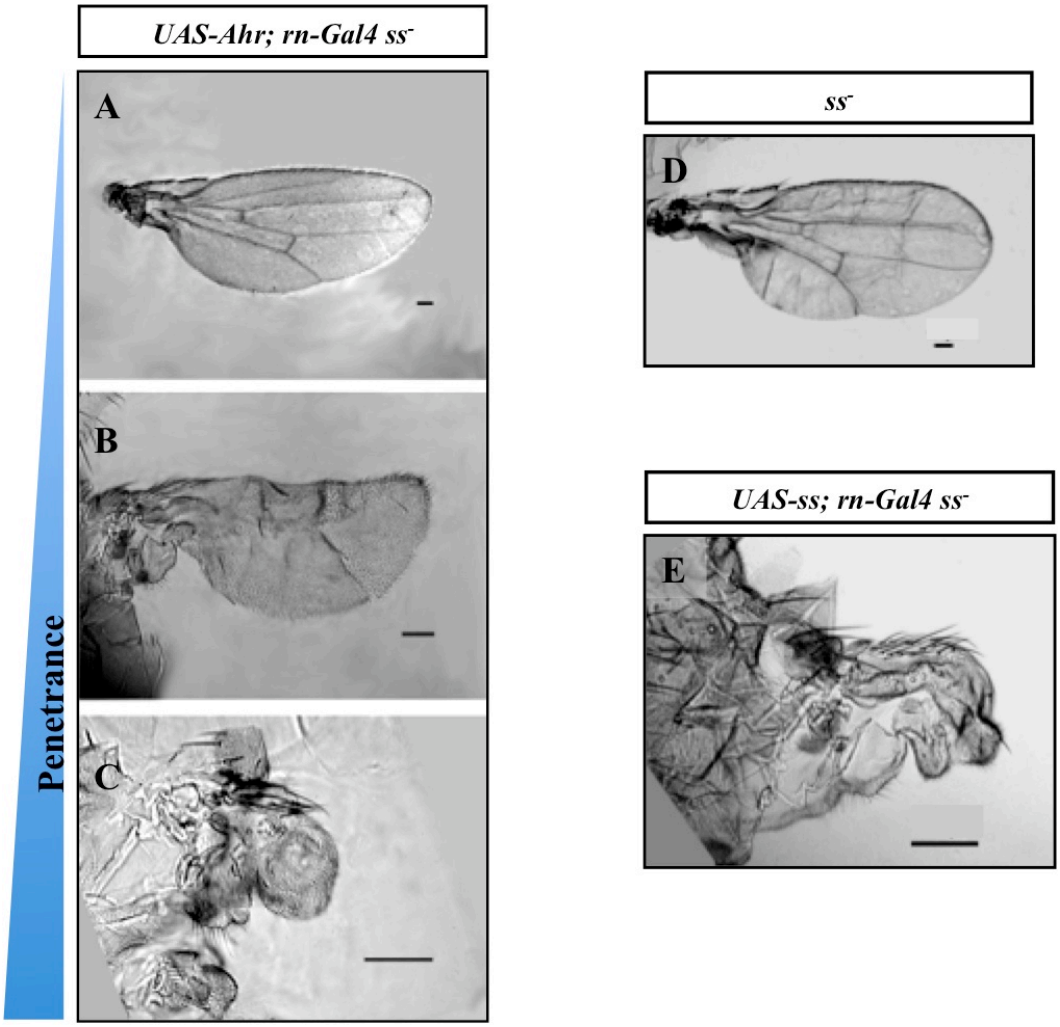

Figure 4.3. In presence of TCDD, expression of Ahr in wing imaginal disc triggers ectopic phenotypes. (A-C) Adult wings of flies *w; UAS-Ahr/+; rn-Gal4* ss^{abr}/ss^{sta} fed with TCDD. Phenotypes are variable. The least penetrant phenotype consists in a slight reduction in size **(A)**, flies with the intermediate penetrance have small veinless wings **(B)**, in severely affected flies wings are almost vestigial **(C)**. **(D)** Wing of a fly *w;; rn-Gal4* ss^{abr}/ss^{sta}. Notice that there is not reduction in size. **(E)** Wing of a fly *w; UAS-ss; rn-Gal4* ss^{abr}/ss^{sta}. Scale bars are 100 μm long.

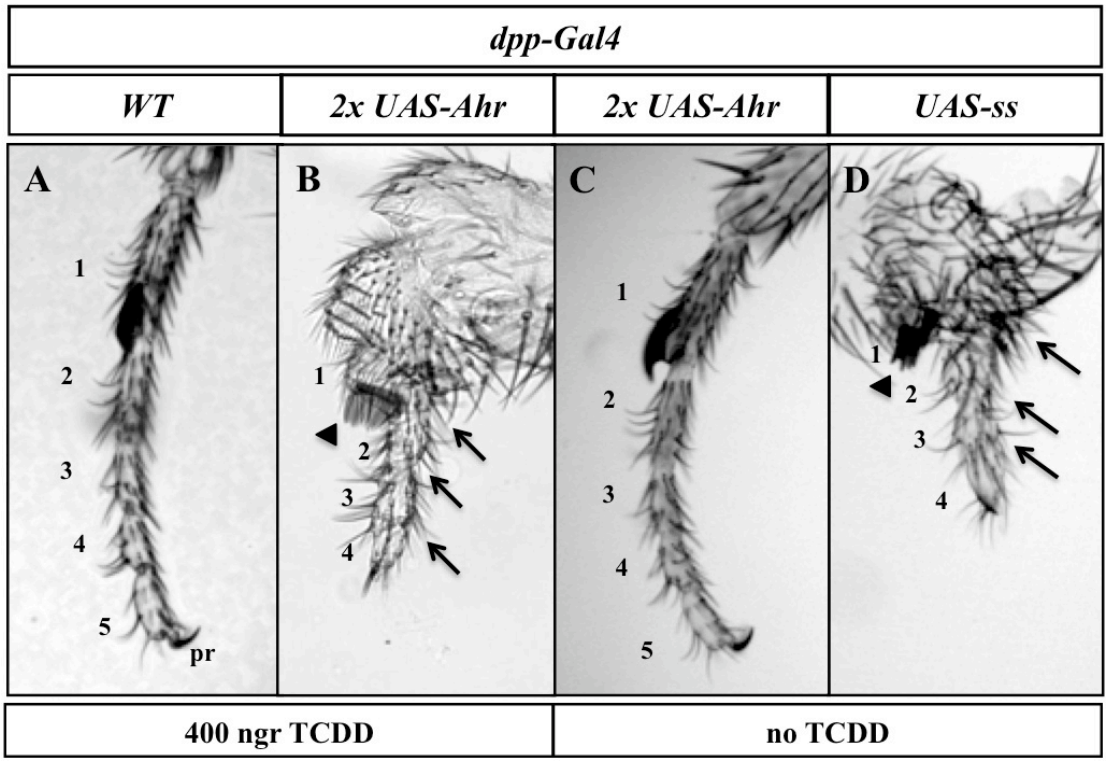

Figure 4.4. Effects of ectopic expression of Ahr on leg development in the presence of TCDD. All images represent the tarsal region of a leg from the first thoracic segment of flies in presence of TCDD (A and B), and in absence of TCDD (C and D). **(A)** Wild-type leg. **(B)** Leg of a *w; UAS-Ahr/UAS-Ahr; dpp-Gal4/+*. **(C)** Leg of a *w; UAS-Ahr/UAS-Ahr; dpp-Gal4/+*. **(D)** Leg of a *w; UAS-ss/+; dpp-Gal4/+*. Numbers indicate the number of present tarsi. Arrowheads point to the presence of sex-combs despite of the changes in phenotype. Arrows point to the presence of indentation between segments.

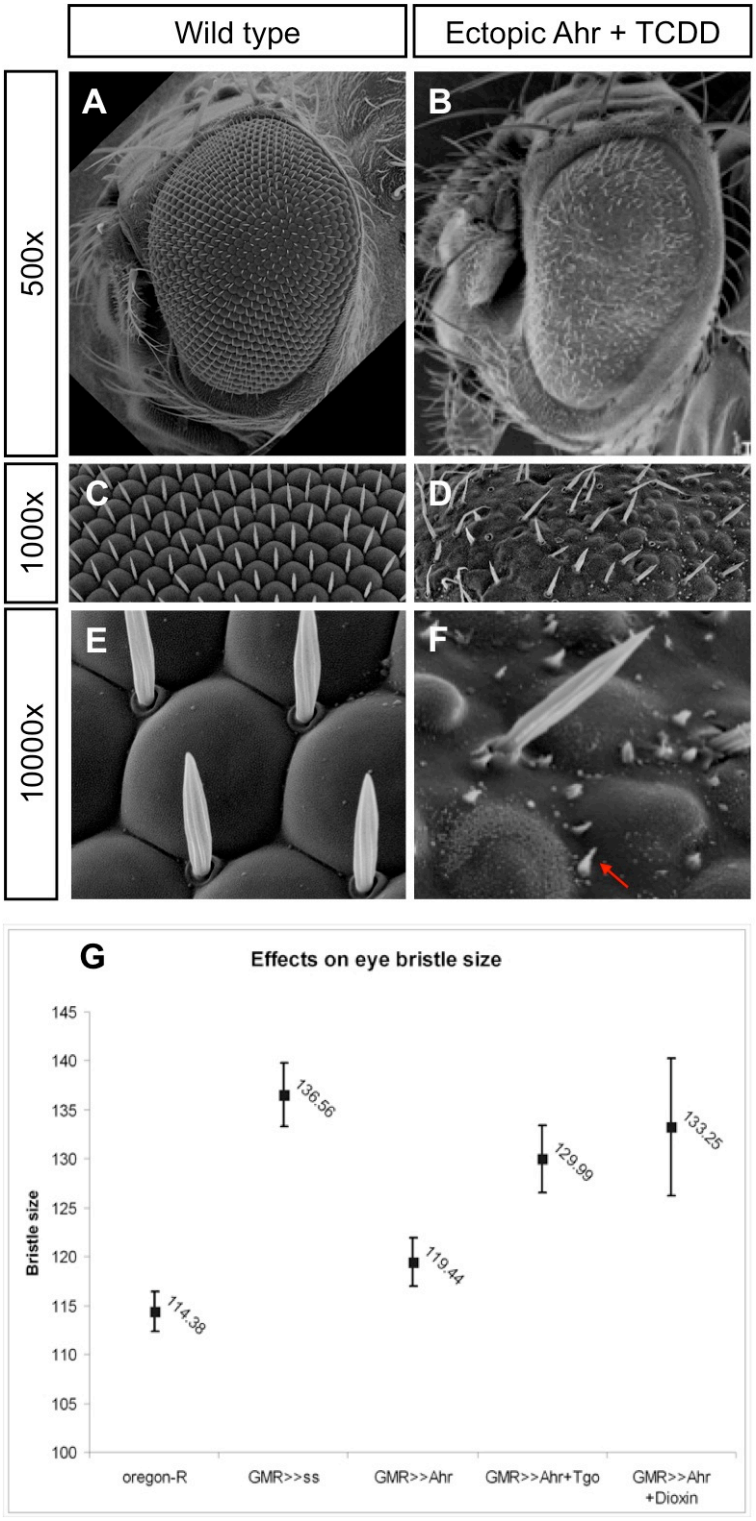

Figure 4.5. Effects on adult eye morphology caused by ectopic expression of Ahr in presence of TCDD. Adult eyes as seen in the scanning electron microscope. Top is dorsal, left is anterior. **(A)** The eye of a wild-type fly. **(B)** Eye of a *w; GMR-Gal4/+; UAS-Ahr/+*. **(C and D)** View at 1000x **(E and F)** View at 10000x. The red arrow points at one of the ectopic structures that resemble trichomes or bracts. **(G)** Average size of eye bristles and their standard errors.

4.2.3. Changes in the affinity of Ahr for its dimerisation partner in the presence of TCDD

The effects on adult morphology and changes in gene expression triggered by TCDD are similar to those caused by Ahr in the presence of Arnt or extra Tgo (see section 3.2.2 and 3.2.3). Both Arnt and Tgo are transcription factors with the ability to form different heterodimeric complexes with bHLH proteins other than Ahr and Ss (Swanson et al., 1995; Ward et al., 1998). Different complexes have different DNA binding sites (Emmons et al., 1999; Swanson et al., 1995). For this reason, competition for the different partners is a mechanism of regulation of the activity of Arnt and Tgo. This way, Arnt and Tgo can have different roles in different tissues at varying times during development (Chan et al., 1999; Emmons et al., 1999; Swanson et al., 1995).

For instance, Arnt forms a complex with HIF1α. This complex binds to the HREs (Hypoxia Response Elements) (Wang et al., 1995). In competition assays using EMSA (Electrophoretic Mobility Shift Assay) Ahr is shown to compete with HIF1α for binding to Arnt (Chan et al., 1999). Addition of Ahr reduces the affinity of Arnt::HIF1α complex to its specific DNA binding site. Ability of Ahr to quench Arnt is clearly higher in presence of β-naptoflavone (βNF); a known ligand of Ahr (Chan et al., 1999; Swanson and Perdew, 1993).

These results suggest that the effects caused by Ahr in the presence of TCDD might be due to an increase in the affinity for endogenous Tgo. I conducted coimmunoprecipitation assays to analyse the ability of Ahr to bind Tgo or Arnt in the presence and absence of TCDD. Synthetic Ahr protein is able to bind TCDD as shown in velocity sedimentation on sucrose gradients (Butler et al., 2001). All proteins were synthesized in the TNT coupled transcription/translation system. Ss and Ahr were labelled with methionine tagged with S^{35}. Protein lysates were incubated together and

TCDD was added during the incubation. Tgo and Arnt were pulled using anti-Tgo and anti-Arnt monoclonal antibodies, respectively. Under my experimental conditions, greater affinity of Ahr for either Tgo or Arnt was not observed (Figure 4.6.A). However, this is an *in vitro* system where no other competitors are present, meaning that there are not limitations for these proteins to interact.

Notice that the amount of Tgo present in the assays is slightly higher than the amount of Arnt (Figure 4. 6.B), whereas more Ahr-S^{35} protein seems to consistently precipitate with Arnt (Figure 4.6.A), indicating that under these conditions Ahr must have greater affinity for Arnt than for Tgo. This is not surprising as Arnt is Ahr's natural partner.

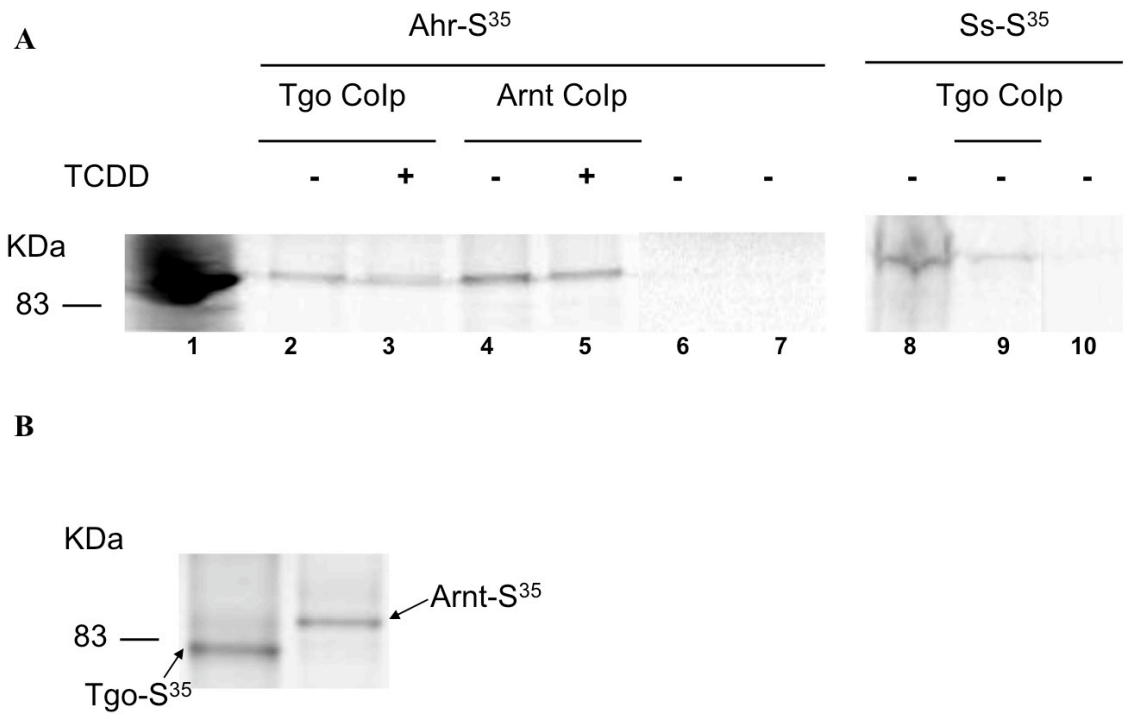

Figure 4.6. Ahr coimmunoprecipitates with Tgo and Arnt. (A) Coimmunoprecipitation assay. All proteins were synthesized in the TNT coupled transcription/translation system. Ahr and Ss were labeled with S^{35}. Lanes 1 and 8 show the load of Ahr and Ss, respectively. The amount of protein added in the assays is ten times higher than the load. Ahr co-precipitates with Tgo (lanes 2 and 3) and Arnt (lanes 4 and 5), in presence and absence of TCDD (lanes 3 and 5). As a negative control the assays were carried out in absence of Tgo and Arnt (lanes 6 and 7 respectively). Ss precipitates with Tgo (lane 9). As a negative control the assay was carried in absence of Tgo (lane 10). **(B)** Tgo-S^{35} and Arnt-S^{35} precipitate with anti-Tgo and anti-Arnt, respectively.

4.3. DISCUSSION

In my experimental system I have placed Ahr in a developmental context and demonstrated that Ahr has the innate ability to fulfil the endogenous functions of Ss; a key regulator in *Drosophila*'s development (as shown in the section 3.2.1). When the same system is exposed to dioxin, Ahr is also able to mimic the response to ectopic expression of Ss. The variability observed in the phenotypes caused by Ahr in the presence of TCDD could be due to fluctuations in the temperature in which the flies were raised. However, the results indicate a clear tendency to enhance the phenotypes and changes in gene expression. Given that in this system none of the examined elements except Ahr are responsive to dioxins, my data suggests that TCDD increases activity of Ahr. This agrees with the hypothesis that dioxin toxicity can be considered as a hyperactivation of Ahr in its developmental functions. Therefore, Ahr seems to have two levels of activity, endogenous and "toxic", with dioxin being the element that triggers the transition between the two levels. Notice that, given the experimental design, the effects I have described in this chapter must be understood as the result of constant exposure to TCDD rather than an acute response.

The current model of Ahr-mediated transcription differentiates between two checkpoints in the regulation of Ahr activity: first, nuclear translocation upon ligand-binding; second, formation of a transcriptional complex with Arnt (McMillan and Bradfield, 2007). In my experimental system, cellular localisation is not a limiting factor as Ahr is nuclear and functional in absence of ligand (as shown in the sextion 3.2.4). This feature is biologically meaningful as, in vertebrates, Ahr has functions in development that are not ligand-dependent (Fernandez-Salguero et al., 1995). These

observations suggest that binding to Arnt might represent the major regulatory event of Ahr activity.

Arnt and Tgo form heterodimeric complexes with other bHLH proteins (Swanson et al., 1995; Ward et al., 1998). Different complexes bind different DNA motifs (Emmons et al., 1999; Swanson et al., 1995). The balance of various bHLH-PAS proteins in the nucleus is a key mechanism of regulation of the activity of Ahr and Ss. Competition between Ahr or Ss and other partners of Arnt or Tgo results in different developmental outcomes (Chan et al., 1999; Emmons et al., 1999). As shown in section 3.2.2, addition of extra Tgo or ectopic expression of Arnt in flies expressing Ahr leads to ectopic phenotypes and changes in gene expression that resemble those caused by exposure to dioxin. Given that Tgo is ubiquitously expressed (Sonnenfeld et al., 1997), this suggests that TCDD might be helping Ahr make more efficient use of the reserves of Tgo in the cell. In other words, TCDD might increase the affinity of Ahr for Tgo, so it would be able to better compete for Tgo. If this was the case, dioxin toxicity could be understood as the disruption of the balance of heterodimeric complexes formed by Arnt/Tgo in the nucleus.

In *in vitro* coimmunoprecipitation assays, TCDD does not seem to increase the affinity of Ahr for Arnt. This result might represent the real biological scenario, meaning that TCDD has no effect on the formation of the heterodimeric complex. However, it might also be due to limitations in the system, since there are no other partners of Arnt to compete against. The later possibility is supported by competition experiments that have been conducted in EMSA assays. Addition of Ahr is able to disrupt the ability of Arnt::HIF1α complexes. The presence of βNF seems to enhance this ability, indicating that addition of βNF unbalances the formation of heterodimers with Arnt (Chan et al., 1999). It has not been addressed in this work whether TCDD is

increasing the transcriptional activity of the Ahr::Tgo dimmer. In fact, TCDD might be enhancing the affinity of the Ahr::Tgo complex by its DNA binding site. This issue will be approached in the future with electrophoretic mobility shift assays .

Ahr has been widely studied in the context of xenobiotic toxicity. However, Ahr also seems to be part of a developmental network. Development happens in three dimensions: time, space, and genetic context. The later means that the fragile balance between the different factors that drive development is key in the formation of a new organism. My results suggest that part of the toxic effects of dioxin can be understood as a disruption of developmental networks.

In a broader sense, we are protected from xenobiotics through a battery of genes activated by the dioxin receptor (Fernandez-Salguero et al., 1995; Mimura et al., 1997). Until today, toxicity triggered by dioxins other than TCDD is believed to be caused by oxidative metabolites released upon digestion of these chemicals. This work demonstrates that the effect of these pollutants on the developmental program remains to be determined.

Chapter 5

The Aryl Hydrocarbon Receptor and Spineless interact with the zinc-finger proteins Squeeze and Rotund

5.1. INTRODUCTION

Most studies on *Ahr* biology have been conducted in the "framework of xenobiotic toxicity" (quoting McMillan and Bradfield (McMillan and Bradfield, 2007)), whereas endogenous roles of *Ahr* are still mostly undetermined. As shown in the previous chapters Ahr and Ss are highly conserved, thus Ahr is able to fulfill Ss functions in leg development, and undergo the same specific interactions with proteins and DNA motifs. For this reason, the study of Ss might help us to understand more about the biology of Ahr and the mechanisms of action involved in its endogenous role.

With the work shown in this chapter I aim to find out new elements of the network in which *ss* operates. Since Ahr and Ss seem to function by similar means, this

will help as to better understand the mechanisms of action of Ahr. For this purpose I conducted an enhancer and suppressor assay in the adult eye of *Drosophila melanogaster* (Figure 5.1). This is not the first time that the eye of the fruit fly has been employed to study the effects of overexpression of mammalian genes (see Figure 1.8) (de Nooij et al., 1996), since mutant phenotypes in the eye do not affect the viability of the organism. The eyes of a fly have a very well defined and repetitive structure, which makes it easy to detect phenotypic changes. In the screen, I used a fly strain that expresses ectopically Ss in the eye imaginal disc (*w; GMR-Gal4; UAS-ss*^{C2}). The adult eye of these flies has a particular phenotype: lack of pigmentation in the centre of the eye, roughness, and thicker and longer bristles in the dorsal anterior part of the eye (referred to as ss-eye phenotype here after) (Figure 5.2.B). I tested the effect of removing one copy of a candidate gene over this ss-eye phenotype. As deficiencies are equivalent to null mutations, I set up crosses between strains carrying individual deficiencies in the third chromosome, and the strain *GMR-Gal4; UAS-ss*^{C2} (Figure 5.1). Removing the copy of a gene upregulated by *ss* would ideally suppress the ss-eye phenotype. The same effect would be seen when removing the copy of a gene coding for an activating co-factor. Reciprocally, removing the copy of a gene downregulated by *ss* or coding for a repressing co-factor would result in an enhancer of the phenotype.

Thus, making use of the *UAS/Gal4* system, clonal analysis, and co-immunoprecipitation assays, in this chapter I will show that:

- *ss* interacts with two genes that encode for zinc-finger proteins of the C_2H_2 Krüppel type: *squeeze* (*sqz*) and *rotund* (*rn*) (St Pierre et al., 2002). *sqz* has been isolated as a candidate to interact with *ss* from the enhancer and suppressor screen. *rn* is the closest homologue of *sqz*, and it is coexpressed with *ss* in leg

imaginal disc. Sqz protein might also repress Rn activity by competition to the same binding site (Terriente Felix et al., 2007).

- *ss* does not control expression of *sqz* or *rn*, in agreement with work recently published (Pueyo and Couso, 2008). I will also show that Ss and Rn interact physically in *in vivo* experiments.
- Ss and Rn are able to repress expression of the *ta5-enhancer*, suggesting that bHLH-PAS and zinc-finger proteins interact physically to drive changes in gene expression.
- *Ahr* is able to interact functionally with *sqz* and *rn*, showing that the ability to interact with zinc-finger proteins from the C_2H_2 Krüppel family might be a trait that has remained conserved between *ss* and *Ahr*.

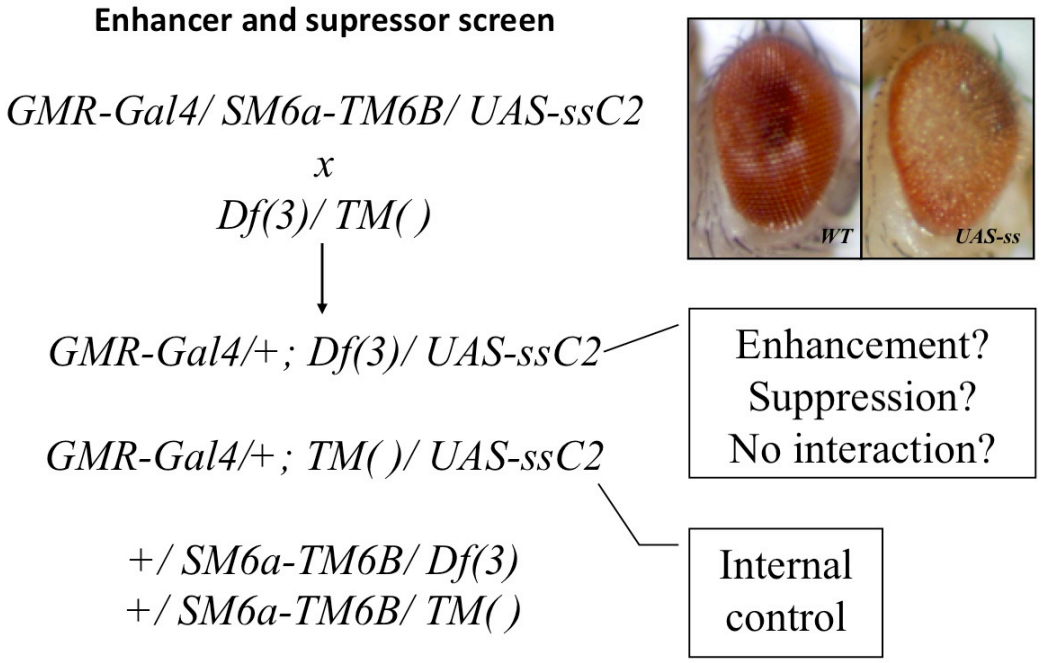

Figure 5.1. Enhancer and suppressor screen. Females from the strain *GMR-Gal4/ SM6a-TM6B/ UAS-ss*^{C2} were crossed to males from 140 different deficiencies located along the third chromosome. The offspring were sorted according to the presence of phenotypic markers. Flies without balancer chromosomes were studied as the experimental group, and were compared to the flies *GMR-Gal4/+; TM( )/UAS*-ss^{C2} (Internal control). The pictures next to the parental cross show the ss-eye phenotype versus a wild type eye.

5.2. RESULTS

5.2.1. Enhancer and suppressor screen

The objective of this work was to identify new factors that might be key to *ss* functions. First, I assessed whether the ss-eye phenotype is specific, i.e. it is due to the effect of ectopic ss on its normal targets or interactors, not to its effects on artefactual or ectopic interactors. For this reason, I tested null alleles of known interactors of *ss* in leg imaginal disc: *tgo*, and *dac.*

tgo and *ss* genes have close functional relationship in leg and antennal development (Emmons et al., 1999). *tgo* is ubiquitously expressed and act as a partner for many other bHLH-PAS transcription factors (Ohshiro and Saigo, 1997; Sonnenfeld et al., 1997). *tgo* mutant alleles enhance ss^{-} phenotypes and tgo^{-} somatic clones show antennal, leg, and bristle defects that are very similar to ss^{-} mutants (Emmons et al., 1999).

dac is a gene that encodes a transcription factor involved in the development of several organs such as the eye, antenna, and leg (Dong et al., 2002; Mardon et al., 1994). In *dac* mutants, the eyes are severely reduced or absent, and the femur, tibia, and proximal three tarsi are reduced. In the eye imaginal disc, *dac* is expressed at the posterior margin before the initiation of the morphogenetic furrow. Posterior to the furrow, *dac* is expressed in photoreceptors R1, R6, and R7, and the cone cells. In the leg imaginal disc, *dac* is expressed in a ring in the distal half (Mardon et al., 1994). Until mid larval instar, the *dac* expression domain abuts distally with the *B* expression domain. *ss* and *rn* are expressed during mid-third larval instar between both domains. *ss* and *rn* repress *dac* proximally and *B* distally thus creating an intermediate domain between *dac* and *B* (Pueyo and Couso, 2008).

I crossed null alleles of *tgo* and *dac* with the strain *w; GMR-Gal4/SM6a-TM6B/UAS-ss*^{C2}. *tgo*$^{-}$ suppressed the ss-eye phenotype (Figure 5.2.C), while over-expression of *tgo* or removing one copy of *dac* enhanced it (Figure 5.2.D and E, respectively). Given that *dac* and *tgo* are closely related to *ss* functions in leg development, the fact that *dac* and *tgo* interact with the ss-eye phenotype suggests that *ss* is driving the same changes in gene expression in eye and leg imaginal disc. This indicates that the adult eye is a good system to carry out an enhancer and suppressor screen.

For my screen I tested 140 deficiencies. These deficiencies were the ones selected by Bloomington for a kit of deletions covering the entire third chromosome. I narrowed interacting regions by comparing the results of overlapping deficiencies. From this search I isolated seven regions on the third chromosome suppressing the ss-eye phenotype, and five that enhanced it (Table 5.1). I followed the regions 91F4-8 and 98B1-5 given that they are the two smallest regions isolated from the screen (Figure 5.3.A and B). The region 91F4-8 suppressed the ss-eye phenotype and region 98B1-5 enhanced it (Table 5.1). I started a systematic search of single candidate genes in these regions, by looking at the expression pattern of *lacZ* reporters. Three of them showed an expression pattern in the leg imaginal disc reminiscent of *ss* (Figure 5.4.A) (Duncan et al., 1998), *l(3)02102*^{02102} (Figure 5.4.B) and *l(3)3675*^{3675} (Figure 5.4.C) in the region 91F4-8 (Figure 5.3.A, green and blue arrowhead, respectively); and *ms(3)98B*^{6302} (Figure 5.4.D) in the region 98B1-5 (Figure 5.3.B, orange arrowhead). The *lacZ* expression of the P-elements *l(3)02102*^{02102} and *l(3)3675*^{3675} was weak or completely absent in early and mid third instar in leg imaginal disc. This observation indicates that, providing that these P-elements represent true interactors, they would be downstream of *ss*.

The P-element *ms(3)98B*^{6302} was generated by single P element mutagenesis in order to create a collection of male-sterile mutants (Castrillon et al., 1993). X-Gal staining shows very strong *lacZ* expression in a ring in the distal part of the leg imaginal disc during later third instar. Expression also extends proximally in the ventral half in a pattern that is reminiscent of *wg* (Figure 5.4.D). No gene related to the P element has been annotated.

The P-element *l(3)3675*^{3675} was first identified in the Berkeley *Drosophila* genome project gene disruption project (Spradling et al., 1999). The *lacZ* gene is expressed faintly in the chordotonal organ and a ring in the distal half of the leg imaginal disc during later third instar (Figure 5.4.C). No related gene is annotated.

The P-element *l(3)02102*^{02102} is a transgenic insertion that was first identified in a screen for zygotic lethal mutations (Perrimon et al., 1996). X-Gal stainings show expression of the *lacZ* reporter in the chordotonal organ and in a ring in the distal part of the leg imaginal disc during late third instar (Figure 5.4.B). The stainings also reveal expression in the presumptive maxillary palp in the antennal imaginal disc, in the morphogenetic furrow, and in the anteroventral part of the wing imaginal disc (Figure 5.4.E and F). The P-element *l(3)02102*^{02102} has been shown to report the expression of *squeeze* (*sqz*) (Allan et al., 2003; McGovern et al., 2003). The *sqz* gene encodes a zinc finger protein of the C_2H_2 Krüppel-type. It forms part of a conserved subfamily of zinc-finger proteins together with *Drosophila* Rotund, *C. elegans* Lin-29, and rat CIZ.

sqz plays a key role in the determination of Tv neurons during CNS development (Allan et al., 2003). *sqz* works in a combinatorial code with other transcription factors to predetermine Tv cell identity (Allan et al., 2003; Miguel-Aliaga et al., 2004). It has been suggested that *sqz* regulates *dachshund* expression in these

neurons (Miguel-Aliaga et al., 2004). *sqz* is also expressed in the wing imaginal disc (Terriente Felix et al., 2007).

When the strain *GMR-Gal4 UAS-ss*^{C2} was crossed to the strain *sqz*$^{i.e}$*/TM6B* the experimental offspring did not show suppression nor enhancement of any of the traits of the ss-eye phenotype (data not shown). The allele *sqz*$^{i.e}$ is reported to be a null allele generated by the imprecise excision of the *P(GawB)* of *sqz-Gal4*, which was generated from the conversion of the P-element *l(3)02102*^{02102} (*sqz-lacZ*) (Allan et al., 2003; McGovern et al., 2003). *sqz*$^{i.e}$*/sqz*^{Df} genotype displays a 100% larval lethality. PCR analysis from genomic DNA confirmed that the excision generated a deletion of the second and the third exon, although the precise 3' breakpoint has not been determined (Allan et al., 2003). Notice that *sqz-lacZ* is expressed in the eye imaginal disc during 3rd larval instar (Figure 5.4.E, arrow), suggesting that Sqz is present when Ss is ectopically expressed. Three different scenarios can be considered. First, *sqz* is not a real interactor of *ss* and therefore it is not responsible for the suppression caused by deletions covering the region 91F4-8. Second, such an interaction might require a second factor contained within the same region. Third, *sqz*$^{i.e}$ is a hypermorph allele (excess of function), explaining why *sqz*$^{i.e}$ and *sqz*^{Df} do not show the same sort of interaction. In this instance *sqz*$^{i.e}$ should enhance the ss-eye phenotype. Since this is not the case, the later possibility seems to be unlikely. Further analysis on the interaction between *ss* and *sqz* was required.

In order to ascertain the role of *sqz* in leg development I induced *sqz*$^{i.e}$ somatic clones by mitotic recombination. Twenty-two clones were found in the tarsal region. Clones showed no phenotype apart from an ectopic sex-comb found in the first tarsal segment and second tarsal segment of two different males (Figure 5.5.B and C). In addition, from the cross *sqz-lacZ x Df(3R)Dl-KX23* (*sqzDf*), two scapers of the genotype

sqz-lacZ /Df(3R)Dl-KX23 (*sqzDf*) were found among the control offspring of five hundred siblings. These two flies did not show any mutant phenotype in adult leg (Figure 5.5.D). Altogether these data suggest that *sqz* is redundant in function with *ss* in leg development, hence the weak and variable interaction observed between *sqz* and *ss*.

Table 5.1. Genomic regions that show interaction with the ss-eye phenotype. The interacting regions were defined by their cytological coordinates. Regions were delimited by the study of overlapping deficiencies. All the deficiencies used in this screen delete parts of the third chromosome. In the table “sup.” stands for suppression, “enh.” stands for enhancer, and “0” stands for no interaction.

Table 5.1

Region	Interaction with region	Deficiency	Deletion	Interaction with deletion
67E3;68A3	Sup.	Df(3L)BSC14	67E3-7;68A2-6	Sup.
		Df(3L)vin5	68A2-3;69A1-3	Enh.
		Df(3L)vin2	67F2-3;68D6	Enh.
68A2;68A6	Enh.	Df(3L)vin5	68A2-3;69A1-3	Enh.
		Df(3L)vin2	67F2-3;68D6	Enh.
		Df(3L)ED4470	68A6;68E1	0
68E1;68F2	Sup.	Df(3L)Exel6115	68E1;68F2	Sup.
		Df(3L)vin7	68C8-11;69B4-5	0
79E3;79F1	Enh.	Df(3L)HD1	79D3-E1;79F3-6	Enh.
		Df(3L)Ten-m-AL29	79C1-3;79E3-8	0
		Df(3L)Delta1AK	79E5-F1;80A2-3	0
85D1;85D11-14	Sup.	Df(3R)BSC24	85C4-9;85D12-14	Sup.
		Df(3R)ED5331	85C3;85D1	0
		Df(3R)ED5339	85D1;85D11	0
85F1-2 or 86C7-8	Enh.	Df(3R)BSC38	85F1-2;86C7-8	Enh.
		Df(3R)Exel6155	85F1;85F10	Sup.
		Df(3R)ED5495	85F16;86C7	0
85F2-10	Sup.	Df(3R)Exel6155	85F1;85F10	Sup.
		Df(3R)Exel6265	85F10;85F16	0
91B1-2 or 91C1-5	Enh.	Df(3R)Cha7	90F1-F4;91F5	Enh.
		Df(3R)DG2	89E1-F4;91B1-2	0
		Df(3R)07280	91B2;91C1	0
		Df(3R)ED5911	91C5;91F4	0
91F4-8	Sup.	Df(3R)Dl-Bx12	91F1-2;92D3	Sup.
		Df(3R)Exel6183	91E4;91F8	Sup.
		Df(3R)ED5911	91C5;91F4	0
92A11-B3	Sup.	Df(3R)Dl-Bx12	91F1-2;92D3	Sup.
		Df(3R)ED5942	91F12-92B3	Sup.
		Df(3R)Ed6025	92A11-E2	Sup.
		Df(3R)Exel6184	92A5;A11	0
92B3;92E2	Enh.	Df(3R)H-B79	92B3;92F13	Enh.
		Df(3R)Exel6185	92E2;92F1	0
98B1-98B5	Sup.	Df(3R)BSC42	98B1-2;98B3-5	Enh.

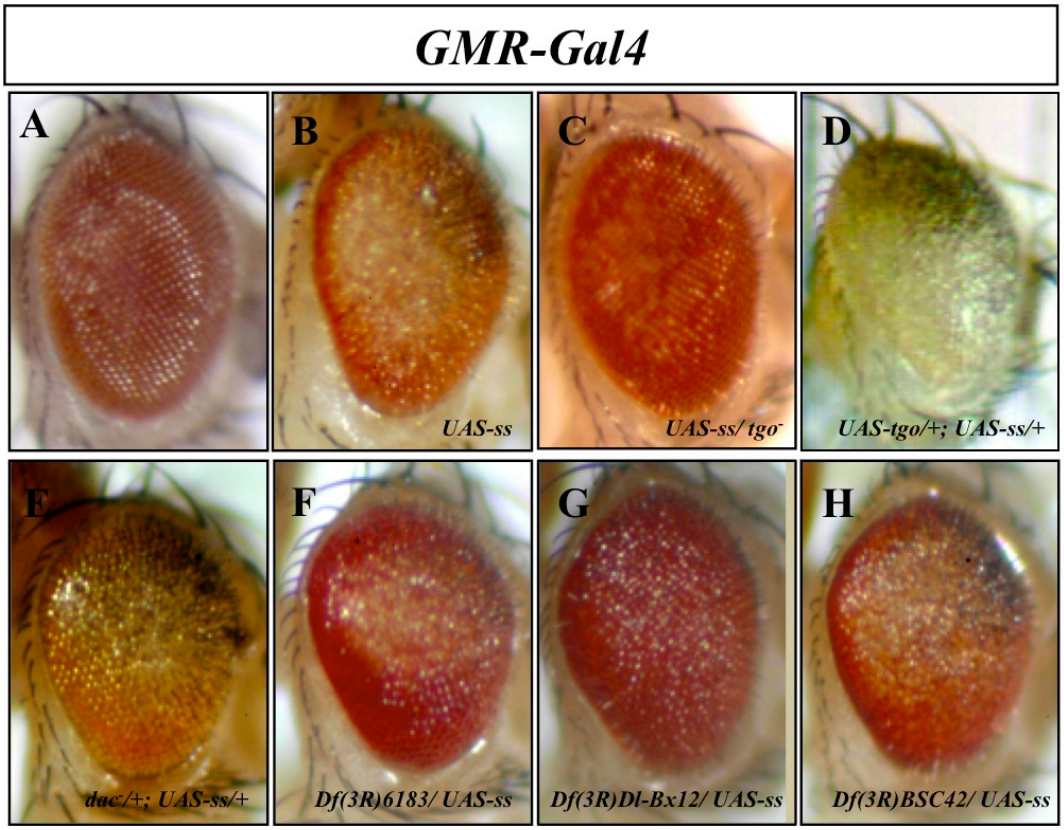

Figure 5.2. Different genotypes interact with the ss-eye phenotype. (A) The eye of a wild-type fly. Top is dorsal, right is anterior. **(B)** Eye of a *w; GMR-Gal4/SM6a-TM6B/UAS-ss^{C2}* (ss-eye phenotype) **(C)** Eye of a *w; GMR-Gal4/+; UAS-ss^{C2}/tgo^{-}*. Removing one copy of the gene *tgo* suppresses the ss-eye phenotype. **(D)** Eye of a *w; GMR-Gal4/UAS-tgo; UAS-ss^{C2}/+*. Overexpression of *tgo* enhances the ss-eye phenotype. **(E)** Eye of a *w; GMR-Gal4/dac^{-}; UAS-ss^{C2}/+*. Removing one copy of the gene *dac* enhances the ss-eye phenotype. **(F)** Flies *w; GMR-Gal4; UAS-ss^{C2}*/Df(3R)6183 show suppression of the ss-eye phenotype. **(G)** Flies *w; GMR-Gal4; UAS-ss^{C2}*/Df(3R)Dl-Bx12 Show suppression of the ss-eye phenotype. **(H)** Flies *w; GMR-Gal4; UAS-ss^{C2}*/Df(3R)BSC42 Show suppression of the ss-eye phenotype.

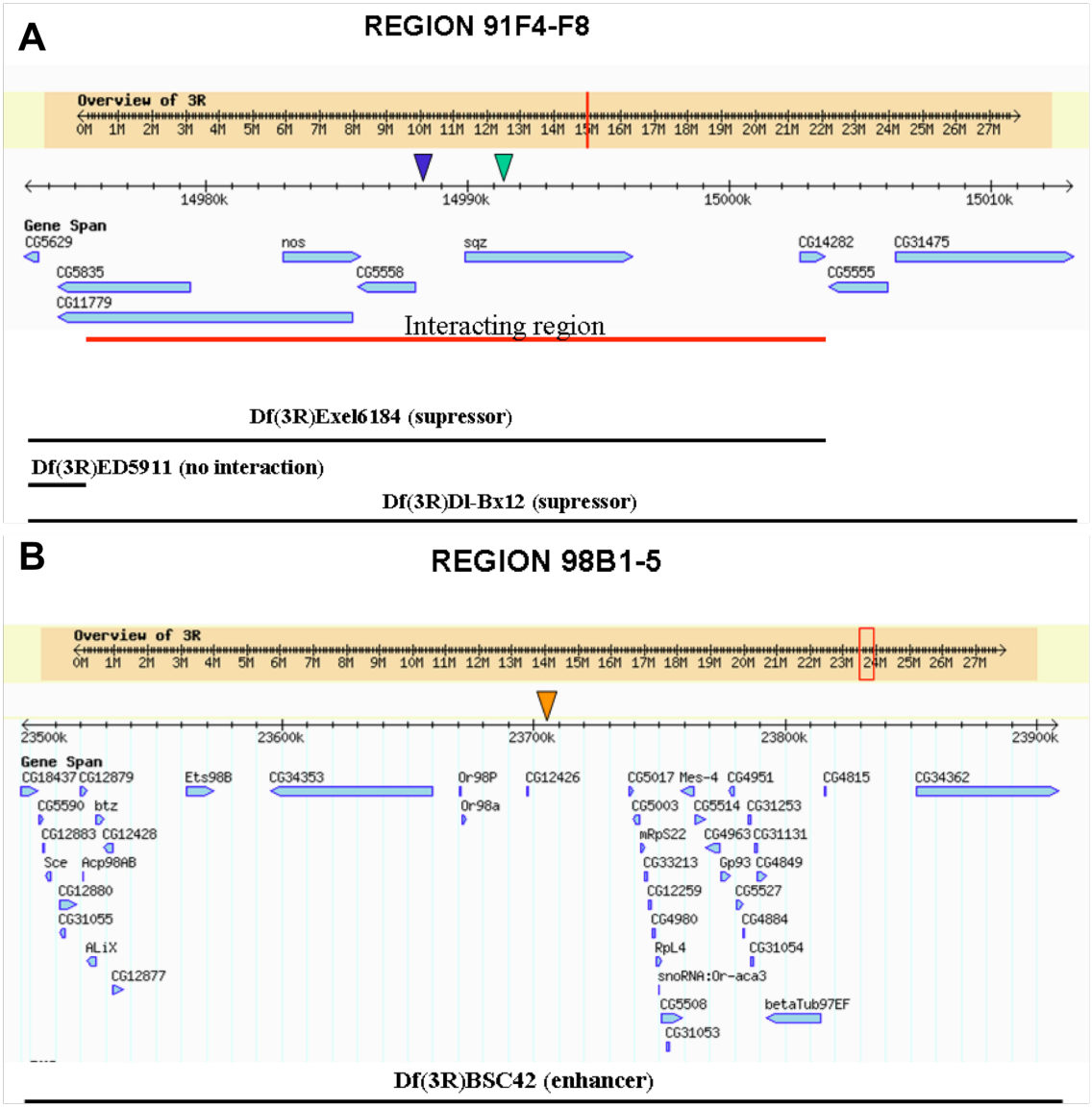

Figure 5.3. Map of interacting regions 91F4-8 and 98B1-5. **(A)** Interacting region 91F4-F8. The red stripe marks the region that suppressed the ss-eye phenotype. The overlapping deficiencies *Df(3R)Exel6183* and *Df(3R)Dl-Bx12* partially suppressed the lack of colour in the centre of the eye, longer bristles, and roughness. The area was narrowed by the non-interacting deficiency *Df(3R)ED5911*. The arrowheads show he transgenic insertions $l(3)02102^{02102}$ (known as *sqz-lacZ*; green arrowhead) and $l(3)03675^{03675}$ (blue arrowhead). **(B)** Interacting region 98B1-B5. This region was narrowed only by the deficiency *Df(3R)BSC42*, which enhanced the ss-eye phenotype. The location of the transgenic insertion $ms(3)98B^{6302}$ is pointed by the orange arrowhead. Notice that the scales of each map are different.

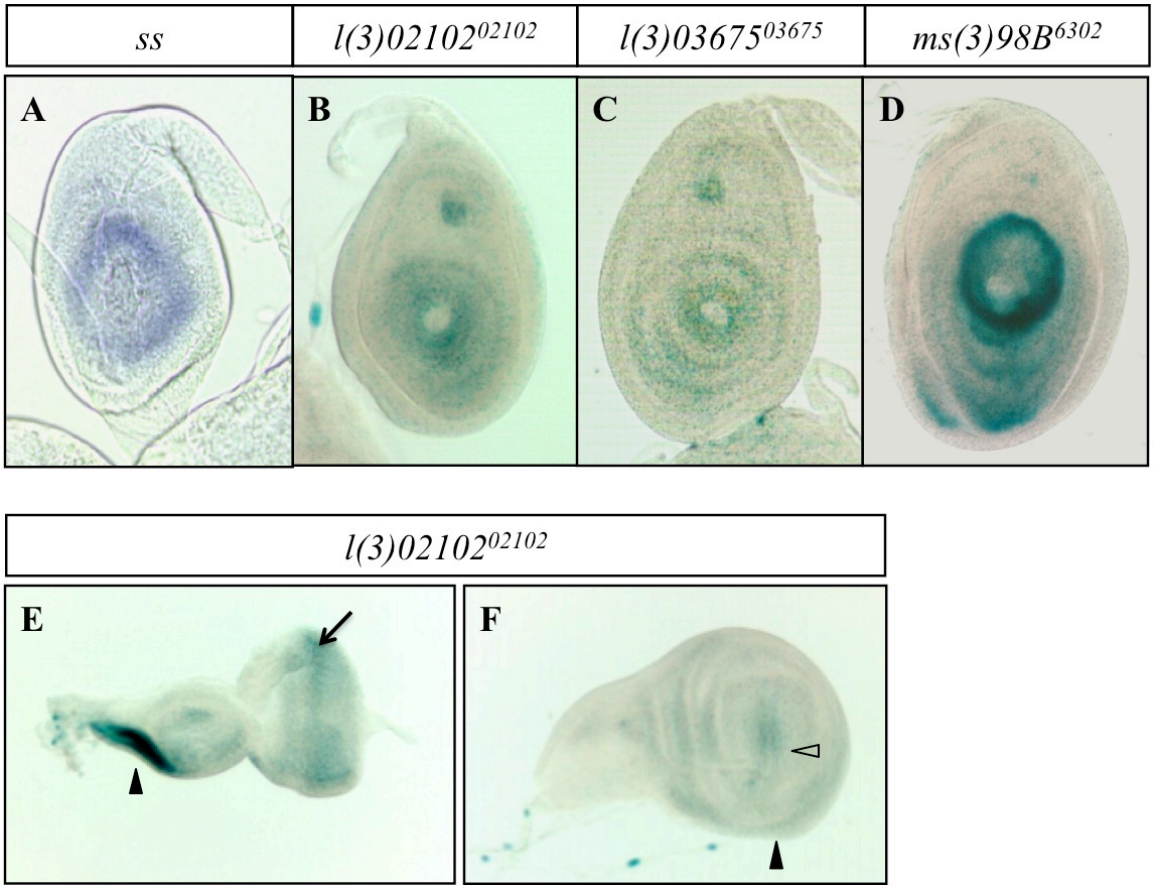

Figure 5.4. Expression pattern of ss and the P-elements found on the enhancer and suppressor screen. (A) Expression of *ss* mRNA in wild type leg imaginal disc in the mid third instar. **(B-D)** X-Gal staining in leg imaginal discs from late third instar larvae. **(B)** P-element $l(3)02102^{02102}$ expression reporting *sqz* expression (interacting region 91F14-8). **(C)** P-element $l(3)3675^{3675}$ *lacZ* expression (interacting region 91F4-8). **(D)** P-element *ms(3)98B6302 lacZ* expression (interacting region 98B1-5). **(E and F)** The P-element $l(3)02102^{02102}$ is expressed in the morphogenetic furrow (arrow) and in the presumptive maxillary palp (arrowhead) **(E)** and in the presumptive wing margin (open arrowhead) and hinge (solid arrowhead) **(F)**.

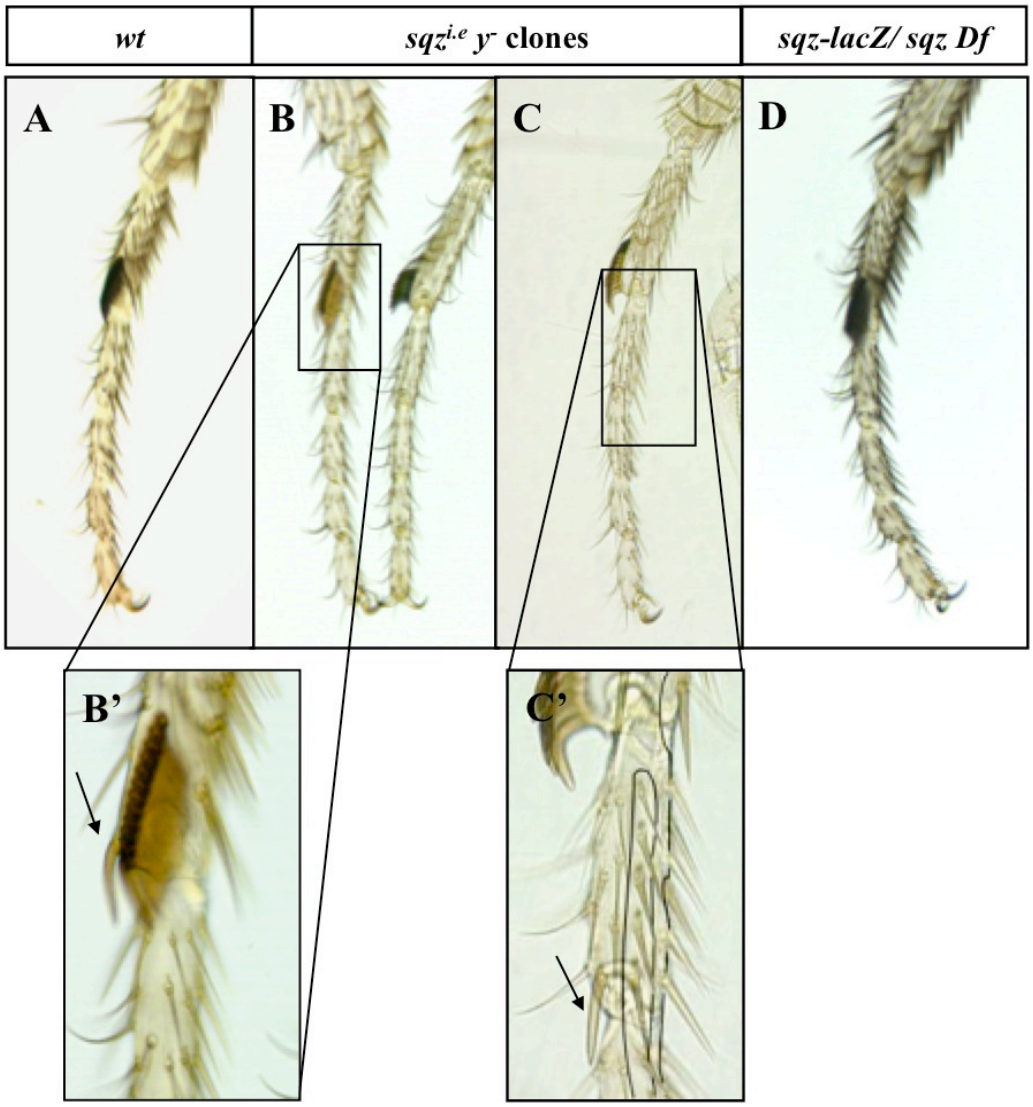

Figure 5.5. *sqz*$^{i.e}$ *y*$^{-}$ clones in adult leg. (A) Tarsal region of a wild type fly. **(B and C)**. Tarsal region of two different male flies *y*$^{-}$*; Frt82B sqz*$^{i.e}$*/Frt82B y*$^{+}$. Clones are marked by the lack of pigmentation caused by the phenotypic marker *yellow* (*y*). **(B')** Detailed view of a clone *y-; Frt82B sqz*$^{i.e}$*/Frt82B sqz*$^{i.e}$ caused by heat shock at 40-50 hours A.E.L. An ectopic sex-comb (arrow) stands in the distal part of the tarsal segment ta1, in the edge between the ventral and the dorsal region. **(C')** Detailed view of a clone *y-; Frt82B sqz*$^{i.e}$*/Frt82B sqz*$^{i.e}$ caused by heat shock at 48-54 hours A.E.L. An ectopic sex-comb (arrow) stands in the distal part of the tarsal segment ta2, in the edge between the ventral and the dorsal region. The limits of the clone are shown by the black line. **(D)** View of the tarsal region of a protorathic leg of a *sqz-lacZ/sqzDf* fly. Larval lethality of this genotype is almost a 100%, however, two scapers were recovered. All legs look wild-type.

5.2.2. Effects of misexpression of Sqz in leg imaginal disc

Ectopic expression of Sqz was driven by *dpp-Gal4*, and its effects were compared to those caused by ectopic expression of Ss. In *w; UAS-sqz; dpp-Gal4* heterozygote flies the joint and the indentation between tarsi ta4 and ta5 are missing leading to the fusion of both tarsi, and the size of the segment ta1 is clearly reduced (Figure 5.6.C). This resembles the phenotype of flies expressing Ss under the *dpp-Gal4* driver at 18^{o}C (Figure 5.6.B). Notice that Gal4 drivers are temperature sensitive, so at 18^{o}C the levels of expression are considerably lower than at 25^{o}C (compare phenotypes caused by ectopic expression of Ss at 18^{o}C and 25^{o}C in Figure 5.6.B and Figure 3.3.G, respectively).

In leg imaginal disc, misexpression of Ss driven by *dpp-Gal4* during the late third instar gave rise to the suppression of *Bar* (*B*) and *dachshund* (*dac*) in the dorsal region of their expression domains (Figure 5.7.B). Ectopic expression of Sqz with the same driver repressed *B* and *dac* dorsally in leg imaginal disc (Figure 5.7.C). *dpp* expression domain consists of a stripe across the dorsal side of the leg imaginal disc (Masucci et al., 1990). Notice that *dac* was derepressed in the *B* expression domain (Figure 5.7.C, arrowhead).

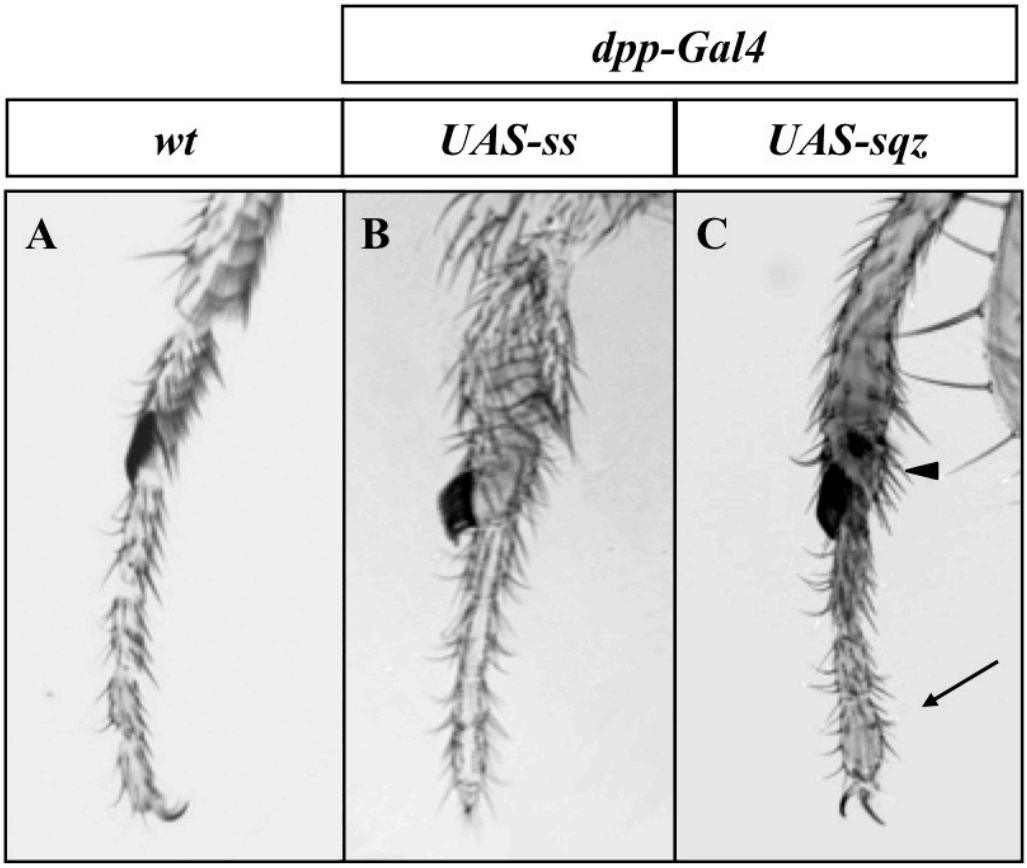

Figure 5.6. **Effects of misexpression of ss and sqz in leg imaginal disc. (A)** Tarsal region of a wild type leg. **(B)** Adult leg from a *dpp-Gal4/ UAS-ss* heterozygote showing fusion of tarsal segments ta4 and ta5. These flies were brought up at 18^{o}C **(C)** Adult leg from a *UAS-sqz; dpp-Gal4* heterozygote showing fusion of tarsal segments ta4 and ta5 (arrow) and the reduction in size of the segment ta1 (arrowhead).

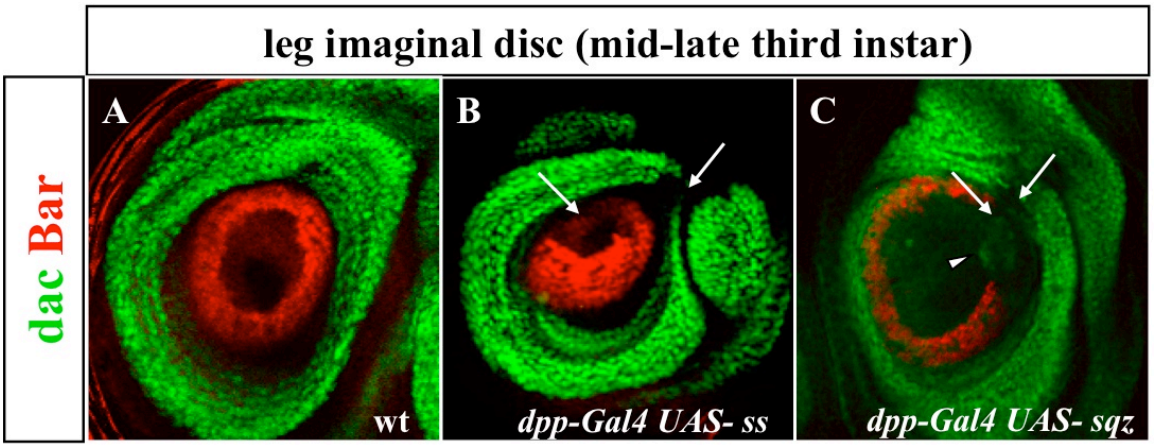

Figure 5.7. Ectopic expression of *ss* and *sqz* repress *B* and *dac* in leg imaginal disc. **(A)** Wild type leg imaginal disc in late third larvae instar showing expression of *B* (red) and *dac* (green). **(B and C)**. Leg imaginal disc in the late third larvae instar showing repression of *B* (red) and *dac* (green) in their dorsal region (white arrows) of their expression domains by *ss* **(B)**, and *sqz* **(C)**. Note that in (C) *dac* is partially de-repressed in the *B* expression domain (white arrow head). Ectopic expression of both *ss* and *sqz* was driven by *dpp-Gal4*. B and Dac proteins were labelled by rabbit anti-Bar (red) and mouse anti-dac (green), respectively.

5.2.3. Sqz is not able to drive the translocation of Tgo into the nucleus

Tgo is the best-known partner of Ss. They interact directly to form a transcription factor complex (Emmons et al., 1999). In the presence of Ss protein, Tgo is translocated into the nucleus where they bind to act as a transcription factor (Emmons et al., 1999). Thus, when Ss is misexpressed in salivary glands during the third instar, tgo protein is accumulated in the nucleus (Figure 5.8.B) in contrast with wild type salivary glands (Figure 5.8.A). In order to test whether Sqz has any control over Tgo sub-cellular localization, *UAS-sqz* was overexpressed in salivary glands by *dpp-Gal4*. Interestingly, in this case, Tgo is accumulated in the periphery of the nucleus (Figure 5.8.C).

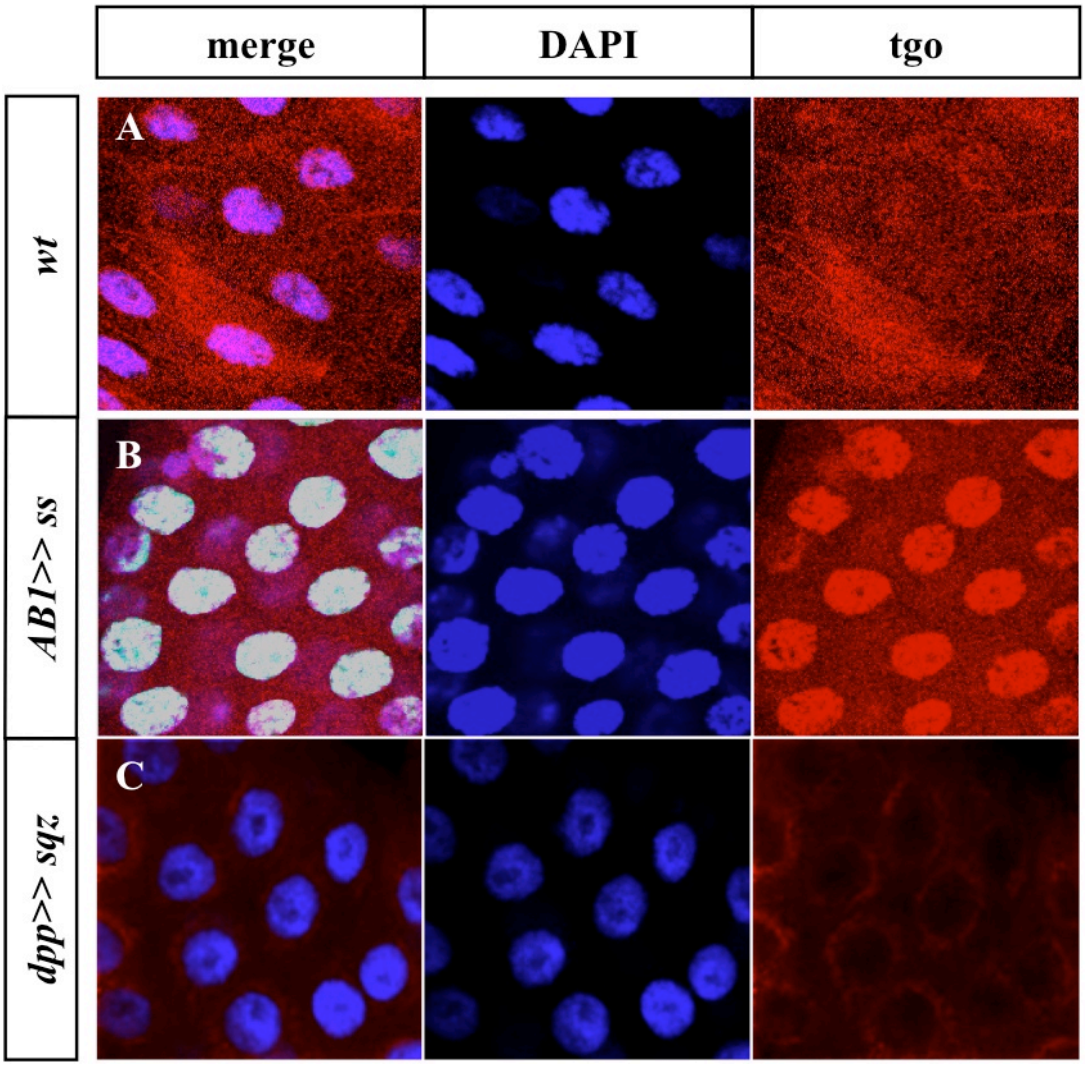

Figure 5.8. Effects of misexperession of *ss* or *sqz* on the sub-cellular localization of Tgo. Tgo was reported with anti-Tgo mouse monoclonal (red), and nucleus were stained with the DNA marker DAPI (blue). **(A)** Wild type salivary gland in the mid third instar showing endogenous Tgo (red). Tgo is located all over the cell in *Or-R* salivary glands. **(B)** Salivary gland of a *AB1-Gal4 UAS-ss-eGFP* in the mid third larvae instar. Tgo is mostly nuclear (red), although some of it remains cytoplasmatic. **(C)** Salivary gland of a *dpp-Gal4 UAS-sqz* in the mid third larvae instar. Note that Tango (red) is mostly cytoplasmatic, but it seems to accumulate around the nucleus.

5.2.4. *sqz* interacts functionally with *ss* and *rn* in leg development

In Terriente et al. (2007), the authors present a model in which the Sqz protein represses Rn activity in wing imaginal disc by competing for the same DNA binding sites (Terriente Felix et al., 2007). *rn* is the closest homologue of *sqz* and is co-expressed with *ss* in a ring in the presumptive distal region of the leg imaginal disc during the third larval instar. *rn* is also involved in the proximo-distal patterning of *Drosophila* leg (Duncan et al., 1998; Pueyo and Couso, 2008; St Pierre et al., 2002). Hence, *rn* might also interact with ss. The *rn* gene expresses two transcripts coding for the proteins Rn and Roe. Roe is expressed in eye imaginal discs, whereas Rn is expressed in the leg imaginal disc. The deficiency covering the genomic region of *roe* did not appear as an interactor candidate, suggesting that roe might not be involved in the ss-eye phenotype. Notice that removing one copy of the gene might not be enough to show an interaction with the ss-eye phenotype. However, it is still possible that *rn*, *sqz*, and *ss* interact in leg development.

In order to test whether there is a functional relationship between *sqz*, *rn* and *ss*, flies *rn-Gal4(13) ss^{sta}/TM3 Ser* were crossed to the strain *sqz$^{i.e}$/TM6B hu*. *rn-Gal4(13)* is a hypomorph allele of *rn* generated by the insertion of a *P(GawB)* element (St Pierre et al., 2002). *ss^{sta}* is a null allele generated by the genomic translocation from the chromosome X to the *spineless* locus in the third chromosome (Melnick et al., 1993; St Pierre et al., 2002). The legs of the different offspring categories were studied. 15% of male flies *rn-Gal4(13) ss^{sta}/TM6B* show alterations in the arrangement of sex-combs, which extend ectopically into the second tarsal segment, indicating transformation towards first tarsal segment (Figure 5.9.B). A more dramatic phenotype can be seen in flies *rn-Gal4(13) ss^{sta}/ sqz$^{i.e}$* where sex-combs extension can be observed in 74.36% of the male flies (Figure 5.9.C). The transformation to ta1 segment might be due to

derepression of the gene *dac*, as in wildtype leg imaginal discs *rn* and *ss* downregulate *dac*, thus creating the distal border of the *dac* expression domain. Notice that ss^{sta} and *rn-Gal4(13)* heterozygote flies have wild type legs (Figure 5.9.A and data not shown, respectively). This result shows that *sqz* interacts functionally with *ss* and *rn* in leg development. Thus, given the level of homology between Sqz and Rn, it is likely that *sqz* is redundant with *rn*, explaining why sqz^{-} mitotic clones showed very mild phenotypes in adult leg (see section 5.2.1).

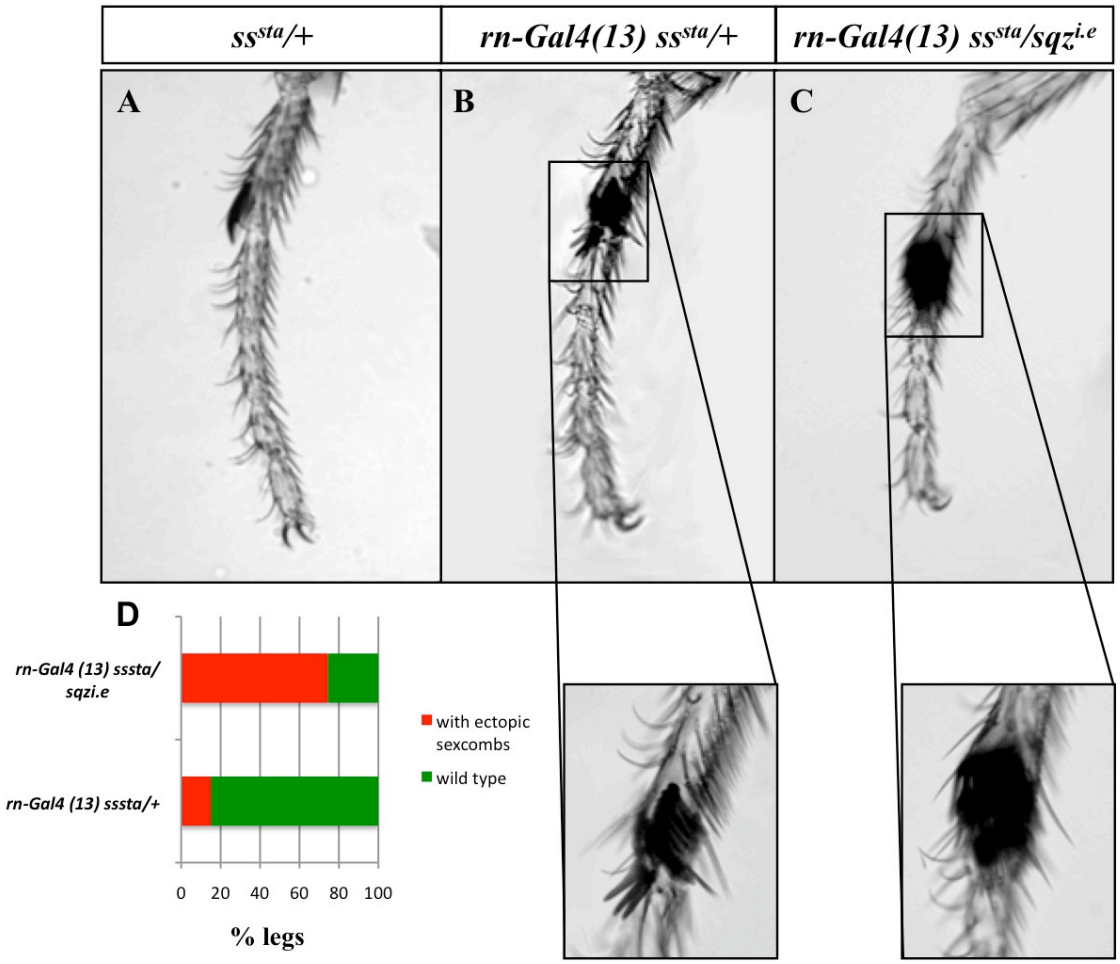

Figure 5.9. Lack of function of *sqz* enhances *rn*⁻ and *ss*⁻ phenotype in adult leg. (A) Tarsal region of a leg of a wild-type adult fly. **(B)** Leg of a *rn-Gal4(13)* ss^{sta} heterozygote fly. 15% of heterozygous flies for *rn* and *ss* mutant alleles show ectopic sex-combs in the second tarsal segment of the protorathic male leg, indicating transformation to first tarsal segment. **(C)** Leg of a *rn-Gal4(13)* $ss^{sta}/sqz^{i.e}$ fly. 74.36% of the flies heterozygous for *rn*, *ss* and *sqz* mutant alleles show ectopic sex-combs in the second tarsal segment of the protorathic male leg. The second tarsi is shorter, and the presence of ectopic sex-combs is more dramatic when a copy of the gene *sqz* is removed. **(D)** Percentage of male protorathic legs that showed ectopic sex-combs in the second tarsal segent (red), or wildtype phenotype (green).

5.2.5 *ss* does not control expression of neither *sqz* nor *rn*

rn and *sqz* seem to interact functionally with *ss*. However, the nature of this interaction is to be determined. In order to ascertain whether *ss* controls *rn* or *sqz* at the transcriptional level, expression of *rn-lacZ* and *sqz-lacZ* was studied when ss was overexpressed. rn-lacZ and sqz-lacZ were generated by the insertion of a lacZ P-element in the 5' region of rn and sqz, respectively (Allan et al., 2003; McGovern et al., 2003; St Pierre et al., 2002). X-Gal stainings show that both *rn-lacZ* and *sqz-lacZ* are expressed in a ring in a distal part of the leg imaginal disc during mid-late 3rd larval instar (Figure 5.10.A and C, respectively)

Ectopic expression of Ss was driven by *dpp-Gal4* in a stripe across the dorsal half of the disc. The *lacZ* reporter indicates that neither *rn-lacZ* or *sqz-lacZ* are activated by addition of extra Ss (Figure 5.10.B and D). *sqz-lacZ* expression in the chordotonal organ was split in two expression domains, this is probably caused by the formation the ectopic furrow across the dorsal half of the disc (Figure 5.10.D, red arrow). Notice that the leg imaginal discs were dissected at approximately the same developmental stage (third larval instar) to allow direct comparison of the effects caused by the ectopic expression of Ss. This data indicates that *ss* does not control expression of *rn* or *sqz*. Instead, they are activated by the gene *tal* and cooperate to determine the fate of the second and third tarsal segments (see section 1.7.1) (Pueyo and Couso, 2008). Therefore, the interaction between these genes might happen at the post-transcriptional level.

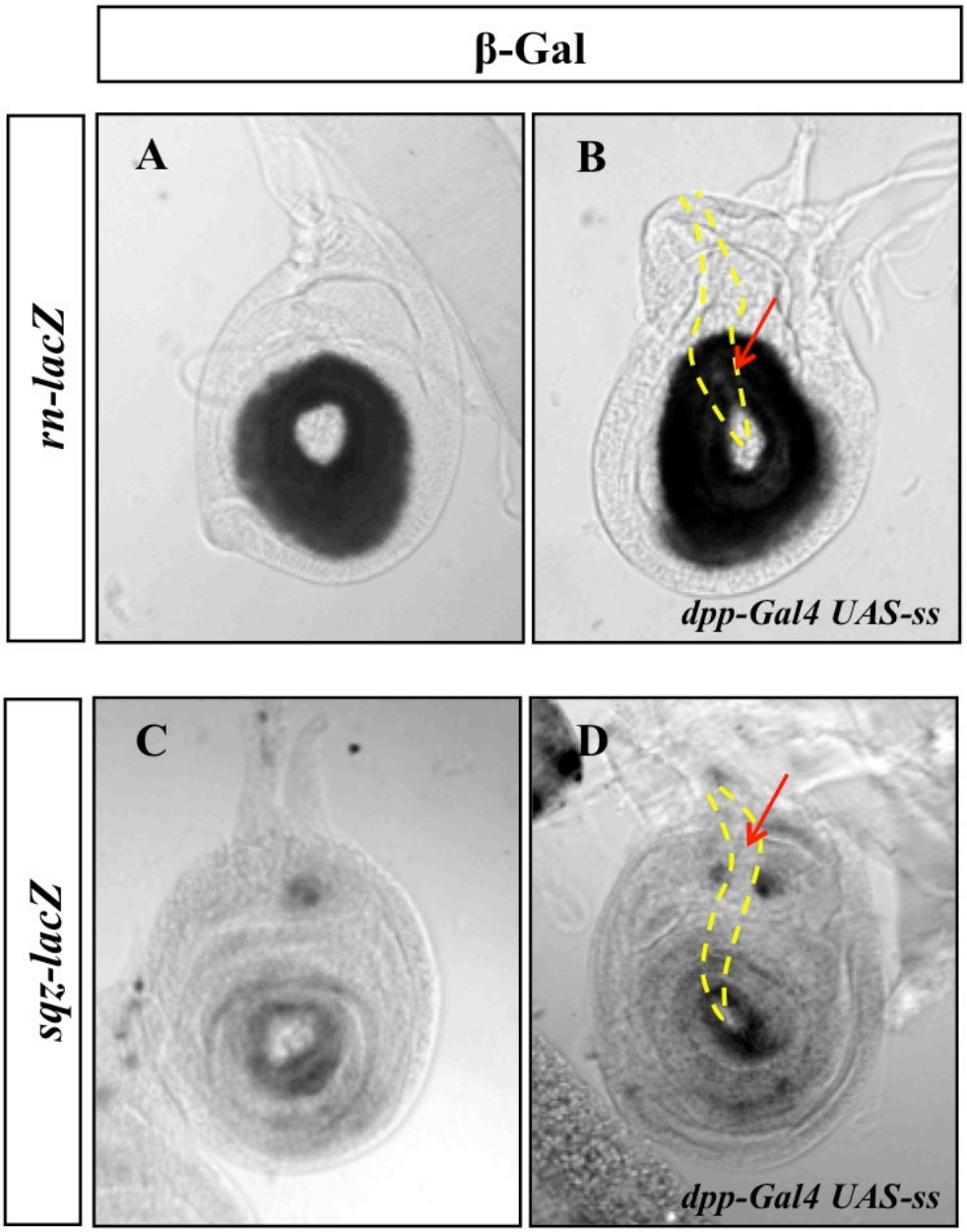

Figure 5.10. *ss* does not control expression of *rn* or *sqz*. All pictures show X-Gal stainings on leg imaginal discs from mid-late 3rd instar larvae. **(A and B)** Expression of the *lacZ* reporter in *rn-lacZ* **(A)** and *rn-lacZ/dpp-Gal4 larvae* **(B)**. **(C and D)** Expression of the *lacZ* reporter in *sqz-lacZ heterozygotes* **(C)** and *sqz-lacZ/dpp-Gal4* **(D)**. Red arrows point at the formation of an ectopic furrow in the dorsal half of the disc. The dashed yellow line shows the approximate *dpp-Gal4* expression pattern.

5.2.6. Rn and Ss are able to repress the ta5 enhancer

Ss downregulates the expression of the gene *Bar* in leg imaginal disc through the binding to a genomic region called *ta5-enhancer*. The sequence of the *ta5-enhancer* has a XRE motif that is highly conserved in other species of *Drosophila*. Ss represses the expression of the gene *lacZ* under the control of the *ta5-enhancer* (*ta5-lacZ*). When the XRE is removed, Ss is not longer able to control the expression of the reporter gene (Kozu et al., 2006). Hence demonstrating that Ss regulates changes in gene expression through the binding to XRE motifs. Since *rn* is expressed in the leg imaginal disc and downregulates *Bar* (Pueyo and Couso, 2008; St Pierre et al., 2002), it is possible that Rn also binds to the *ta5-enhancer*. I aimed to test whether these genes are able to control the expression of the *ta5-lacZ*.

X-Gal stainings show that ectopic expression of Rn driven by *dpp-Gal4* seems to repress weakly the *ta5-lacZ* (Figure 5.11.C, arrow). Notice that ectopic Ss also downregulates the expression of the reporter gene (Figure 5.11.B, arrow). It is possible that Rn binds a DNA motif in the *ta5-enhancer*, thus regulating the expression of *Bar*. These experiments require more accurate immunohistochemestry and analysis of the ta5 enhancer (this will be addressed in further directions). Electrophoretic mobility shift assays might be carried out in the future to test whether Rn controls expression of *Bar* by direct binding to the *ta5* enhancer.

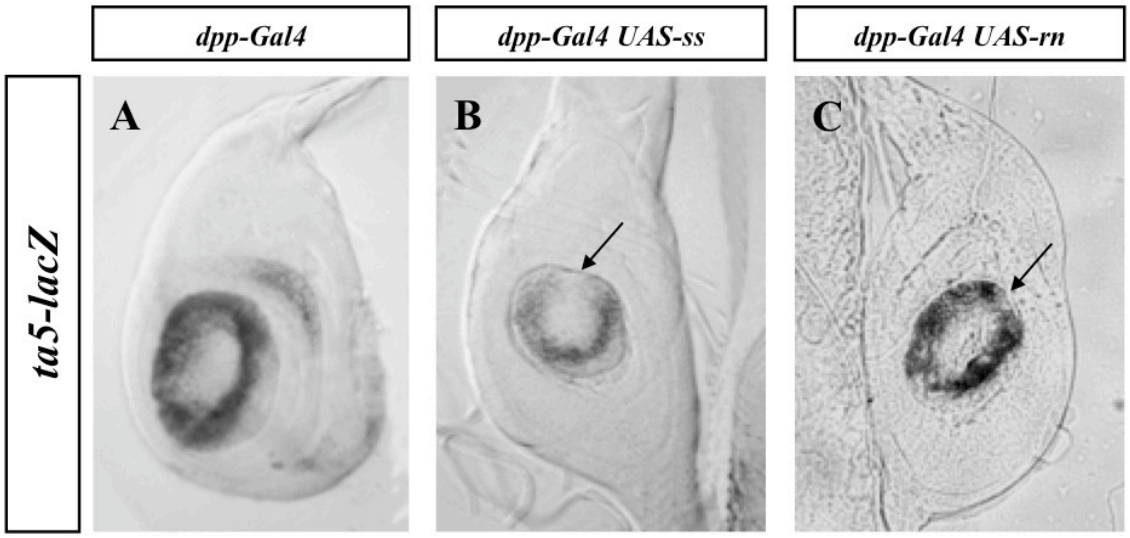

Figure 5.11. Ectopic expression of Ss or Rn represses expression of the *ta5-lacZ* reporter. (A) Expression of the *ta5-lacZ* reporter gene in leg imaginal discs from mid-late 3rd instar larvae (*lacZ* expression was detected by X-Gal staining). **(B)** *ta5-lacZ* expression in *ta5-lacZ/+; dpp-Gal4/UAS-ss* larvae. **(D)** X-Gal staining in *ta5-lacZ/UAS-rn; dpp-Gal4/+ larvae*. Notice that the *ta5-lacZ* reporter is repressed by the ectopic expression of Ss, and Rn (arrows in C and D respectively).

5.2.7 Ss interacts physically with Rn

One possibility is that Ss might control Rn and Sqz activity by a physical interaction.

This seems to be a likely scenario given the following premises:

- Ahr interacts with the proteins Slug and Sp1; two zinc-finger proteins from the Krüppel family (Ikuta and Kawajiri, 2006; Kobayashi et al., 1996; Roman et al., 2008). Recently, it has been shown that Ahr binds Slug to repress the expression of genes downstream of XRE motifs and Slug binding sites (Roman et al., 2008). Ahr and Sp1 control the expression of the gene CYP1A1 through the binding of XRE and BTE (Basic Transcription Element) motifs, respectively (Kobayashi et al., 1996). BTEs are GC box sequences. *In vitro* assays showed that Sp1 is able to interact physically with Ahr via its zinc finger domain with the bHLH and PAS domains of Ahr, and the bHLH domain of Arnt (Kobayashi et al., 1996).
- Cases of bHLH proteins interacting with zinc-finger factors in the development of *Drosophila* have been described. For instance, proneural bHLH proteins bind senseless via its zinc finger to regulate gene expression during the development of the embryonic PNS (Acar et al., 2006).
- As shown in the previous section, both Rn and Ss are able to repress the expression of the *ta5-lacZ* repoter. A likely scenario is that Rn and Ss form a heteromeric complex to regulate changes in gene expression.

These data suggest that Ss might interact with Rn and Sqz. In order to address this possibility I conducted co-immunoprecipitation assays from *in vivo* extracts from third instar larvae. Both *UAS-ss-GFP* and *UAS-Ahr-GFP* proteins were expressed ectopically using the *heat shock-Gal4* (*hs-Gal4*). The *hs-Gal4* activates expression of

the *UAS* constructs when flies are incubated at 37^{o}C. Anti-GFP mouse monoclonal antibody (Crameri et al., 1996) was used to precipitate Ahr-GFP and Ss-GFP from the protein extracts. After precipitation, presence of Rn was detected by Western-blot with an anti-Rn polyclonal anti-body (del Alamo and Mlodzik, 2008). In this experiment Rn interacts physically with Ss (Figure 5.12.A. lane 4), but it does not show interaction with Ahr (Figure 5.12.A. lane 2). Notice that Ahr-GFP protein seems to be more abundant than Ss-GFP (Figure 5.12.B. lane 1), meaning that the amount of protein is not a limiting factor. Hence, Ahr might not be able to interact with Rn or the interaction is not detectable in this assay. Interaction with Sqz could no be tested in the co-immunoprecipitation assays as there is not available anti-body.

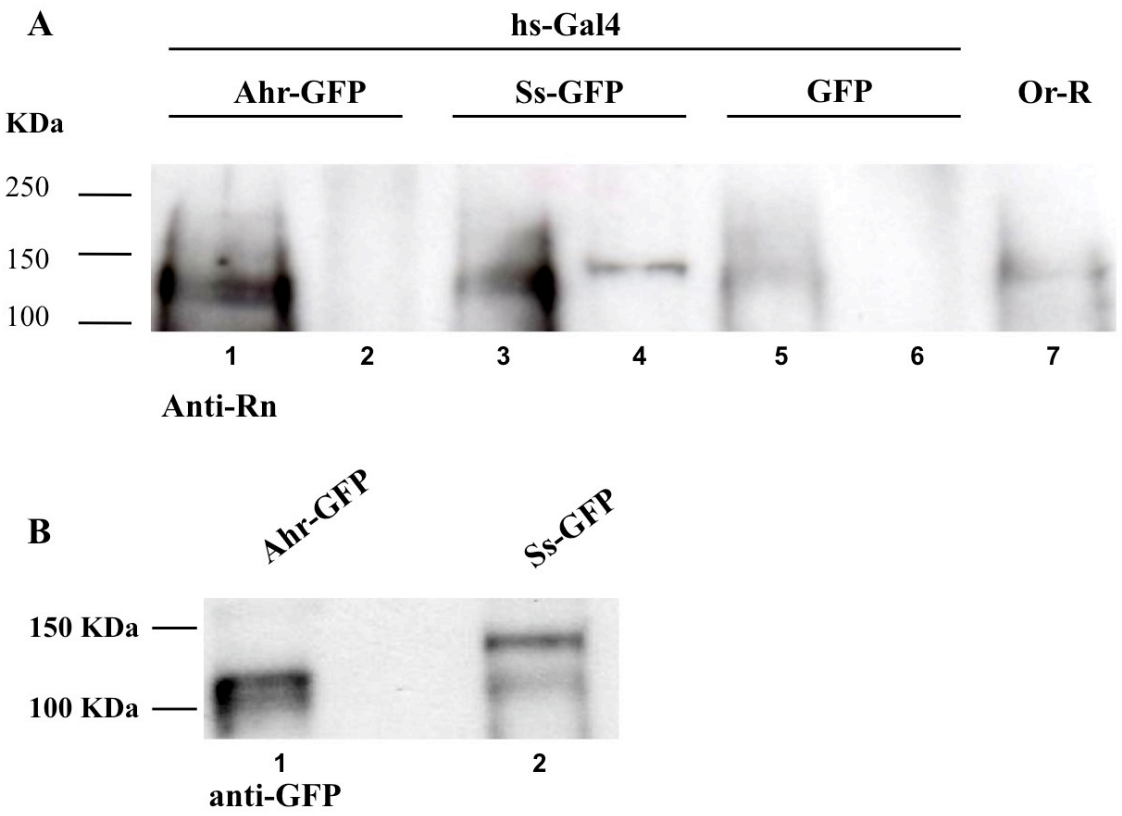

Figure 5.12. Ss interacts physically with Rn. *hs-Gal4* was used to drive the expression of the transgenic contructs *UAS-Ahr-GFP, UAS-ss-GFP*, and *UAS-GFP* in third larval instar larvae. Anti-GFP monoclonal antibody was used to precipitate the GFP quimeric proteins. **(A)** Presence of Rn was detected by western-blot with an anti-Rn polyclonal antibody. Lanes 1, 3, and 5 were loaded with extracts before the assay. Lanes 2, 4, and 6 were loaded with the precipitates. Lane 7 was loaded with OR-R protein extract. **(B)** Presence of GFP was confirmed by western-blot with anti-GFP. Notice that Ahr-GFP is more abundant than Ss-GFP.

5.2.8. *Ahr* is able to interact functionally with *sqz* and *rn*

The high degree of functional equivalence between *ss* and *Ahr* suggests that the molecular context in which they operate might be conserved. However, developmental genetic networks have also derived in both vertebrate and invertebrate lineages. *sqz* and *rn* genes are two potential candidates to be functional interactors of *ss* and might reveal a general characteristic of *ss*: the ability to interact functionally with zinc-finger proteins from the C_2H_2 Krüppel family. In order to assess whether this is also a feature of Ahr, I tested the ability of the dioxin receptor to interact with *sqz* and *rn*.

Ectopic expression of *rn*, driven by *GMR-Gal4* in the eye imaginal disc during the third larval instar, causes lack of pigmentation and roughness in the adult eye (Figure 5.13.B) (St Pierre et al., 2002). The eye is also reduced in size appearing narrower than the wild-type eye. This change in size might be caused by cell death as the eye is covered by scattered necrotic tissue. Addition of *Ahr* enhances the *rn* phenotype as necrosis extends to most of the eye surface (Figure 5.13.C). Notice that ectopic *Ahr* does not cause any visible phenotype (Figure 5.13.D). Ectopic expression of *sqz* with the same *GMR-Gal4* triggers a less severe phenotype. Pigmentation is partially absent and the surface of the eye is rough (Figure 5.13.E). In contrast with *rn*, ectopic *sqz* does not cause visible cell death. In flies ectopically expressing *sqz* together with *Ahr* the lack of pigmentation extends to most of the adult eye (Figure 5.13.F).

Expression of Ahr in leg imaginal disc also rescues *rn-Gal4(5)* phenotypes in adult leg. *rn-Gal4(5)* was generated by a *P[GawB]* insertion in the 5' region of the *rn* gene (St Pierre et al., 2002). 73% of *rn-Gal4(5)* heterozygous mutant flies have extra sex combs and shorter ta2 segments that are fused with ta1 (Figure 5.14.B and E). Addition of *Ahr* rescues the phenotype to wild type almost 100 % (Figure 5.14.C, D, and E). This demonstrates that *Ahr* is able to compensate for the lack of *rn* activity.

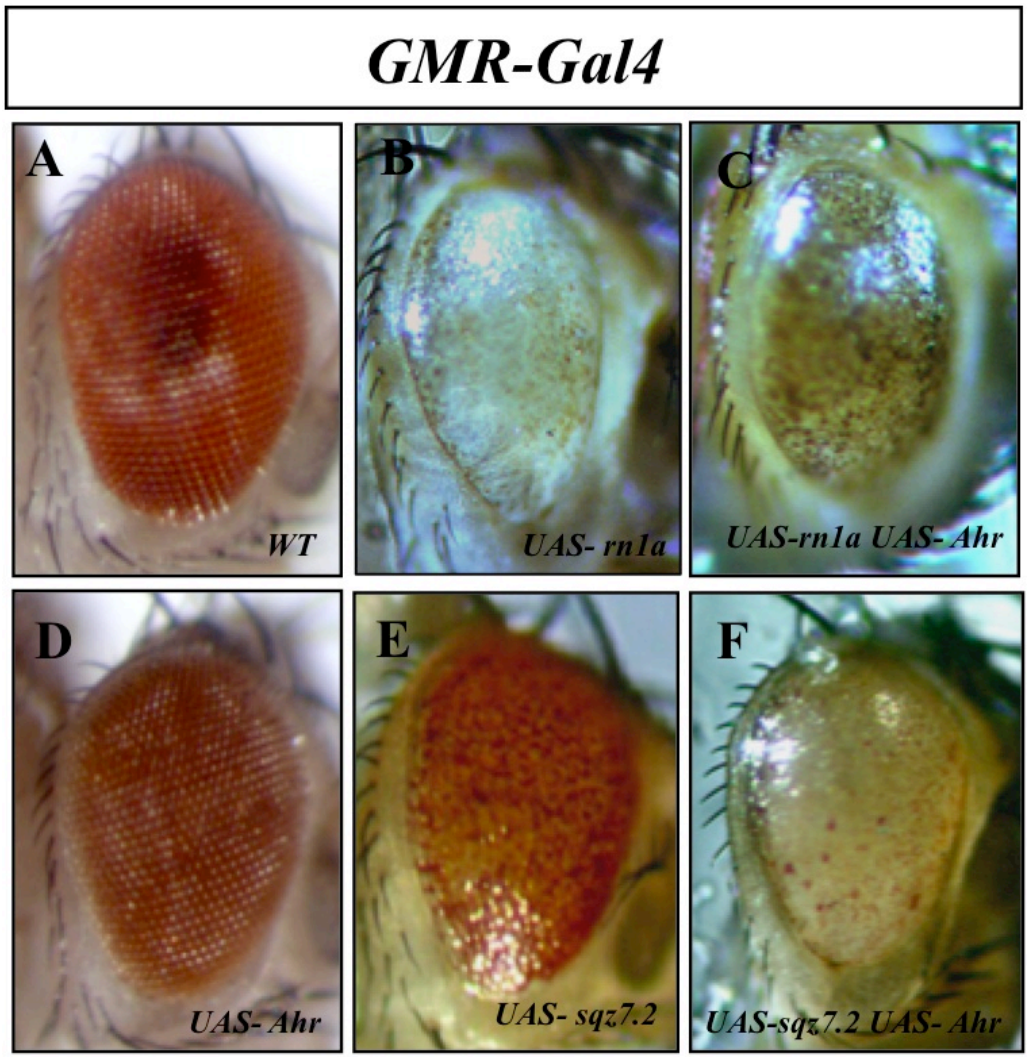

Figure 5.13. Ahr is able to interact with rn and sqz in eye imaginal disc. (A) The eye of a wild-type fly. Top is dorsal, right is anterior. **(B)** Eye of a *w; GMR-Gal4; UAS-rn* heterozygote. **(C)** Eye of a *w; GMR-Gal4/UAS-Ahr; UAS-rn/+*. Addition of Ahr enhances the phenotype caused by ectopic expression of rn in eye imaginal disc. **(D)** Eye of a *w; GMR-Gal4; UAS-Ahr* heterozygote. Ectopic expression of Ahr does not cause any visible phenotype. **(E)** Eye of a *w; GMR-Gal4; UAS-sqz7.2* heterozygote. **(F)** Eye of a *w; GMR-Gal4/UAS-Ahr; UAS-sqz7.2/+*. The eye phenotype caused by ectopic expression of *sqz* is enhanced by the addition of *Ahr*.

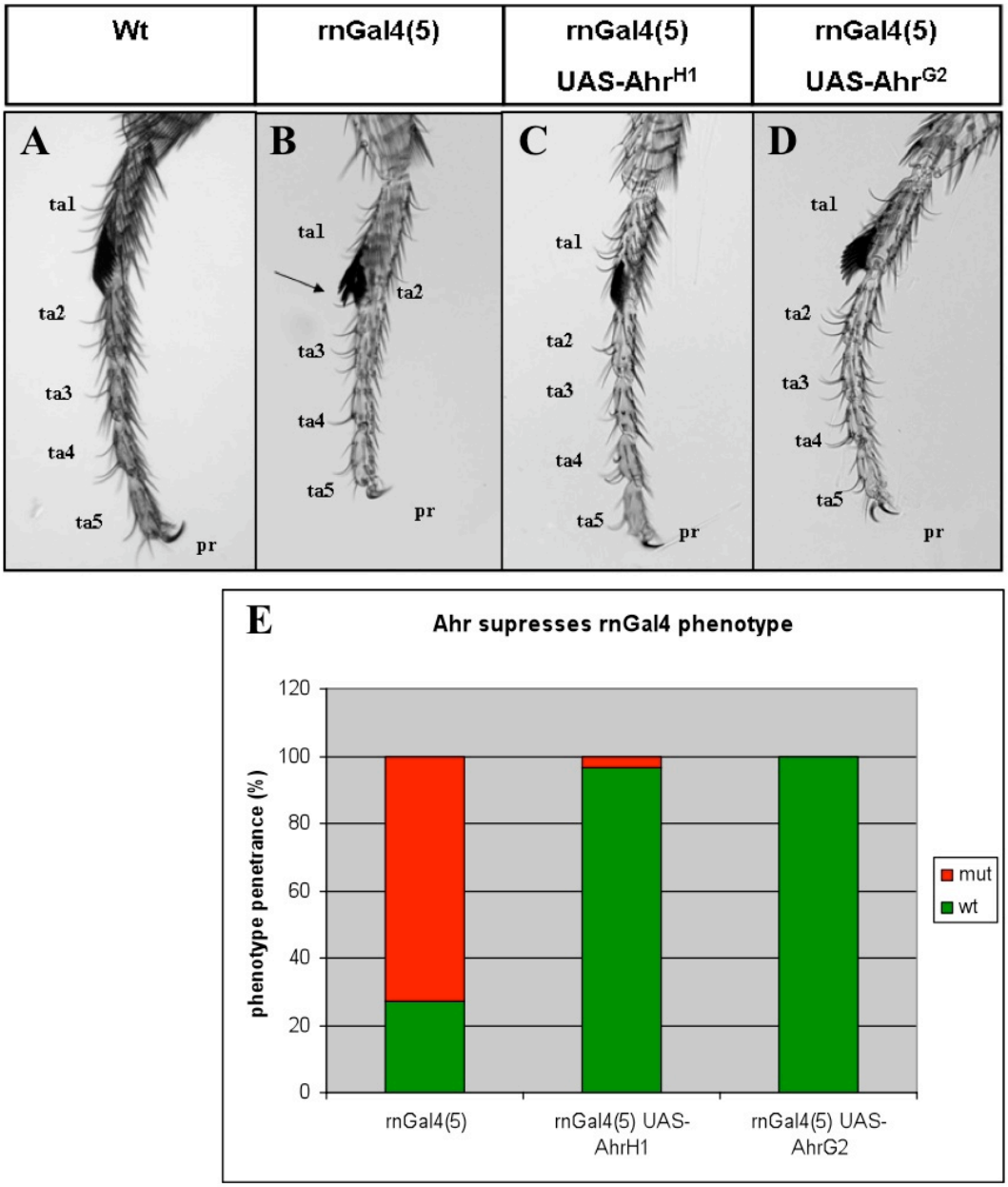

Figure 5.14. Ahr rescues *rn-Gal4(5)* phenotype in adult leg. (A-B) Tarsal region of a male protorathic leg. ta1, ta2, ta3, ta4, ta5, and pr stand for the first, second, third, fourth, and fifth tarsal segment and the pretarsi, respectively. **(A)** wild type. **(B)** *rnGal4(5)* heterozygote. The second tarsal segment is severely reduced and fused to the first tarsal segment (arrow). **(C)** *UAS-AhrH1; rnGal4(5)* heterozygote. **(D)** *UAS-AhrG2; rnGal4(5)* heterozygote. **(E)** Histogram showing the ratio of phenotypic classes per genotype. Green shows the percentage of wild type legs, and red shows the percentage of legs that exhibit the mutant phenotype.

5.3. DISCUSSION

With the work shown in this chapter I aimed to find new elements that interact with *ss* and to test to what extent these interactions might remain conserved with *Ahr*. For this purpose, I carried out an enhancer and suppressor screen using the adult eye of *Drosophila* as a system. The reliability of the screen was assessed by testing known interactors of *ss* in leg development. These interactors, *tgo* and *dac*, did interact with the ss-eye phenotype. *tgo* is a molecular partner of ss in leg and antennal development (Emmons et al., 1999). Removing one copy of *tgo* suppressed the ss-eye phenotype, whereas overexpression of Tgo enhanced it. *dac* is downregulated by ss in leg imaginal disc (Pueyo and Couso, 2008). Accordingly, a *dac* mutant allele enhanced the ss-eye phenotype.

From the screen I isolated the *sqz* gene as a candidate interactor. *sqz* is located in one of the suppressor regions. This region was corroborated for two different deficiencies and narrowed by deficiencies that did not show any interaction. *sqz* codes for a zinc-finger protein. Interestingly, it has been shown that Sqz works in a combinatorial code with other transcription factors such as Dac in the development of the CNS (Allan et al., 2003; Miguel-Aliaga et al., 2004). *sqz-lacZ* expression pattern in leg imaginal disc is reminiscent of the pattern of *ss*. *sqz-lacZ* is expressed in a ring in the presumptive distal region during late-third instar. This expression domain is broader than *ss* extending further from the distal border. *ss* is expressed slightly earlier (early-mid third instar) than *sqz-lacZ* (mid-late third instar). However, it is still possible that the Ss protein half life is long enough as to interact with Sqz in the same cells. In agreement with this possibility, staining with anti-Ss of leg imaginal discs during late third larval instar gave a low background, suggesting that some Ss might still be present

(Pueyo and Couso, 2008). *sqz* is also expressed in the chordotonal organ. Notice that this pattern is reminiscent of *tal*, which controls expression of *ss* and *rn* in leg imaginal disc. Further tests to assess the interaction between *ss* and *sqz* were required.

sqz is the closest homologue of *rn*, with a 90% homology in the zinc-finger domain. *rn* plays a key role in distal leg and wing blade development (St Pierre et al., 2002). It has been suggested that Sqz represses Rn activity in the wing imaginal disc by competing for the same DNA binding sites (Terriente Felix et al., 2007). In the leg imaginal disc, *rn* is co-expressed with *ss* in a ring in the presumptive tarsal region. Both, *rn* and *ss* downregulate *dac* proximally and *B* distally, thus creating the boundaries of the intermediate tarsal segments. Although ss and rn seem to cooperate in leg development, they do not regulate each other expression in leg imaginal disc (Pueyo and Couso, 2008). Sqz was able to repress expression of *dac* and *Bar* when it was expressed ectopically in leg imaginal disc suggesting that there might be some kind of functional interaction with *rn* and *sqz* in leg imaginal disc.

About 15 % of the *rn-Gal4(13)* ss^{sta} heterozygote males have ectopic sex-combs in the most proximal region of the ta2 segment of the prothoracic leg. Among the transheterozygote males *rn-Gal4(13)* $ss^{sta}/sqz^{i.e}$ almost 75% show the same phenotype, which is also more dramatic: the second tarsal segment is reduced in size and the ectopic sex-combs are more abundant. These results indicate that there is a functional relationship between *sqz*, *rn* and *ss* in leg development, and that *sqz* is a true interactor of *ss*.

One question remains unanswered, why does $sqz^{i.e}$ not show interaction with the ss-eye phenotype? On one hand, there might be other elements in the region 91F4-8 that are required for the interaction between *ss* and *sqz*. On the other, $sqz^{i.e}$ might not be a null allele. $sqz^{i.e}$ was created by the imprecise excision of the P-element insertion

P(l)02102^{02102}. This excision deletes the second and third exon of the gene, although the precise 3' breakpoint has not been determined. The *sqz* gene is formed by three exons. It is possible that the sequence coded in the first exons might account for the interaction with the ss-eye phenotype. Further analysis of the region 91F4-8 and the allele *sqz*$^{i.e}$ is required.

5.3.1 Sqz in leg development

Clonal analysis of *sqz*$^{i.e}$ somatic clones was carried out in order to ascertain the function of sqz in leg development. Only two somatic clones in the tarsal region out of twenty-two showed the presence of an ectopic sex-comb (from the twenty-two clones, eight were in prothoracic legs from male flies). In both cases, the ectopic sex-comb was found in a tarsal segment in the male prothoracic leg. No other phenotype was found in the rest of the adult leg. This data suggests that *sqz* has a limited function in leg development. However, given the high degree of homology between *rn* and *sqz*, it is also possible that *sqz* is redundant with *rn*. In the absence of *rn*, *sqz* could partially substitute *rn*, explaining why *sqz*$^{i.e}$ interacts with *rnGal4(13) ss*^{sta}.

Ectopic expression of *ss* and *sqz* in leg imaginal disc causes comparable phenotypes in tarsal region: loss of joints and shorter ta1. Ectopic expression of *sqz* downregulates *B* and *dac*. *sqz* is able to drive the same changes in gene expression as *ss* and *rn*, supporting the notion that *sqz* is redundant to *rn* in leg development. Repression of *dac* is consistent with the presence of ectopic sex-combs, indicating transformation to first tarsal segment.

sqz does not drive translocation of Tgo to the nucleus, instead Tgo accumulates around the nucleus. This indicates that overexpresion of *sqz* might affect the localization of Tgo and hence its accessibility to Ss.

5.3.4. Ss interacts physically with Rn

Ectopic expression of Ss in the leg imaginal disc did not alter the pattern of expression of the reporter genes *sqz-lacZ* and *rn-lacZ*, suggesting that *ss* does not control expression of *sqz* or *rn*; this agrees with recently published data (Pueyo and Couso, 2008). Hence, the interaction between these proteins must lay at the posttranscriptional level.

In the literature review there are several cases of bHLH-PAS transcriptions factors that interact physically with zinc-finger proteins. For instance, Ahr binds to Slug and to Sp1 (Kobayashi et al., 1996; Roman et al., 2008). Thus, I resolved to test whether Ss is able to bind to Rn. Co-immunoprecipitation assays showed that Ss and Rn interact physically in *in vivo* extracts from 3rd instar larvae. This indicates that Ss and Rn might form a protein complex to drive changes in gene expression. Interaction with Sqz could not be tested as there is not available antibody.

These results suggest that Ss and Rn might bind to the same regulatory regions of their immediately downstream genes. Ss represses expression of *Bar* in leg imaginal disc through the direct binding to the *ta5-enhancer* (Kozu et al., 2006). Since Ss and Rn are coexpressed in leg imaginal disc, it is possible that Rn also binds to the *ta5-enhancer* to downregulate *Bar*. This could be the case since ectopic expression of Rn driven by *dpp-Gal4* repressed the *ta5-lacZ* reporter in the dorsal part of the leg imaginal disc. Further analysis of the *ta5-enhancer* and Electrophoretic Mobility Shift Assays (EMSA) will be required to determine Rn's DNA binding site.

5.3.3. *ss* and *Ahr* interact with zinc-finger genes from the Krüppel family

Ahr is also able to interact functionally with *sqz* and *rn*. Addition of *Ahr* enhances the phenotypes caused by ectopic expression of either *sqz* or *rn*. *Ahr* also rescues *rn*$^{-}$ phenotypes in adult leg. These results indicate that *Ahr* can act as a positive

co-factor for *rn* and *sqz*. These data and the fact that Ahr binds to Slug and to Sp1 to drive changes in gene expression (Kobayashi et al., 1996; Roman et al., 2008) suggest that C_2H_2 Krüppel-type zinc-finger proteins possibly are part of the common mechanisms of action of the dioxin receptor. Thus, Ahr might interact with the homologue of Sqz and Rn in vertebrates to target specific promoters and drive changes in gene expression. This possibility will be addressed in the discussion chapter (section 6.2).

Ahr did not show interaction to Rn in co-immunoprecipitation assays. The amount of protein in the samples was not a limiting factor as Ahr-GFP seemed to be more abundant than Ss-GFP, and the amount of Rn was comparable in all samples. Thus, Ahr might not be able to interact to Rn, or the interaction is not strong enough as to be shown in my assays. Thus, it remains unclear whether Sqz interacts physically with Ss and Ahr, and whether Rn binds Ahr. This issue will be addressed in the future using other techniques such as GST-pull downs and mass spectrometry.

As shown in chapter 4, Ahr seems to have two levels of activity: endogenous and toxic. Addition of TCDD or either Tgo or Arnt also enhanced Ahr activity and led to ectopic phenotypes that resemble ectopic expression of Ss. Competition assays showed that dioxins increase the affinity of Ahr for Arnt (Chan et al., 1999). Hence, TCDD might trigger the transition between the two levels of Ahr activity by helping Ahr to make better use of other molecular cofactors.

Since addition of Ahr enhances the phenotypes caused by ectopic Rn or ectopic Sqz, one interesting possibility is that TCDD is increasing the affinity of Ahr for these proteins and so leading to ectopic phenotypes that resemble those caused by ectopic expression of Ss. In other words, in absence of dioxins the affinity of Ahr for Rn or Sqz might be low compared to Ss, explaining why it is not seen in my interaction assays.

Addition of dioxin might help Ahr to recruit all the cofactors that interact with Ss, thus leading to similar ectopic phenotypes. The ability of Ahr to bind to Rn in presence of TCDD will be addressed in the future experiments.

Chapter 6

General discussion

6.1. What have we learned about dioxin toxicity?

The Ligand Binding Domain (LBD) represses Ahr activity in the absence of an exogenous ligand. Addition of TCDD drives a comformational change in the LBD that allows Ahr to be released from the cytoplasmic complex and shuttled to the nucleus (Ikuta et al., 1998; Kudo et al., 2009). However, my data demonstrates that, in the absence of dioxins, Ahr is still functional at least to a certain level. This is supported by the fact that Ahr mutant mice have developmental defects and a shorter life span (Fernandez-Salguero et al., 1995; Mimura et al., 1999; Schmidt et al., 1996). Therefore, there must be mechanims of control of Ahr activity other than presence of aryl hydrocarbons and the conformation of the LBD.

My work shows that the availability of the molecular partner Arnt (or Tgo in *Drosophila*) is also a key element in the control of Ahr activity. As shown in section

4.2.3, the ability of Ahr to compete for its partner will be decisive in its functions. Thus, addition of the ligand βNF increases affinity of Ahr for Arnt, enhancing the binding to XREs in electrophoretic mobility shift assays (Chan et al., 1999).

To what extent is dioxin toxicity due to the disruption of Ahr activity? My work, put together with others, indicates that dioxins can compromise the fine-tuning between specific transcription factors in the cell. This is developed in the following model:

> Ahr has endogenous functions in the organism at a low level of activity. TCDD binds and upregulates Ahr and possibly enhances its affinity for Arnt. This higher level of Ahr activity has two immediate consequences. First, it leads to the activation of a battery of genes involved in xenobiotic metabolism and Ahr's developmental functions (Schmidt and Bradfield, 1996). Second, Ahr will "kidnap" Arnt, breaking the balance with other bHLH-PAS proteins. The later event could be deleterious and contribute, at least partially, to the toxic effects of dioxins.

Further directions:

I intend to clarify whether the effects of TCDD in the transgenic lines expressing Ahr are due to an increase in the affinity of the Ahr/Tgo complex for XREs. For this purpose, I plan to carry out EMSA with Ahr and Tgo at increasing concentrations of TCDD.

Here I have set a system in *Drosophila* in which the Ahr-mediated effects of dioxins can be studied and quantified. In the future, this system could be used to screen for potential therapeutic treatments. For example, drug libraries could be screened in the search of chemical compounds that might suppress the effects caused by exposure to dioxin in flies expressing Ahr.

6.2. Ahr and the Krüppel type Zinc-finger proteins

As shown in chapter 3, the mechanisms of action of Ahr and Ss are highly conserved, i.e. interaction with the same molecular partner (Arnt or Tgo) and binding to the same DNA motifs (XREs). bHLH-PAS proteins can be sorted in two groups: class I and class II. The proteins from the class I are only able to form heterodimers with the class II. In a functional sense, the class I protein of the heterodimer will attribute DNA specificity to the complex, whereas the class II will work like some sort of adaptor. Ahr and Ss are class I bHLH-PAS proteins, whereas Arnt and Tgo belong to the class II (Furness et al., 2007). The only known partner for Ahr is Arnt. The Ahr/Arnt complex binds to XREs (Swanson et al., 1995; Whitlock, 1990). However, Arnt can also bind, for instance, to the HIFα protein, which belongs to the class I. Arnt and HIFα bind to HREs (Hipoxia Response Elements; CACGTA) (Wang et al., 1995). The dynamics of this system seems to be preserved, as Tgo binds to CMEs (CNS Midline Element) when it dimerises with the class I protein Trachealess (Thr), but binds to XREs when it forms a complex with Ss (Duncan et al., 1998; Emmons et al., 1999; Ohshiro and Saigo, 1997). It seems that the context in which these proteins function is very conserved. Hence, Ahr and Ss might operate by similar means. In order to test whether Ss is able to fulfill Ahr functions in a vertebrate system, I will consider to use cell culture experiments to test the ability of Ss to rescue Ahr-/- phenotypes.

Later on in this work I have shown that the gene *ss* interacts with *rn* and *sqz*, which code for zinc-finger proteins from the Krüppel C_2H_2 family (Allan et al., 2003; St Pierre et al., 2002). The relationship between *ss, rn* and *sqz* will be addressed in section 6.3. The orthologue of Sqz and Rn in mammals is the protein CIZ (Cas-Interacting Zinc-finger) (St Pierre et al., 2002). It could be possible that Ahr and CIZ are functionally related. Three facts support this hypothesis. First, Ahr enhances the

phenotypes caused by ectopic expression of Rn and Sqz. Second, Ahr and Ss are highly conserved and the interaction between Ss and Rn might be a feature that has remained preserved through evolution. Third, Ahr binds to Slug and Sp1, two Krüppel type zinc-fingers proteins (Kobayashi et al., 1996; Roman et al., 2008).

CIZ is ubiquitously expressed in mice and rats (Alvarez et al., 2005; Nakamoto et al., 2000). It has been reported to be involved in extracellular matrix remodeling during osteogenesis (Nakamoto et al., 2000; Shen et al., 2002) and in the development of male sex organs and spermatogensis (Nakamoto et al., 2004). How does this relate to Ahr functions?

On one hand, *Ahr* might play a key role in EMT (Ephitelium to Meshemchyma Transition; see section 1.3.5) during palatal closure (Abbott and Birnbaum, 1991; Bock and Kohle, 2006). Ahr activates the expression of the gene *Slug*, which in turn will repress the expression of *E-Cadherins* (Ikuta and Kawajiri, 2006). In EMT, cells that are bound in an organized monolayer have to detach and rearrange. This process possibly requires degradation of the extracellular matrix to allow cells to move and acquire a new position and shape. In bone development, CIZ activates the expression of certain matrix metalloproteinases (MMPs) that will drive the degradation of the extracellular matrix. CIZ binds directly to a specific DNA motif ((G/C)AAAAA(A)) in the promoter of genes that encode for MMPs (Nakamoto et al., 2000; Shen et al., 2002). Thus, *CIZ* might be involved in *Ahr*-mediated EMT. CIZ is a nucleocytoplasmic shuttling protein that is located in the nucleus and in the focal adhesions (Nakamoto et al., 2000). Ahr and CIZ might meet in the nucleus to form part of a protein complex that could drive changes in gene expression during EMT. This relationship must be taken with caution as it is merely

speculative. No function of *CIZ* has been reported in palate development, although this does not necessarily mean that *CIZ* is not involved in palatal closure.

On the other hand, both *CIZ* and *Ahr* are involved in spermatogenesis and male-sex organ development (Lin et al., 2002; Nakamoto et al., 2004). In $Ahr^{-/-}$ mice, testis are smaller and normal development of the prostate and seminal vesicles is impaired (Lin et al., 2002). In $CIZ^{-/-}$ mice, there is also a reduction in the size of the testis and the levels of sperm production (Nakamoto et al., 2004). Given these similarities, *Ahr* and *CIZ* might work together in the development of the male reproductive organs.

Further directions:

In the work that will follow this thesis, I intend to ascertain whether Ahr and CIZ are real interactors. To do this I will:

- Conduct *in vitro* co-immunoprecipitation assays to test whether Ahr and CIZ are able to interact physically.
- Study the promoter of genes directly downstream of CIZ in the search of putative XREs.
- Search for CIZ-DNA binding sites in the promoter of genes directly regulated by Ahr.

In the long run, if these experiments indicate a possible interaction between Ahr and CIZ, it would be interesting to study the role of Ahr in the control of expression of metalloproteinases during EMT and the role of CIZ in dioxin toxicity.

6.3. *rn* and *ss* work in a combinatorial code that determines a specific tarsal identity

As shown in chapter 5, *ss* interacts with the genes *sqz* and *rn,* while the role of *sqz* in leg development remains to be elucidated, my data suggests that *sqz* is redundant to *rn* in tarsal development as removing one copy of *sqz* does not seem to affect leg development unless it is in a rn^{-} ss^{-} heterozygote background. This theory is also supported by the mosaic analysis of *sqz* mutant mitotic clones. In Terriente et al. (2008) the authors propose a model in which Sqz represses Rn activity by competing for the same binding sites during the development of the wing (Terriente Felix et al., 2007). This does not seem the case in leg development, as in that instance I should expect that removing one copy of *sqz* would suppress the leg phenotype of rn^{-} ss^{-} heterozygote flies.

rn and *ss*, on the other hand, share a biological context: the development of the intermediate tarsal segments (Pueyo and Couso, 2008). My results and published data demonstrate that *rn* and *ss* do not regulate each other at the transcriptional level (Pueyo and Couso, 2008), instead the proteins that they encode interact physically. Rn might also downregulate expression of *Bar* through the direct binding to the *ta5-enhancer*. The following is a model of distal leg development that I have implemented with my own data:

> During second larval instar the expression of the signaling protein Dpp from the dorsal half and Wg from the ventral half subdivides the leg in different proximo-distal domains. Dpp and Wg cooperate to activate the genes *Distal-less* (*Dll*) and *dachshund* (*dac*) in the distal (centre of the disc) and medial presumptive regions, respectively (Estella and Mann, 2008; Lecuit and Cohen, 1997). Coming from the most distal region, EGFR signaling activates *B*

expression (Galindo et al., 2005). *B* represses *dac* expression, creating two major expression domains in the distal part of the disc. Around mid-third larval instar the gene *tarsal-less* (*tal*) is expressed in the boundary between *dac* and *B* expression domains. *tal* activates *ss* and *rn* expression in the presumptive second and third tarsal segments. Ss, Rn and Tgo form a heteromeric complex that binds to the XRE and possibly other Rn-binding elements nearby in the *ta5-enhancer* to repress expression of *Bar*. In the fourth tarsal segment, *tal* activates expression of Bar non-autonomously, which in turn upregulates the gene *apterous* (*ap*). In the fifth tarsal segment, the bHLH-PAS protein Trachealess (Trh) interacts with Tgo to bind to the *ta5-enhancer* and activate expression of Bar. Trch and Tgo might bind to CMEs (ACGTG) present in the *ta5-enhancer* (Tajiri et al., 2007). In the pretarsus *trh* cooperates with *aristaless* (*al*), *Chip*, and *Lim1* to repress expression of *Bar* (Tajiri et al., 2007). The proteins coded by *al*, *Chip*, and *Lim1* form a heteromeric complex (Pueyo and Couso, 2004). However, it has not been determined whether such a complex controls *Bar* via the *ta5-enhancer* (Figure 6.1 and Figure 6.2)

Differential expression of transcription factors and protein interactions work in a combinatorial code to control the expression of *Bar* and to give specific tarsal identity to a different set of cells in the distal region of the leg imaginal disc.

Further directions:

Published data shows that Sp1 binds via its zinc-finger domain to the bHLH domain of both Ahr and Arnt (Kobayashi et al., 1996). These premises suggest that:

- Ss and Rn interact through their bHLH and zinc-finger domains, respectively. In order to test this hypothesis, I will conduct *in vitro* co-immunoprecipitation assays with different parts of Rn and Ss.

- Tgo and Rn also interact physically and I aim to test whether both proteins are able to co-precipitate. This will be useful to understand the structure of the transcription factor complex they might form.

It is likely that Rn represses expression of *Bar* via the *ta5-enhancer* during tarsal development. I plan to study the expression of the *ta5-lacZ* reporter in *rn* mutant mitotic clones. I will also carry out EMSA. The design of the oligos will be based on sequences from the *ta5-enhancer* and the CIZ-DNA binding site.

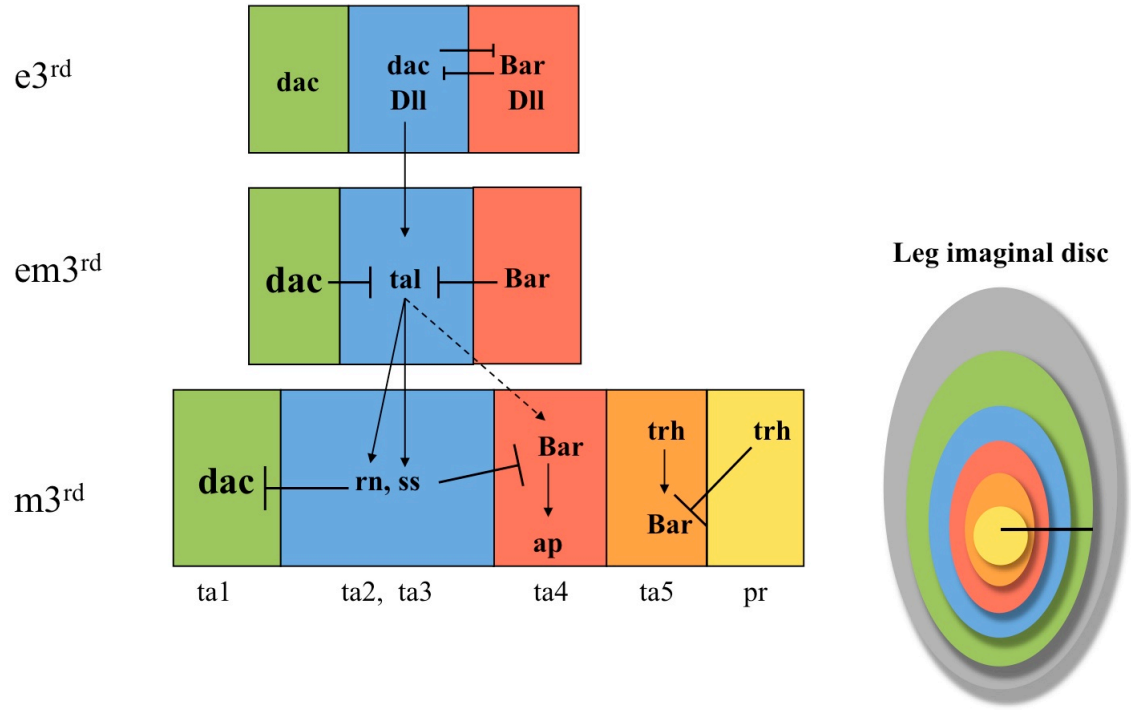

Figure 6.1. The genetic network that drives the fruit fly's distal leg development. The box diagram represents a section from the leg imaginal disc (black bar). E3rd, em3rd, and m3rd indicate the early, early-mid, and mid 3rd larval stages, respectively. ta1, ta2, ta3, ta4, ta5, and pr indicate the formation of the first, second, third, fourth, and fifth tarsal segments, and the pretarsus, respectively.

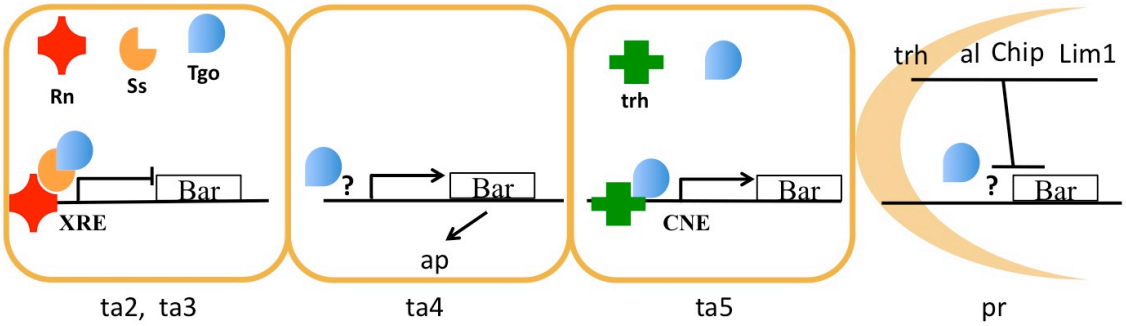

Figure 6.2. A combinatorial code of transcription factors and the interactions between them control expression of Bar and tarsal identity. Rn, Ss, and Tgo repress expression of *Bar* via the *ta5-enhancer* in the presumptive second and third tarsal segments. Expression of *Bar* upregulates *ap* in the presumptive fourth tarsal segment. Trh and Tgo enhance expression of Bar in the presumptive fifth tarsal segment via the *ta5-enhancer*. However, in the developing pretarsus, *trh* cooperates with *al, Chip* and *Lim1* to repress *Bar*. It is currently unknown whether Tgo and the *ta5-enhancer* control expression of *Bar* in the presumptive ta4 and pr segments.

6.4. Acquisition or preservation of the functional duality?

ss has a dual function that depends on the amount of protein that it expresses. In antennal development, *ss* seems to work as a homeotic gene. Certain combinations of *ss* mutant alleles (i.e. ss^{sta}/ss^{a}) lead to a transformation form distal antenna to distal leg, whereas legs remain wild type (Melnick et al., 1993). On the other hand, overexpression of Ss in leg leads to a transformation to distal antenna (Duncan et al., 1998). Thus, antennal/leg fate depends on the amount of Ss protein. The homeotic role of ss is also seen in the beetle *Tribolium castaneum*. RNA interferance of *ss* mRNA leads to a homeotic transformation of antenna to leg, whereas legs had wildtype appearance (Figure 6.3) (Toegel et al., 2009). It should be taken into account that RNAi is not necessarily equivalent to a null allele, meaning that in the *ss* RNAi experiments some *ss* mRNA might remain unaffected, which could be enough for the leg to develop. In the same work, the authors also show expression of *ss*, by in situ hybridation, in leg and antennal primordium (Figure 6.4) (Toegel et al., 2009). In summary, the similarities between *Drosophila* and *Tribolium* indicate that *ss* is required and sufficient to give antennal identity. *ss* seems to play a homeotic role in the development of antenna, whereas it might have a more morphological role in the formation of the adult leg. The arthropod leg and antenna are related structures. It is commonly accepted that they have evolved from the same ancestral appendage (Callahan, 1979). In Duncan et al. (1998), the authors speculate that the ancestral function of *ss* in arthropods was antennal specification (formation of a sensory organ that comprises mechanoreceptors and chemoreceptors) and later in evolution it acquired a role in leg elongation (Duncan et al., 1998).

In *C. elegans*, the homologue of *Ahr* (*Ahr-1)* is expressed during embryonic and larval development. The study of mutations in the *Ahr-1* locus indicate that it has a role

in neuronal development and detection of the concentraion of oxygen (Huang et al., 2004; Qin and Powell-Coffman, 2004). Thus, *Ahr-1* seems to be involved in the development of the worm chemosensitive system, supporting that the ancestral role of *ss* was related to the formation of sensory organs. As worms lack leg-like structures, the role of *ss* in leg development could not be compared with *Ahr-1*.

From a functional perspective, *Ahr* is very similar to its invertebrate orthologues. The current models support the theory that *Ahr* detoxification functions appeared after the invertebrate and vertebrate linage split (Butler et al., 2001; Hahn, 2002; McMillan and Bradfield, 2007). Indeed, Ss, Ahr-1, and Ahr's orthologue in the soft shell clam (clam-Ahr) fail to bind dioxins in *in vitro* experiments (Butler et al., 2001) and exposing flies, worms or clams to TCDD does not seem to have any discernable effect (Butler et al., 2001; Powell-Coffman et al., 1998). However, in evolution, new functions do not arise out of the blue. Instead, "evolution works as a tinkerer" (quoting François Jacob (Jacob, 1977)), using what is available as far as the acquisition of new functions can compromise with the existing ones. Why was *Ahr* "chosen" to detect and signal the presence of aryl hydrocarbons? Although, I am afraid, an answer to this question would require an extensive analysis of different species among vertebrates and invertebrates, it seems plausible that the ancestor of *Ahr* was involved in the transduction of chemosensory signals. As certain xenobiotics became an adaptive pressure for the organism, *Ahr* was possibly in the right place at the right time to evolve to detect and transduct the presence of dioxins.

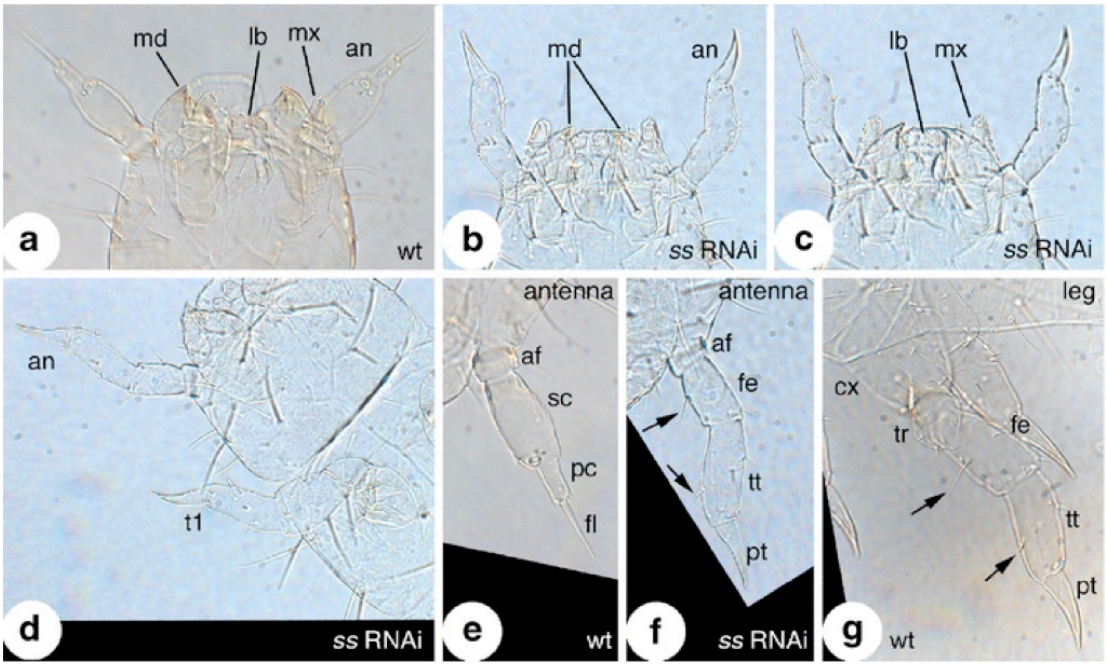

Figure 6.3. RNA interference of *ss* leads to a homeotic transformation from antenna to leg in the beetle *Tribolium castaneum*. Figure extracted from Toegel et al. 2009. **(A)** Head of a wild type beetle. The cephalic appendages are identified as antenna (an) labium (lb), mandible (md) and maxilla (mx). **(B and C)** Two different plane of focus of the head of a beetle injected with *ss* RNAi during the pupal stage. **(D)** View of the anterior part of a beetle treated with *ss* RNAi. Notice the antenna and the first thoracic leg (t1) are similar. **(E)** Detailed view of a wild type antenna. Segments are identified as antennifer (af), scapus (sc), pedicellus (pc), and flagellum (fl). **(F)** Antenna of a beetle treated with *ss* RNAi. Segments are identified as femur (fe), tibiotarsus (tt), and pretarsus (pt). **(G)** The leg of a wild type beetle. Additional abbreviations: coxa (cx) and trochanter (tr). Arrows point at the femur and tibiotarsus.

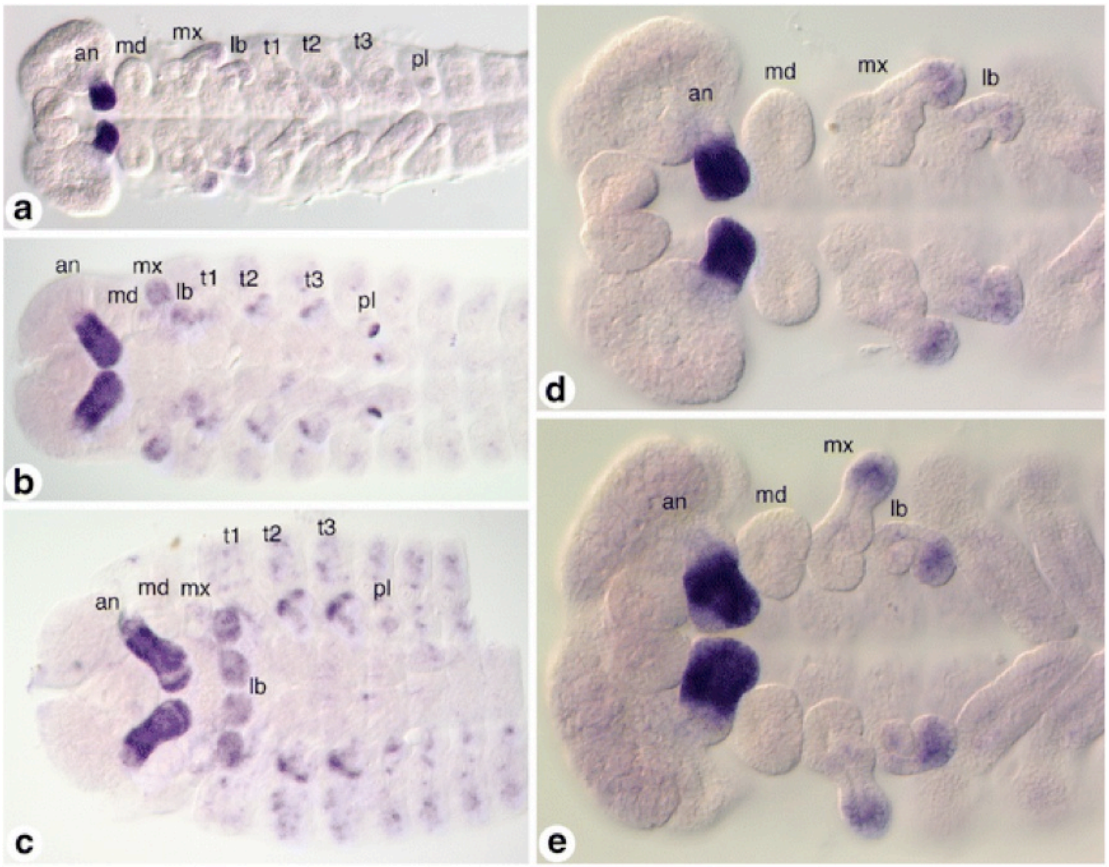

Figure 6.4. Expression of *ss* in *Tribolium* embryos. Figure extracted from Toegel et al. (2009). **(A)** A triboliium embryo with fully elongated germ band. **(B)** Embryo during mid-germ band retraction. **(C)** Fully retracted germ band. **(D)** Magnification of the head in A. **(E)** Head of an embryo at the beginning of the germ band retraction. Abbreviations: antenna (an), mandible (md), maxilla (mx), labium (lb), first, second and third thoracic leg (t1, t2, t3), and pleuropodium (pl).

REFERENCES

Abbott, B. D., Birnbaum, L. S., 1991. TCDD exposure of human embryonic palatal shelves in organ culture alters the differentiation of medial epithelial cells. Teratology. 43**,** 119-32.

Abbott, B. D., Harris, M. W., Birnbaum, L. S., 1992. Comparisons of the effects of TCDD and hydrocortisone on growth factor expression provide insight into their interaction in the embryonic mouse palate. Teratology. 45**,** 35-53.

Abbott, B. D., Probst, M. R., 1995. Developmental expression of two members of a new class of transcription factors: II. Expression of aryl hydrocarbon receptor nuclear translocator in the C57BL/6N mouse embryo. Dev Dyn. 204**,** 144-55.

Acar, M., Jafar-Nejad, H., Giagtzoglou, N., Yallampalli, S., David, G., He, Y., Delidakis, C., Bellen, H. J., 2006. Senseless physically interacts with proneural proteins and functions as a transcriptional co-activator. Development. 133**,** 1979-89.

Ainsley, J. A., Pettus, J. M., Bosenko, D., Gerstein, C. E., Zinkevich, N., Anderson, M. G., Adams, C. M., Welsh, M. J., Johnson, W. A., 2003. Enhanced locomotion caused by loss of the Drosophila DEG/ENaC protein Pickpocket1. Curr Biol. 13**,** 1557-63.

Allan, D. W., St Pierre, S. E., Miguel-Aliaga, I., Thor, S., 2003. Specification of neuropeptide cell identity by the integration of retrograde BMP signaling and a combinatorial transcription factor code. Cell. 113**,** 73-86.

Alonso, M. C., Cabrera, C. V., 1988. The achaete-scute gene complex of Drosophila melanogaster comprises four homologous genes. EMBO J. 7**,** 2585-91.

Alvarez, M., Shah, R., Rhodes, S. J., Bidwell, J. P., 2005. Two promoters control the mouse Nmp4/CIZ transcription factor gene. Gene. 347**,** 43-54.

Andreola, F., Fernandez-Salguero, P. M., Chiantore, M. V., Petkovich, M. P., Gonzalez, F. J., De Luca, L. M., 1997. Aryl hydrocarbon receptor knockout mice (AHR-/-) exhibit liver retinoid accumulation and reduced retinoic acid metabolism. Cancer Res. 57**,** 2835-8.

Andreola, F., Hayhurst, G. P., Luo, G., Ferguson, S. S., Gonzalez, F. J., Goldstein, J. A., De Luca, L. M., 2004. Mouse liver CYP2C39 is a novel retinoic acid 4-hydroxylase. Its down-regulation offers a molecular basis for liver retinoid accumulation and fibrosis in aryl hydrocarbon receptor-null mice. J Biol Chem. 279**,** 3434-8.

Baba, T., Mimura, J., Gradin, K., Kuroiwa, A., Watanabe, T., Matsuda, Y., Inazawa, J., Sogawa, K., Fujii-Kuriyama, Y., 2001. Structure and expression of the Ah receptor repressor gene. J Biol Chem. 276**,** 33101-10.

Baba, T., Mimura, J., Nakamura, N., Harada, N., Yamamoto, M., Morohashi, K., Fujii-Kuriyama, Y., 2005. Intrinsic function of the aryl hydrocarbon (dioxin) receptor as a key factor in female reproduction. Mol Cell Biol. 25**,** 10040-51.

BBC, Deadly dioxin used on Yushchenko. In: http://news.bbc.co.uk/1/hi/world/europe/4105035.stm, (Ed.), 2004.

BBC, Irish Republic recalls all pork. In: http://news.bbc.co.uk/1/hi/world/europe/7769391.stm, (Ed.), 2008.

BBC, Ukranian opposition leader Viktor yushchenko first claimed that he had been poisoned in September, when he was admitted to a clinic suffering from stomach pains. 2004.

Bertazzi, P. A., 1991. Long-Term Effects of Chemical Disasters - Lessons and Results from Seveso. Science of the Total Environment. 106**,** 5-20.

Bier, E., 2005. Drosophila, the golden bug, emerges as a tool for human genetics. Nat Rev Genet. 6**,** 9-23.

Bissell, M. J., Radisky, D., 2001. Putting tumours in context. Nat Rev Cancer. 1**,** 46-54.

Blair, S. S., 2003. Genetic mosaic techniques for studying Drosophila development. Development. 130**,** 5065-72.

Boag, S. a. S., A. , 2007. Immunology. Hodder Arnold.

Bock, K. W., Kohle, C., 2006. Ah receptor: dioxin-mediated toxic responses as hints to deregulated physiologic functions. Biochem Pharmacol. 72**,** 393-404.

Border, W. A., Noble, N. A., 1994. Transforming growth factor beta in tissue fibrosis. N Engl J Med. 331**,** 1286-92.

Brand, A. H., Perrimon, N., 1993. Targeted gene expression as a means of altering cell fates and generating dominant phenotypes. Development. 118**,** 401-15.

Branton, M. H., Kopp, J. B., 1999. TGF-beta and fibrosis. Microbes Infect. 1**,** 1349-65.

Brumby, A. M., Richardson, H. E., 2005. Using Drosophila melanogaster to map human cancer pathways. Nat Rev Cancer. 5**,** 626-39.

Brunnberg, S., Pettersson, K., Rydin, E., Matthews, J., Hanberg, A., Pongratz, I., 2003. The basic helix-loop-helix-PAS protein ARNT functions as a potent coactivator of estrogen receptor-dependent transcription. Proc Natl Acad Sci U S A. 100**,** 6517-22.

Butler, R. A., Kelley, M. L., Powell, W. H., Hahn, M. E., Van Beneden, R. J., 2001. An aryl hydrocarbon receptor (AHR) homologue from the soft-shell clam, Mya arenaria: evidence that invertebrate AHR homologues lack 2,3,7,8-

tetrachlorodibenzo-p-dioxin and beta-naphthoflavone binding. Gene. 278**,** 223-34.

Callahan, P. S., Evolution of antennae, their sensilla and the mechanism of scent detection in Arthropoda. In: A. P. Gupta, (Ed.), Arthropod Phylogeny. Van Nostrand Reinhold Co. , New York, 1979, pp. 259-298.

Castrillon, D. H., Gonczy, P., Alexander, S., Rawson, R., Eberhart, C. G., Viswanathan, S., DiNardo, S., Wasserman, S. A., 1993. Toward a molecular genetic analysis of spermatogenesis in Drosophila melanogaster: characterization of male-sterile mutants generated by single P element mutagenesis. Genetics. 135**,** 489-505.

Chan, W. K., Yao, G., Gu, Y. Z., Bradfield, C. A., 1999. Cross-talk between the aryl hydrocarbon receptor and hypoxia inducible factor signaling pathways. Demonstration of competition and compensation. J Biol Chem. 274**,** 12115-23.

Chou, W. H., Huber, A., Bentrop, J., Schulz, S., Schwab, K., Chadwell, L. V., Paulsen, R., Britt, S. G., 1999. Patterning of the R7 and R8 photoreceptor cells of Drosophila: evidence for induced and default cell-fate specification. Development. 126**,** 607-16.

Corchero, J., Martin-Partido, G., Dallas, S. L., Fernandez-Salguero, P. M., 2004. Liver portal fibrosis in dioxin receptor-null mice that overexpress the latent transforming growth factor-beta-binding protein-1. Int J Exp Pathol. 85**,** 295-302.

Cox, M. B., Miller, C. A., 3rd, 2002. The p23 co-chaperone facilitates dioxin receptor signaling in a yeast model system. Toxicol Lett. 129**,** 13-21.

Crameri, A., Whitehorn, E. A., Tate, E., Stemmer, W. P., 1996. Improved green fluorescent protein by molecular evolution using DNA shuffling. Nat Biotechnol. 14**,** 315-9.

Dahmann, C., 2008. Drosophila. Methods and Protocols. Humana Press.

de Nooij, J. C., Hariharan, I. K., 1995. Uncoupling cell fate determination from patterned cell division in the Drosophila eye. Science. 270**,** 983-5.

de Nooij, J. C., Letendre, M. A., Hariharan, I. K., 1996. A cyclin-dependent kinase inhibitor, Dacapo, is necessary for timely exit from the cell cycle during Drosophila embryogenesis. Cell. 87**,** 1237-47.

del Alamo, D., Mlodzik, M., 2008. Self-modulation of Notch signaling during ommatidial development via the Roughened eye transcriptional repressor. Development. 135**,** 2895-904.

Diaz-Benjumea, F. J., Cohen, B., Cohen, S. M., 1994. Cell interaction between compartments establishes the proximal-distal axis of Drosophila legs. Nature. 372**,** 175-9.

Dolwick, K. M., Swanson, H. I., Bradfield, C. A., 1993. In vitro analysis of Ah receptor domains involved in ligand-activated DNA recognition. Proc Natl Acad Sci U S A. 90**,** 8566-70.

Dong, P. D., Dicks, J. S., Panganiban, G., 2002. Distal-less and homothorax regulate multiple targets to pattern the Drosophila antenna. Development. 129**,** 1967-74.

Duncan, D. M., Burgess, E. A., Duncan, I., 1998. Control of distal antennal identity and tarsal development in Drosophila by spineless-aristapedia, a homolog of the mammalian dioxin receptor. Genes Dev. 12**,** 1290-303.

Edelstone, D. I., Rudolph, A. M., Heymann, M. A., 1978. Liver and ductus venosus blood flows in fetal lambs in utero. Circ Res. 42**,** 426-33.

Emmons, R. B., Duncan, D., Duncan, I., 2007. Regulation of the Drosophila distal antennal determinant spineless. Dev Biol. 302**,** 412-26.

Emmons, R. B., Duncan, D., Estes, P. A., Kiefel, P., Mosher, J. T., Sonnenfeld, M., Ward, M. P., Duncan, I., Crews, S. T., 1999. The spineless-aristapedia and tango bHLH-PAS proteins interact to control antennal and tarsal development in Drosophila. Development. 126**,** 3937-45.

EPA, Exposure and Human Health Reassessment of 2,3,7,8-Tetrachlorodibenzo-p-Dioxin (TCDD) and Related Compounds National Academy Sciences (NAS) Review Draft. In: http://www.epa.gov/ncea/pdfs/dioxin/nas-review/, (Ed.), 2005.

Estella, C., Mann, R. S., 2008. Logic of Wg and Dpp induction of distal and medial fates in the Drosophila leg. Development. 135**,** 627-36.

Feiler, R., Bjornson, R., Kirschfeld, K., Mismer, D., Rubin, G. M., Smith, D. P., Socolich, M., Zuker, C. S., 1992. Ectopic expression of ultraviolet-rhodopsins in the blue photoreceptor cells of Drosophila: visual physiology and photochemistry of transgenic animals. J Neurosci. 12**,** 3862-8.

Fernandez-Salguero, P., Pineau, T., Hilbert, D. M., McPhail, T., Lee, S. S., Kimura, S., Nebert, D. W., Rudikoff, S., Ward, J. M., Gonzalez, F. J., 1995. Immune system impairment and hepatic fibrosis in mice lacking the dioxin-binding Ah receptor. Science. 268**,** 722-6.

Fernandez-Salguero, P. M., Hilbert, D. M., Rudikoff, S., Ward, J. M., Gonzalez, F. J., 1996. Aryl-hydrocarbon receptor-deficient mice are resistant to 2,3,7,8-tetrachlorodibenzo-p-dioxin-induced toxicity. Toxicol Appl Pharmacol. 140**,** 173-9.

Fernandez-Salguero, P. M., Ward, J. M., Sundberg, J. P., Gonzalez, F. J., 1997. Lesions of aryl-hydrocarbon receptor-deficient mice. Vet Pathol. 34**,** 605-14.

Fischer, J. A., Giniger, E., Maniatis, T., Ptashne, M., 1988. GAL4 activates transcription in Drosophila. Nature. 332**,** 853-6.

Fortini, M. E., Rubin, G. M., 1990. Analysis of cis-acting requirements of the Rh3 and Rh4 genes reveals a bipartite organization to rhodopsin promoters in Drosophila melanogaster. Genes Dev. 4**,** 444-63.

Fortini, M. E., Skupski, M. P., Boguski, M. S., Hariharan, I. K., 2000. A survey of human disease gene counterparts in the Drosophila genome. J Cell Biol. 150**,** F23-30.

Furness, S. G., Lees, M. J., Whitelaw, M. L., 2007. The dioxin (aryl hydrocarbon) receptor as a model for adaptive responses of bHLH/PAS transcription factors. FEBS Lett. 581**,** 3616-25.

Galindo, M. I., Bishop, S. A., Couso, J. P., 2005. Dynamic EGFR-Ras signalling in Drosophila leg development. Dev Dyn. 233**,** 1496-508.

Galindo, M. I., Bishop, S. A., Greig, S., Couso, J. P., 2002. Leg patterning driven by proximal-distal interactions and EGFR signaling. Science. 297**,** 256-9.

Galindo, M. I., Pueyo, J. I., Fouix, S., Bishop, S. A., Couso, J. P., 2007. Peptides encoded by short ORFs control development and define a new eukaryotic gene family. PLoS Biol. 5**,** e106.

Ghysen, A., Richelle, J., 1979. Determination of sensory bristles and pattern formation in Drosophila. II. The achaete-scute locus. Dev Biol. 70**,** 438-52.

Golic, K. G., Lindquist, S., 1989. The FLP recombinase of yeast catalyzes site-specific recombination in the Drosophila genome. Cell. 59**,** 499-509.

Gomez, M. R., 1988. Varieties of expression of tuberous sclerosis. Neurofibromatosis. 1**,** 330-8.

Gray, L. E., Jr., Kelce, W. R., 1996. Latent effects of pesticides and toxic substances on sexual differentiation of rodents. Toxicol Ind Health. 12**,** 515-31.

Greenspan, R. J., 2004. Fly Pushing. Cold Spring Harbor Laboratory Press.

Grueber, W. B., Jan, L. Y., Jan, Y. N., 2002. Tiling of the Drosophila epidermis by multidendritic sensory neurons. Development. 129**,** 2867-78.

Hahn, M. E., 2002. Aryl hydrocarbon receptors: diversity and evolution. Chem Biol Interact. 141**,** 131-60.

Hannah-Alava, A., 1958. Developmental Genetics of the Posterior Legs in Drosophila Melanogaster. Genetics. 43**,** 878-905.

Hauck, B., Gehring, W. J., Walldorf, U., 1999. Functional analysis of an eye specific enhancer of the eyeless gene in Drosophila. Proc Natl Acad Sci U S A. 96**,** 564-9.

Heisenberg, M. B., E., 1977. The role of retinula cell types in visual behavior of Drosophila melanogaster. J. Comp. Physiol. 177**,** 127-162.

Held, L. I., Jr., 2002. Bristles induce bracts via the EGFR pathway on Drosophila legs. Mech Dev. 117**,** 225-34.

Henklova, P., Vrzal, R., Ulrichova, J., Dvorak, Z., 2008. Role of mitogen-activated protein kinases in aryl hydrocarbon receptor signaling. Chem Biol Interact. 172**,** 93-104.

Hoffman, E. C., Reyes, H., Chu, F. F., Sander, F., Conley, L. H., Brooks, B. A., Hankinson, O., 1991. Cloning of a factor required for activity of the Ah (dioxin) receptor. Science. 252**,** 954-8.

Huang, X., Powell-Coffman, J. A., Jin, Y., 2004. The AHR-1 aryl hydrocarbon receptor and its co-factor the AHA-1 aryl hydrocarbon receptor nuclear translocator specify GABAergic neuron cell fate in C. elegans. Development. 131**,** 819-28.

IARC, 1997. IARC Working Group on the Evaluation of Carcinogenic Risks to Humans: Polychlorinated Dibenzo-Para-Dioxins and Polychlorinated

Dibenzofurans. Lyon, France, 4-11 February 1997. IARC Monogr Eval Carcinog Risks Hum. 69**,** 1-631.

Ikuta, T., Eguchi, H., Tachibana, T., Yoneda, Y., Kawajiri, K., 1998. Nuclear localization and export signals of the human aryl hydrocarbon receptor. J Biol Chem. 273**,** 2895-904.

Ikuta, T., Kawajiri, K., 2006. Zinc finger transcription factor Slug is a novel target gene of aryl hydrocarbon receptor. Exp Cell Res. 312**,** 3585-94.

Jacob, F., 1977. Evolution and tinkering. Science. 196**,** 1161-6.

Jeon, M. S., Esser, C., 2000. The murine IL-2 promoter contains distal regulatory elements responsive to the Ah receptor, a member of the evolutionarily conserved bHLH-PAS transcription factor family. J Immunol. 165**,** 6975-83.

Joulia, L., Deutsch, J., Bourbon, H. M., Cribbs, D. L., 2006. The specification of a highly derived arthropod appendage, the Drosophila labial palps, requires the joint action of selectors and signaling pathways. Dev Genes Evol. 216**,** 431-42.

Kahn, P. C., Gochfeld, M., Nygren, M., Hansson, M., Rappe, C., Velez, H., Ghent-Guenther, T., Wilson, W. P., 1988. Dioxins and dibenzofurans in blood and adipose tissue of Agent Orange-exposed Vietnam veterans and matched controls. JAMA. 259**,** 1661-7.

Kazlauskas, A., Poellinger, L., Pongratz, I., 2000. The immunophilin-like protein XAP2 regulates ubiquitination and subcellular localization of the dioxin receptor. J Biol Chem. 275**,** 41317-24.

Kazlauskas, A., Sundstrom, S., Poellinger, L., Pongratz, I., 2001. The hsp90 chaperone complex regulates intracellular localization of the dioxin receptor. Mol Cell Biol. 21**,** 2594-607.

Kim, M. D., Jan, L. Y., Jan, Y. N., 2006. The bHLH-PAS protein Spineless is necessary for the diversification of dendrite morphology of Drosophila dendritic arborization neurons. Genes Dev. 20**,** 2806-19.

Kiserud, T., 2000. Liver length in the small-for-gestational-age fetus and ductus venosus flow. Am J Obstet Gynecol. 182**,** 252-3.

Klinge, C. M., Kaur, K., Swanson, H. I., 2000. The aryl hydrocarbon receptor interacts with estrogen receptor alpha and orphan receptors COUP-TFI and ERRalpha1. Arch Biochem Biophys. 373**,** 163-74.

Kobayashi, A., Sogawa, K., Fujii-Kuriyama, Y., 1996. Cooperative interaction between AhR.Arnt and Sp1 for the drug-inducible expression of CYP1A1 gene. J Biol Chem. 271**,** 12310-6.

Kohle, C., Gschaidmeier, H., Lauth, D., Topell, S., Zitzer, H., Bock, K. W., 1999. 2,3,7,8-Tetrachlorodibenzo-p-dioxin (TCDD)-mediated membrane translocation of c-Src protein kinase in liver WB-F344 cells. Arch Toxicol. 73**,** 152-8.

Kozu, S., Tajiri, R., Tsuji, T., Michiue, T., Saigo, K., Kojima, T., 2006. Temporal regulation of late expression of Bar homeobox genes during Drosophila leg development by Spineless, a homolog of the mammalian dioxin receptor. Dev Biol. 294**,** 497-508.

Kudo, K., Takeuchi, T., Murakami, Y., Ebina, M., Kikuchi, H., 2009. Characterization of the region of the aryl hydrocarbon receptor required for ligand dependency of transactivation using chimeric receptor between Drosophila and Mus musculus. Biochim Biophys Acta.

Lahvis, G. P., Lindell, S. L., Thomas, R. S., McCuskey, R. S., Murphy, C., Glover, E., Bentz, M., Southard, J., Bradfield, C. A., 2000. Portosystemic shunting and

persistent fetal vascular structures in aryl hydrocarbon receptor-deficient mice. Proc Natl Acad Sci U S A. 97**,** 10442-7.

Lahvis, G. P., Pyzalski, R. W., Glover, E., Pitot, H. C., McElwee, M. K., Bradfield, C. A., 2005. The aryl hydrocarbon receptor is required for developmental closure of the ductus venosus in the neonatal mouse. Mol Pharmacol. 67**,** 714-20.

Lecuit, T., Cohen, S. M., 1997. Proximal-distal axis formation in the Drosophila leg. Nature. 388**,** 139-45.

Lewis, E. B., 1960. A new standard food medium. Drosophila Information Service. 34.

Lin, T. M., Ko, K., Moore, R. W., Simanainen, U., Oberley, T. D., Peterson, R. E., 2002. Effects of aryl hydrocarbon receptor null mutation and in utero and lactational 2,3,7,8-tetrachlorodibenzo-p-dioxin exposure on prostate and seminal vesicle development in C57BL/6 mice. Toxicol Sci. 68**,** 479-87.

Lindsley, D. L. a. G. G. Z., 1992. The Genome of Drosophila melanogaster. Academic Press.

Liu, L., Yermolaieva, O., Johnson, W. A., Abboud, F. M., Welsh, M. J., 2003. Identification and function of thermosensory neurons in Drosophila larvae. Nat Neurosci. 6**,** 267-73.

Luebeck, E. G., Buchmann, A., Stinchcombe, S., Moolgavkar, S. H., Schwarz, M., 2000. Effects of 2,3,7,8-tetrachlorodibenzo-p-dioxin on initiation and promotion of GST-P-positive foci in rat liver: A quantitative analysis of experimental data using a stochastic model. Toxicol Appl Pharmacol. 167**,** 63-73.

Mann, H. B., Whitney, D. R., 1947. On a Test of Whether One of 2 Random Variables Is Stochastically Larger Than the Other. Annals of Mathematical Statistics. 18**,** 50-60.

Mardon, G., Solomon, N. M., Rubin, G. M., 1994. dachshund encodes a nuclear protein required for normal eye and leg development in Drosophila. Development. 120**,** 3473-86.

Masucci, J. D., Miltenberger, R. J., Hoffmann, F. M., 1990. Pattern-specific expression of the Drosophila decapentaplegic gene in imaginal disks is regulated by 3' cis-regulatory elements. Genes Dev. 4**,** 2011-23.

McGovern, V. L., Pacak, C. A., Sewell, S. T., Turski, M. L., Seeger, M. A., 2003. A targeted gain of function screen in the embryonic CNS of Drosophila. Mech Dev. 120**,** 1193-207.

McMillan, B. J., Bradfield, C. A., 2007. The aryl hydrocarbon receptor sans xenobiotics: endogenous function in genetic model systems. Mol Pharmacol. 72**,** 487-98.

McMillan, P. A., McGuire, T. R., 1992. The homeotic gene spineless-aristapedia affects geotaxis in Drosophila melanogaster. Behav Genet. 22**,** 557-73.

Melnick, M. B., Noll, E., Perrimon, N., 1993. The Drosophila stubarista phenotype is associated with a dosage effect of the putative ribosome-associated protein D-p40 on spineless. Genetics. 135**,** 553-64.

Michalek, J. E., Wolfe, W. H., Miner, J. C., Papa, T. M., Pirkle, J. L., 1995. Indices of TCDD exposure and TCDD body burden in veterans of Operation Ranch Hand. J Expo Anal Environ Epidemiol. 5**,** 209-23.

Miguel-Aliaga, I., Allan, D. W., Thor, S., 2004. Independent roles of the dachshund and eyes absent genes in BMP signaling, axon pathfinding and neuronal specification. Development. 131**,** 5837-48.

Miller, G., Hansen, K. & Stark, W. , 1981. Phototaxis in Drosophila: R1-R6 input and interaction among ocellar and compound eye receptors. J. Insect Physiol. 27**,** 813-819.

Mimura, J., Ema, M., Sogawa, K., Fujii-Kuriyama, Y., 1999. Identification of a novel mechanism of regulation of Ah (dioxin) receptor function. Genes Dev. 13**,** 20-5.

Mimura, J., Yamashita, K., Nakamura, K., Morita, M., Takagi, T. N., Nakao, K., Ema, M., Sogawa, K., Yasuda, M., Katsuki, M., Fujii-Kuriyama, Y., 1997. Loss of teratogenic response to 2,3,7,8-tetrachlorodibenzo-p-dioxin (TCDD) in mice lacking the Ah (dioxin) receptor. Genes Cells. 2**,** 645-54.

Mitchell, H. K., Edens, J., Petersen, N. S., 1990. Stages of cell hair construction in Drosophila. Dev Genet. 11**,** 133-40.

Mocarelli, P., Gerthoux, P. M., Ferrari, E., Patterson, D. G., Jr., Kieszak, S. M., Brambilla, P., Vincoli, N., Signorini, S., Tramacere, P., Carreri, V., Sampson, E. J., Turner, W. E., Needham, L. L., 2000. Paternal concentrations of dioxin and sex ratio of offspring. Lancet. 355**,** 1858-63.

Moolgavkar, S. H., Luebeck, E. G., Buchmann, A., Bock, K. W., 1996. Quantitative analysis of enzyme-altered liver foci in rats initiated with diethylnitrosamine and promoted with 2,3,7,8-tetrachlorodibenzo-p-dioxin or 1,2,3,4,6,7,8-heptachlorodibenzo-p-dioxin. Toxicol Appl Pharmacol. 138**,** 31-42.

Muller, H. J., 1918. Genetic Variability, Twin Hybrids and Constant Hybrids, in a Case of Balanced Lethal Factors. Genetics. 3**,** 422-99.

Muller, H. J., Kaplan, W. D., 1966. The dosage compensation of Drosophila and mammals as showing the accuracy of the normal type. Genet Res. 8**,** 41-59.

Murre, C., McCaw, P. S., Vaessin, H., Caudy, M., Jan, L. Y., Jan, Y. N., Cabrera, C. V., Buskin, J. N., Hauschka, S. D., Lassar, A. B., et al., 1989. Interactions between

heterologous helix-loop-helix proteins generate complexes that bind specifically to a common DNA sequence. Cell. 58**,** 537-44.

Nakamoto, T., Shiratsuchi, A., Oda, H., Inoue, K., Matsumura, T., Ichikawa, M., Saito, T., Seo, S., Maki, K., Asai, T., Suzuki, T., Hangaishi, A., Yamagata, T., Aizawa, S., Noda, M., Nakanishi, Y., Hirai, H., 2004. Impaired spermatogenesis and male fertility defects in CIZ/Nmp4-disrupted mice. Genes Cells. 9**,** 575-89.

Nakamoto, T., Yamagata, T., Sakai, R., Ogawa, S., Honda, H., Ueno, H., Hirano, N., Yazaki, Y., Hirai, H., 2000. CIZ, a zinc finger protein that interacts with p130(cas) and activates the expression of matrix metalloproteinases. Mol Cell Biol. 20**,** 1649-58.

Nieto, M. A., 2002. The snail superfamily of zinc-finger transcription factors. Nat Rev Mol Cell Biol. 3**,** 155-66.

Ohshiro, T., Saigo, K., 1997. Transcriptional regulation of breathless FGF receptor gene by binding of TRACHEALESS/dARNT heterodimers to three central midline elements in Drosophila developing trachea. Development. 124**,** 3975-86.

Ohtake, F., Baba, A., Takada, I., Okada, M., Iwasaki, K., Miki, H., Takahashi, S., Kouzmenko, A., Nohara, K., Chiba, T., Fujii-Kuriyama, Y., Kato, S., 2007. Dioxin receptor is a ligand-dependent E3 ubiquitin ligase. Nature. 446**,** 562-6.

Pavuk, M., Michalek, J. E., Schecter, A., Ketchum, N. S., Akhtar, F. Z., Fox, K. A., 2005. Did TCDD exposure or service in Southeast Asia increase the risk of cancer in air force Vietnam veterans who did not spray agent orange? J Occup Environ Med. 47**,** 335-42.

Perrimon, N., Lanjuin, A., Arnold, C., Noll, E., 1996. Zygotic lethal mutations with maternal effect phenotypes in Drosophila melanogaster. II. Loci on the second

and third chromosomes identified by P-element-induced mutations. Genetics. 144**,** 1681-92.

Pesatori, A. C., Consonni, D., Bachetti, S., Zocchetti, C., Bonzini, M., Baccarelli, A., Bertazzi, P. A., 2003. Short- and long-term morbidity and mortality in the population exposed to dioxin after the "Seveso accident". Ind Health. 41**,** 127-38.

Peters, J. M., Narotsky, M. G., Elizondo, G., Fernandez-Salguero, P. M., Gonzalez, F. J., Abbott, B. D., 1999. Amelioration of TCDD-induced teratogenesis in aryl hydrocarbon receptor (AhR)-null mice. Toxicol Sci. 47**,** 86-92.

Poland, A., Knutson, J. C., 1982. 2,3,7,8-tetrachlorodibenzo-p-dioxin and related halogenated aromatic hydrocarbons: examination of the mechanism of toxicity. Annu Rev Pharmacol Toxicol. 22**,** 517-54.

Pollenz, R. S., 1996. The aryl-hydrocarbon receptor, but not the aryl-hydrocarbon receptor nuclear translocator protein, is rapidly depleted in hepatic and nonhepatic culture cells exposed to 2,3,7,8-tetrachlorodibenzo-p-dioxin. Mol Pharmacol. 49**,** 391-8.

Pollenz, R. S., 2002. The mechanism of AH receptor protein down-regulation (degradation) and its impact on AH receptor-mediated gene regulation. Chem Biol Interact. 141**,** 41-61.

Pollenz, R. S., Sattler, C. A., Poland, A., 1994. The aryl hydrocarbon receptor and aryl hydrocarbon receptor nuclear translocator protein show distinct subcellular localizations in Hepa 1c1c7 cells by immunofluorescence microscopy. Mol Pharmacol. 45**,** 428-38.

Pongratz, I., Mason, G. G., Poellinger, L., 1992. Dual roles of the 90-kDa heat shock protein hsp90 in modulating functional activities of the dioxin receptor.

Evidence that the dioxin receptor functionally belongs to a subclass of nuclear receptors which require hsp90 both for ligand binding activity and repression of intrinsic DNA binding activity. J Biol Chem. 267**,** 13728-34.

Powell-Coffman, J. A., Bradfield, C. A., Wood, W. B., 1998. Caenorhabditis elegans orthologs of the aryl hydrocarbon receptor and its heterodimerization partner the aryl hydrocarbon receptor nuclear translocator. Proc Natl Acad Sci U S A. 95**,** 2844-9.

Pueyo, J. I., Couso, J. P., 2004. Chip-mediated partnerships of the homeodomain proteins Bar and Aristaless with the LIM-HOM proteins Apterous and Lim1 regulate distal leg development. Development. 131**,** 3107-20.

Pueyo, J. I., Couso, J. P., 2008. The 11-aminoacid long Tarsal-less peptides trigger a cell signal in Drosophila leg development. Developmental Biology. 324**,** 192-201.

Qin, H., Powell-Coffman, J. A., 2004. The Caenorhabditis elegans aryl hydrocarbon receptor, AHR-1, regulates neuronal development. Dev Biol. 270**,** 64-75.

Refaeli, Y., Van Parijs, L., London, C. A., Tschopp, J., Abbas, A. K., 1998. Biochemical mechanisms of IL-2-regulated Fas-mediated T cell apoptosis. Immunity. 8**,** 615-23.

Reiter, L. T., Potocki, L., Chien, S., Gribskov, M., Bier, E., 2001. A systematic analysis of human disease-associated gene sequences in Drosophila melanogaster. Genome Res. 11**,** 1114-25.

Rier, S., Foster, W. G., 2003. Environmental dioxins and endometriosis. Semin Reprod Med. 21**,** 145-54.

Roman, A. C., Benitez, D. A., Carvajal-Gonzalez, J. M., Fernandez-Salguero, P. M., 2008. Genome-wide B1 retrotransposon binds the transcription factors dioxin

receptor and Slug and regulates gene expression in vivo. Proc Natl Acad Sci U S A. 105**,** 1632-7.

Santiago-Josefat, B., Mulero-Navarro, S., Dallas, S. L., Fernandez-Salguero, P. M., 2004. Overexpression of latent transforming growth factor-beta binding protein 1 (LTBP-1) in dioxin receptor-null mouse embryo fibroblasts. J Cell Sci. 117**,** 849-59.

Schecter, A., Birnbaum, L., Ryan, J. J., Constable, J. D., 2006. Dioxins: an overview. Environ Res. 101**,** 419-28.

Schmidt, J. V., Bradfield, C. A., 1996. Ah receptor signaling pathways. Annu Rev Cell Dev Biol. 12**,** 55-89.

Schmidt, J. V., Su, G. H., Reddy, J. K., Simon, M. C., Bradfield, C. A., 1996. Characterization of a murine Ahr null allele: involvement of the Ah receptor in hepatic growth and development. Proc Natl Acad Sci U S A. 93**,** 6731-6.

Shen, Z. J., Nakamoto, T., Tsuji, K., Nifuji, A., Miyazono, K., Komori, T., Hirai, H., Noda, M., 2002. Negative regulation of bone morphogenetic protein/Smad signaling by Cas-interacting zinc finger protein in osteoblasts. J Biol Chem. 277**,** 29840-6.

Shimizu, Y., Nakatsuru, Y., Ichinose, M., Takahashi, Y., Kume, H., Mimura, J., Fujii-Kuriyama, Y., Ishikawa, T., 2000. Benzo[a]pyrene carcinogenicity is lost in mice lacking the aryl hydrocarbon receptor. Proc Natl Acad Sci U S A. 97**,** 779-82.

Simpson, P., 2007. The stars and stripes of animal bodies: evolution of regulatory elements mediating pigment and bristle patterns in Drosophila. Trends Genet. 23**,** 350-8.

Sonnenfeld, M., Ward, M., Nystrom, G., Mosher, J., Stahl, S., Crews, S., 1997. The Drosophila tango gene encodes a bHLH-PAS protein that is orthologous to mammalian Arnt and controls CNS midline and tracheal development. Development. 124**,** 4571-82.

Spradling, A. C., Stern, D., Beaton, A., Rhem, E. J., Laverty, T., Mozden, N., Misra, S., Rubin, G. M., 1999. The Berkeley Drosophila Genome Project gene disruption project: Single P-element insertions mutating 25% of vital Drosophila genes. Genetics. 153**,** 135-77.

St Pierre, S. E., Galindo, M. I., Couso, J. P., Thor, S., 2002. Control of Drosophila imaginal disc development by rotund and roughened eye: differentially expressed transcripts of the same gene encoding functionally distinct zinc finger proteins. Development. 129**,** 1273-81.

Stapleton, M., Liao, G., Brokstein, P., Hong, L., Carninci, P., Shiraki, T., Hayashizaki, Y., Champe, M., Pacleb, J., Wan, K., Yu, C., Carlson, J., George, R., Celniker, S., Rubin, G. M., 2002. The Drosophila gene collection: identification of putative full-length cDNAs for 70% of D. melanogaster genes. Genome Res. 12**,** 1294-300.

Steenland, K., Bertazzi, P., Baccarelli, A., Kogevinas, M., 2004. Dioxin revisited: developments since the 1997 IARC classification of dioxin as a human carcinogen. Environ Health Perspect. 112**,** 1265-8.

Stinchcombe, S., Buchmann, A., Bock, K. W., Schwarz, M., 1995. Inhibition of apoptosis during 2,3,7,8-tetrachlorodibenzo-p-dioxin-mediated tumour promotion in rat liver. Carcinogenesis. 16**,** 1271-5.

Struhl, C., 1981. A homeotic mutation transforming leg to antenna in Drosophila. Nature. 292**,** 635-638.

Su, A. I., Cooke, M. P., Ching, K. A., Hakak, Y., Walker, J. R., Wiltshire, T., Orth, A. P., Vega, R. G., Sapinoso, L. M., Moqrich, A., Patapoutian, A., Hampton, G. M., Schultz, P. G., Hogenesch, J. B., 2002. Large-scale analysis of the human and mouse transcriptomes. Proc Natl Acad Sci U S A. 99**,** 4465-70.

Swanson, H. I., Chan, W. K., Bradfield, C. A., 1995. DNA binding specificities and pairing rules of the Ah receptor, ARNT, and SIM proteins. J Biol Chem. 270**,** 26292-302.

Swanson, H. I., Perdew, G. H., 1993. Half-life of aryl hydrocarbon receptor in Hepa 1 cells: evidence for ligand-dependent alterations in cytosolic receptor levels. Arch Biochem Biophys. 302**,** 167-74.

Swanson, H. I., Tullis, K., Denison, M. S., 1993. Binding of transformed Ah receptor complex to a dioxin responsive transcriptional enhancer: evidence for two distinct heteromeric DNA-binding forms. Biochemistry. 32**,** 12841-9.

Tajiri, R., Tsuji, T., Ueda, R., Saigo, K., Kojima, T., 2007. Fate determination of Drosophila leg distal regions by trachealess and tango through repression and stimulation, respectively, of Bar homeobox gene expression in the future pretarsus and tarsus. Dev Biol. 303**,** 461-73.

Tapon, N., Ito, N., Dickson, B. J., Treisman, J. E., Hariharan, I. K., 2001. The Drosophila tuberous sclerosis complex gene homologs restrict cell growth and cell proliferation. Cell. 105**,** 345-55.

Terriente Felix, J., Magarinos, M., Diaz-Benjumea, F. J., 2007. Nab controls the activity of the zinc-finger transcription factors Squeeze and Rotund in Drosophila development. Development. 134**,** 1845-52.

Toegel, J. P., Wimmer, E. A., Prpic, N. M., 2009. Loss of spineless function transforms the Tribolium antenna into a thoracic leg with pretarsal, tibiotarsal, and femoral identity. Dev Genes Evol. 219**,** 53-8.

Tracey, W. D., Jr., Wilson, R. I., Laurent, G., Benzer, S., 2003. painless, a Drosophila gene essential for nociception. Cell. 113**,** 261-73.

Tseng, A. S., Hariharan, I. K., 2002. An overexpression screen in Drosophila for genes that restrict growth or cell-cycle progression in the developing eye. Genetics. 162**,** 229-43.

Tsubota, T., Saigo, K., Kojima, T., 2008. Hox genes regulate the same character by different strategies in each segment. Mech Dev. 125**,** 894-905.

Van den Berg, M., Birnbaum, L., Bosveld, A. T., Brunstrom, B., Cook, P., Feeley, M., Giesy, J. P., Hanberg, A., Hasegawa, R., Kennedy, S. W., Kubiak, T., Larsen, J. C., van Leeuwen, F. X., Liem, A. K., Nolt, C., Peterson, R. E., Poellinger, L., Safe, S., Schrenk, D., Tillitt, D., Tysklind, M., Younes, M., Waern, F., Zacharewski, T., 1998. Toxic equivalency factors (TEFs) for PCBs, PCDDs, PCDFs for humans and wildlife. Environ Health Perspect. 106**,** 775-92.

Wang, G. L., Jiang, B. H., Rue, E. A., Semenza, G. L., 1995. Hypoxia-inducible factor 1 is a basic-helix-loop-helix-PAS heterodimer regulated by cellular O2 tension. Proc Natl Acad Sci U S A. 92**,** 5510-4.

Ward, M. P., Mosher, J. T., Crews, S. T., 1998. Regulation of bHLH-PAS protein subcellular localization during Drosophila embryogenesis. Development. 125**,** 1599-608.

Warner, M., Eskenazi, B., Mocarelli, P., Gerthoux, P. M., Samuels, S., Needham, L., Patterson, D., Brambilla, P., 2002. Serum dioxin concentrations and breast

cancer risk in the Seveso Women's Health Study. Environ Health Perspect. 110**,** 625-8.

Wenger, R. H., Camenisch, G., Desbaillets, I., Chilov, D., Gassmann, M., 1998. Up-regulation of hypoxia-inducible factor-1alpha is not sufficient for hypoxic/anoxic p53 induction. Cancer Res. 58**,** 5678-80.

Wernet, M. F., Labhart, T., Baumann, F., Mazzoni, E. O., Pichaud, F., Desplan, C., 2003. Homothorax switches function of Drosophila photoreceptors from color to polarized light sensors. Cell. 115**,** 267-79.

Wernet, M. F., Mazzoni, E. O., Celik, A., Duncan, D. M., Duncan, I., Desplan, C., 2006. Stochastic spineless expression creates the retinal mosaic for colour vision. Nature. 440**,** 174-80.

Whitlock, J. P., Jr., 1990. Genetic and molecular aspects of 2,3,7,8-tetrachlorodibenzo-p-dioxin action. Annu Rev Pharmacol Toxicol. 30**,** 251-77.

Wolff, T. R., D. F., 1993. The Development of Drosophila melanogaster Cold Spring Harbor Laboratory Press.

Young, J. M., Burley, M. W., Jeremiah, S. J., Jeganathan, D., Ekong, R., Osborne, J. P., Povey, S., 1998. A mutation screen of the TSC1 gene reveals 26 protein truncating mutations and 1 splice site mutation in a panel of 79 tuberous sclerosis patients. Ann Hum Genet. 62**,** 203-13.

Zack, J. A., Suskind, R. R., 1980. The mortality experience of workers exposed to tetrachlorodibenzodioxin in a trichlorophenol process accident. J Occup Med. 22**,** 11-4.

Zaher, H., Fernandez-Salguero, P. M., Letterio, J., Sheikh, M. S., Fornace, A. J., Jr., Roberts, A. B., Gonzalez, F. J., 1998. The involvement of aryl hydrocarbon

receptor in the activation of transforming growth factor-beta and apoptosis. Mol Pharmacol. 54**,** 313-21.

Zuker, C. S., Cowman, A. F., Rubin, G. M., 1985. Isolation and structure of a rhodopsin gene from D. melanogaster. Cell. 40**,** 851-8.

Appendix I

The following is the list of primers employed for cloning and DNA sequencing in this work.

ss SDK

Tail + **Kozak start site** +3nt + ss coding sequence (1>19)

AGGAGG**TACC**ATCATGAGCCAGCTGGGCACCG

ss reverse

Tail + ss coding sequence (2654>2628)

GCTAGCTAGCGGTGGCCGTGGTGCAGGTGATG

ss seq1

ss coding sequence (638>659)

CCGCTGCCTGCTGGACAACACG

ss seq2

ss coding sequence (1214>1235)

GGTAGTGCCTCCGAGCACCTCC

XbaI-ssA5 forw

Tail+**XbaI**+ss coding sequence (-13>8)

GAGAGA**TCTAGA**ATCCGCCCTAGCAATGAGCCA

ssA5 rev

pgEX-2T vector (downstream of ss insertion)

CCGGGAGCTGCATGTGTCAGAGG

Ahr SDK

Tail + **Kozak start site** +3nt + Ahr coding sequence (1>23)

AGGAGG**TACC**ATCATGAGCAGCGGCGCCAACATCAC

Ahr reverse

Tail + Ahr coding sequence (2427>2395)

GCTAGCTAGTCAACTCTGCACCTTGCTTAGGAATGCC

Ahr seq1

Ahr coding sequence (751>773)

GCGCTGCTTCCTCCACAACTGG

t7 promoter

pCR4-TOPO forward primer

TAATACGACTCACTATAGGG

M13 rev

pCR4-TOPO reverse primer

CAGGAAACAGCTATGAC

Appendix II

The following are the maps of the vectors and constructs that I have employed and generated.

***pUASt* constructs**

I carried out cloning of *Arnt* from *pCMV-Sport6-Arnt* in the the *pUASt* vector in order to generate transgenic lines. *pUASt-Ahr* was used to extract *Ahr* for cloning in the *pCR4-TOPO* vector. The yellow segment represents the gene *white*, which is used for phenotypical selection of transgenics. The UAS promoter is represented by the pink triangle.

pUASt

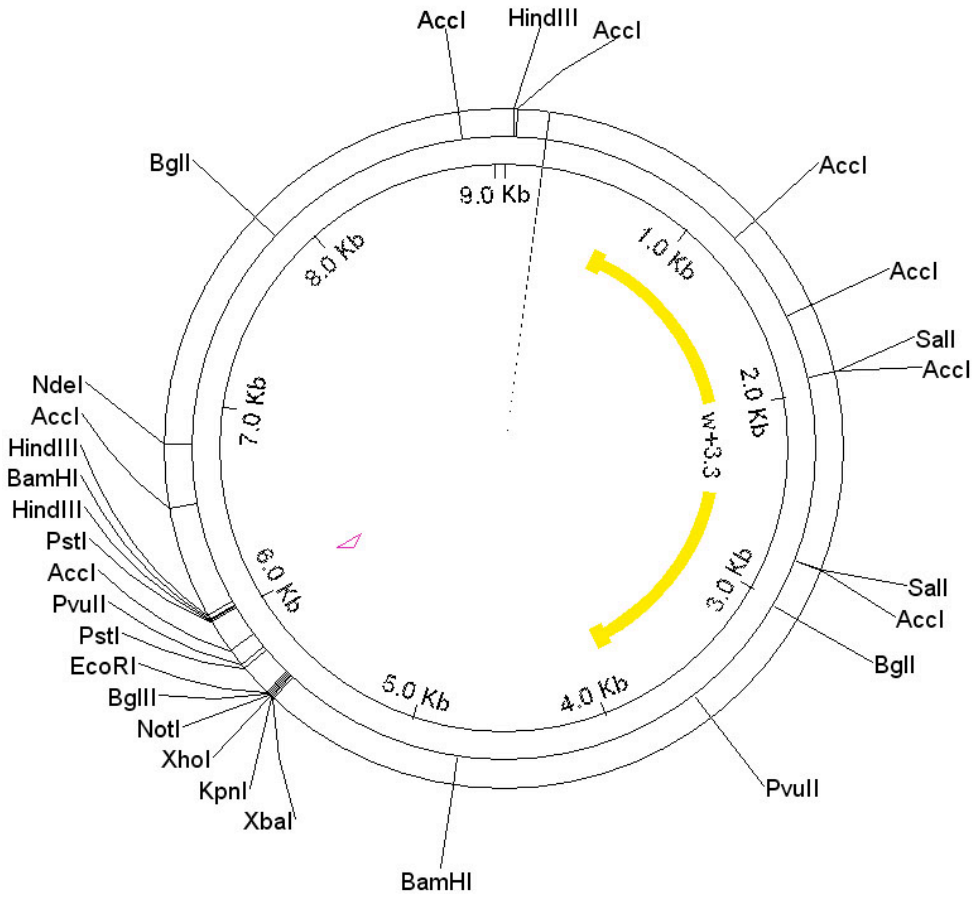

pCMV-Sport6-Arnt

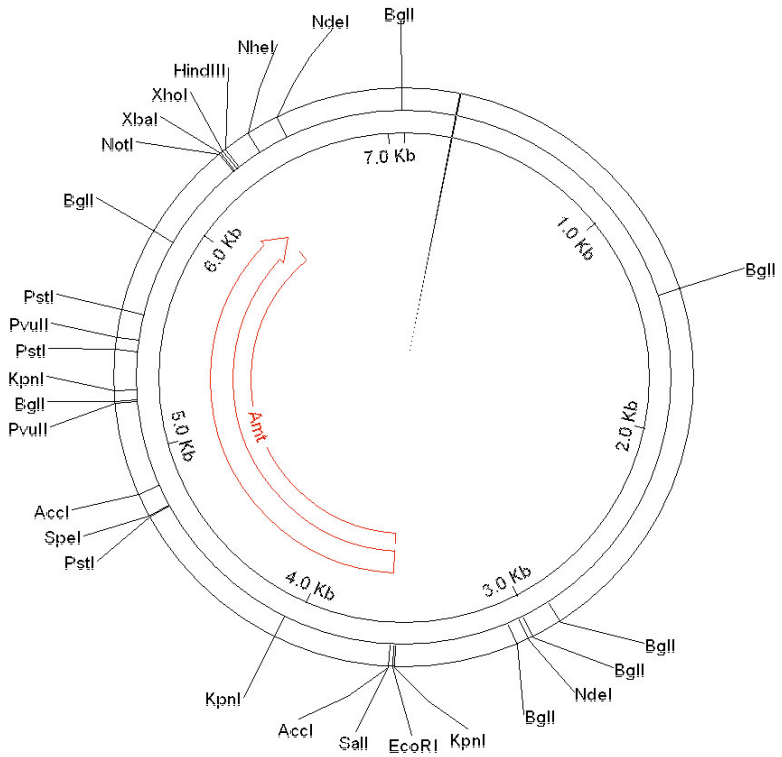

pUASt-Arnt

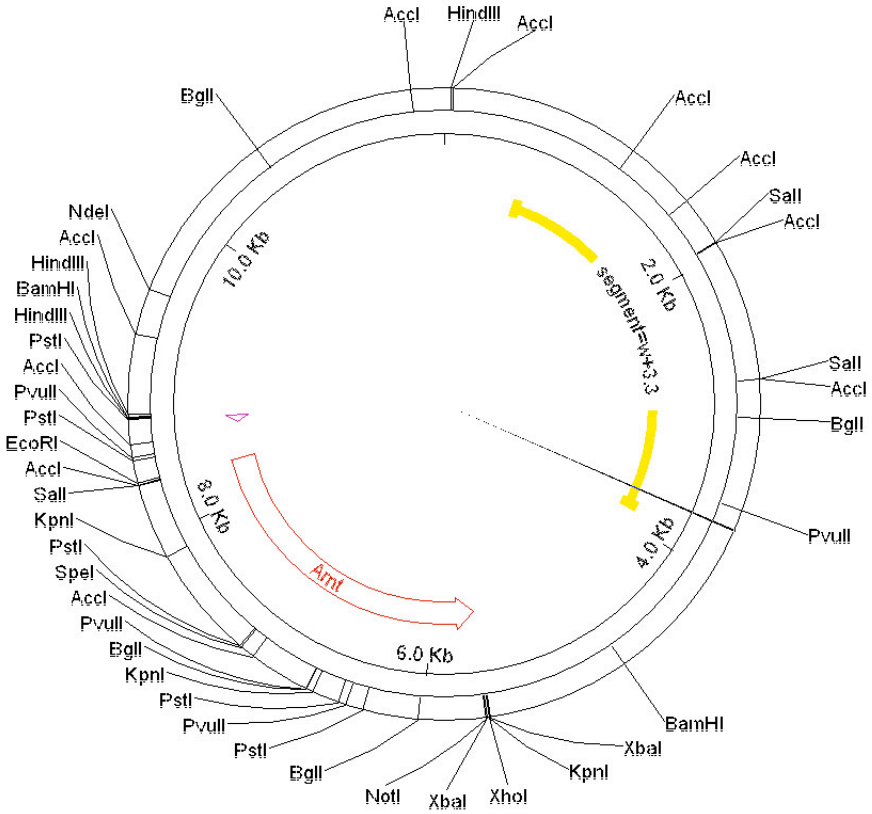

pUASt-Ahr

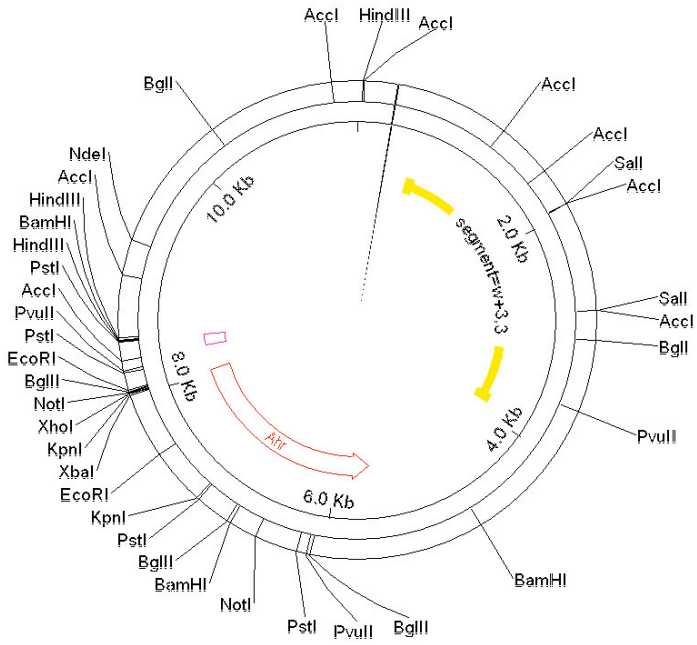

***pCR4-TOPO* constructs**

I performed cloning in the *pCR4-TOPO* in order to express proteins in a cell-free system under the control of the T7 promoter (green segment).

pCR4-TOPO

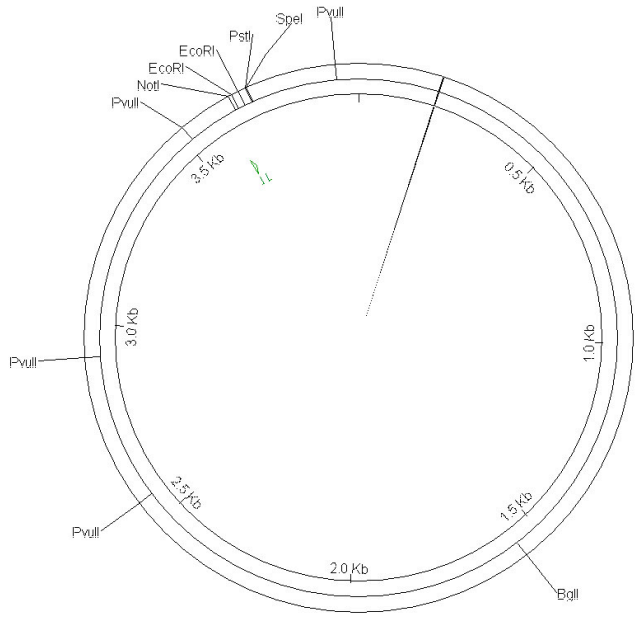

pCR4-TOPO-SDK-Ahr

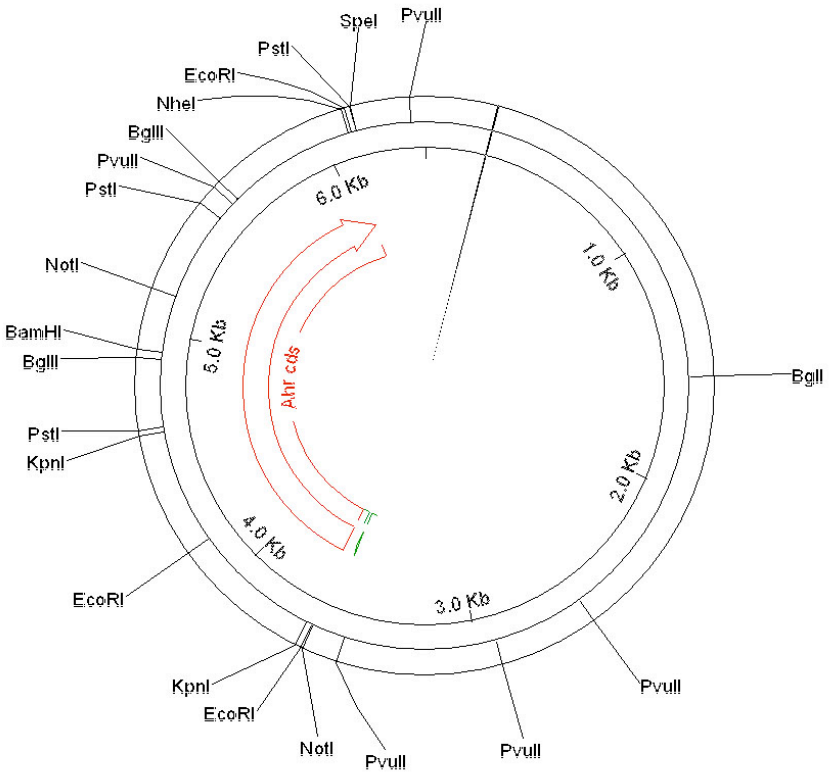

pGEX-2T-ss

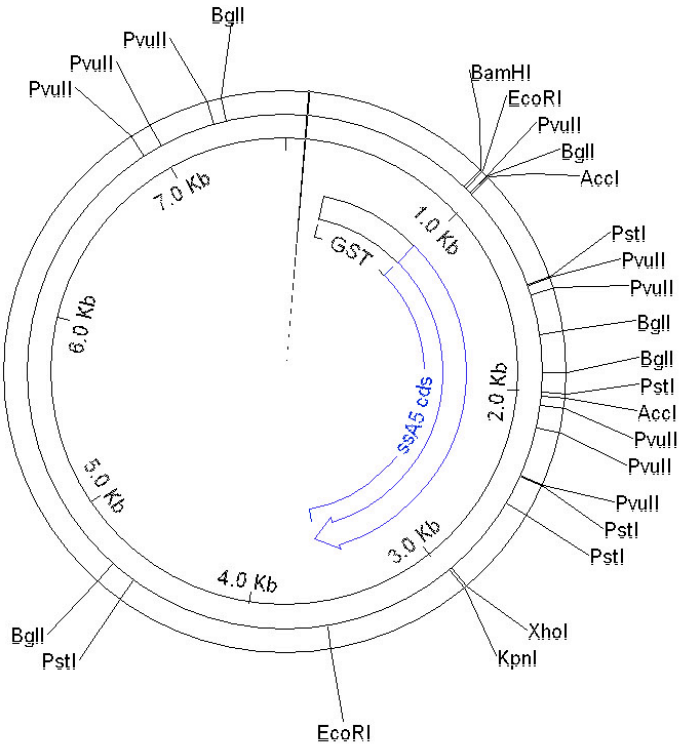

pCR4-TOPO-SDK-ss

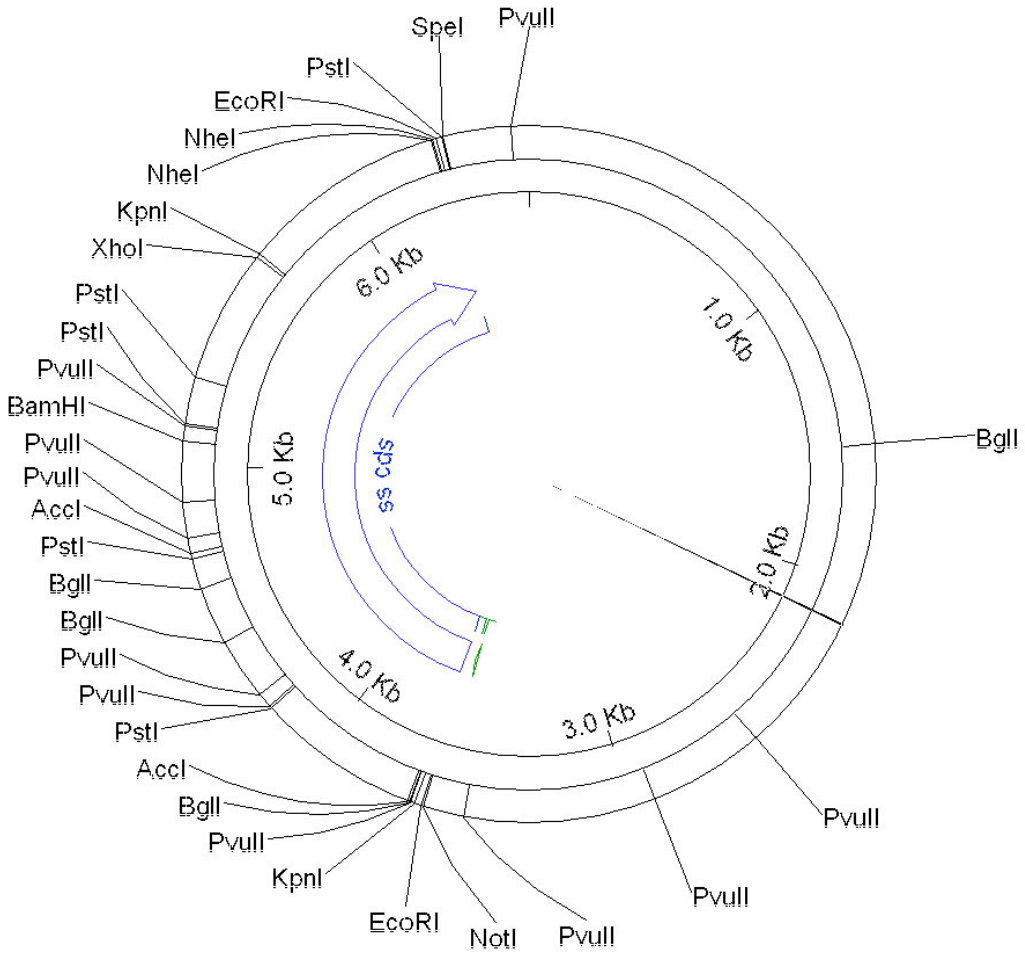

***pOT2* constructs**

Arnt and Tgo were expressed in the rabbit TnT cell-free system under the control of the T7 promoter of the *pOT2* vector. *pOT2-tgo* was obtained in the cDNA *Drosophila* Gold Collection from the BDGP. *Arnt* was extracted from *pCMV-Sport6-Arnt* and cloned in *pOT2*, which was extracted from *pOT2-tgo*.

pOT2-tgo

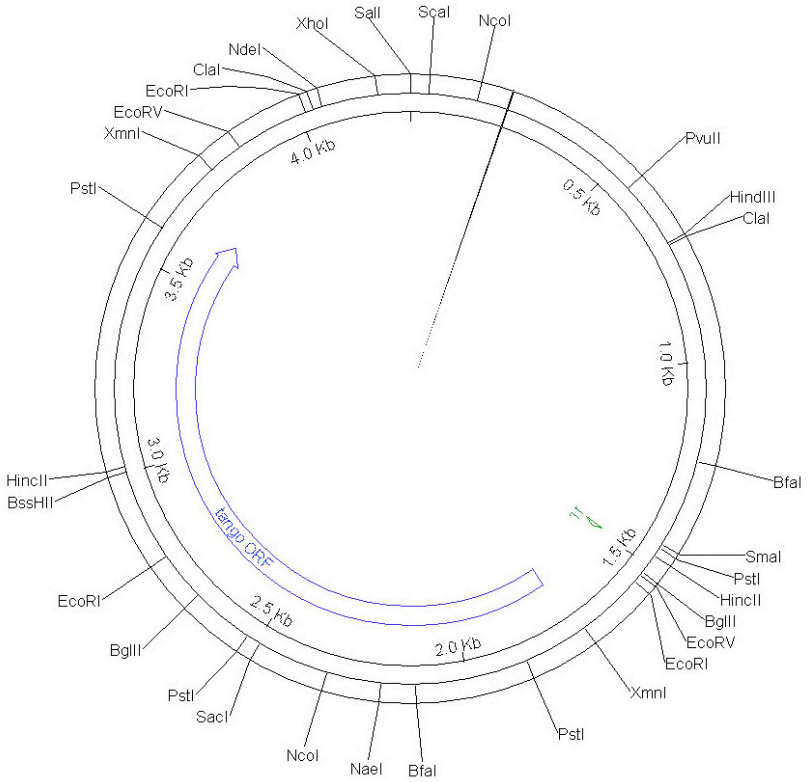

pOT2-Arnt